UNIVERSITY OF CALIFORNIA SAN DIEGO

Activity of Antibiotic Molecules Present in the Eukaryotic/Prokaryotic Interface

A dissertation submitted in partial satisfaction of the requirements for the degree Doctor of Philosophy

in

Biology

by

Roland B. Liu

Committee in charge:

Professor Kit Pogliano, Chair
Professor Eric Schmelz, Co-Chair
Professor Douglas Bartlett
Professor Joe Pogliano
Professor Emmanuel Theodorakis

The dissertation of Roland B. Liu is approved, and it is acceptable in quality and form for publication on microfilm and electronically.

_____

_____

_____

_____
Co-Chair

_____
Chair

University of California San Diego

2020

DEDICATION

This dissertation is dedicated to all the
friends, family, coworkers, and mentors
that have,
in each their own special way,
made me who I am.

TABLE OF CONTENTS

LIST OF FIGURES

Chapter 1

Chapter 2

Chapter 3

LIST OF TABLES

Chapter 1

No tables within Chapters 2 or 3.

ACKNOWLEDGEMENTS

I would like to acknowledge Dr. Kit Pogliano and Dr. Joe Pogliano for their amazing mentorship throughout my graduate school career. They have made the past five years a truly enjoyable and educational experience, and I could not have picked a better lab to have joined.

I would also like to thank all the members of the Pogliano labs for their companionship, guidance, and instruction. Whenever someone asks me what my favorite part about my lab is, I always respond with "the people", and it is thanks to all of you.

Furthermore, thank you to all the friends I've made during my time here at UC San Diego, in the biology cohort, in my singing groups, and elsewhere. Thanks to my DnD groups, especially my DM's Tim and Matt, for helping me keep my imagination alive, and to Acamazing and Encore for giving me an outlet for my musical side. I'd also like to specifically thank the townhouse – Sam, Nathan, Antonia, and Topher – for being such wonderful roommates and making sure I'm alive; Nina, for always being on my side and for sharing so many amazing stories and cartoons with me; Brian, for our brotherly bond over waifus and husbandos; and Chi-wei and Lia, for their unconditional friendship and for testing out all of their recipes on me. Finally, I'd like to again thank Sam, for always being there for me since I first stepped off of the airplane in San Diego for my interview

weekend; and Hannah, whose unceasing loyalty and enthusiasm – and appreciation for the color orange – left me no choice but for me to be her best friend.

Chapter 1, in full is currently being prepared for submission for publication of the material. Liu R., Jespersen A., Tsunemoto H., Lamsa A., Mahoney P., Pogliano J., Pogliano K. The dissertation author was the primary author of this paper.

Chapter 2, in part, is a reprint of the material as it appears in Nature Microbiology 2020. Pierce, E.C., Morin, M., Little, J.C., Liu R.B., Tannous J., Keller N.P., Pogliano K., Wolfe B.E., Sanchez L.M., Dutton R.J. Bacterial–fungal interactions revealed by genome-wide analysis of bacterial mutant fitness. Nat Microbiol (2020). The dissertation author was a co-author on this paper.

Chapter 3, in full, is a reprint of the material as it appears in the Journal of Antimicrobial Chemotherapy 2018. Gupta, N., Liu R., Shin. S., Sinha R., Pogliano J., Pogliano K., Griffin J., Nizet V., Corriden R. "SCH79797 improves outcomes in experimental bacterial pneumonia by boosting neutrophil killing and direct antibiotic activity." The Journal of Antimicrobial Chemotherapy vol. 73,6 (2018). The dissertation author was a co-author on this paper.

VITA

2009-2012	Teaching Assistant, Olin College of Engineering
2012	Bachelor of Science, Olin College of Engineering
2012-2015	Senior Research Associate, Pronutria
2016-2018	Instructional Assistant, University of California San Diego
2018-2019	Head Final Exam Writer, USA Biology Olympiad
2020	Doctor of Philosophy, University of California San Diego

SELECTED PUBLICATIONS

Gupta, N., Liu R., Shin. S., Sinha R., Pogliano J., Pogliano K., Griffin J., Nizet V., Corriden R. SCH79797 improves outcomes in experimental bacterial pneumonia by boosting neutrophil killing and direct antibiotic activity. *The Journal of Antimicrobial Chemotherapy* vol. 73,6 (2018).

Pierce, E.C., Morin, M., Little, J.C., Liu R.B., Tannous J., Keller N.P., Pogliano K., Wolfe B.E., Sanchez L.M., Dutton R.J. Bacterial–fungal interactions revealed by genome-wide analysis of bacterial mutant fitness. *Nat Microbiol* (2020).

Liu R., Jespersen A., Tsunemoto H., Lamsa A., Mahoney P., Pogliano J., Pogliano K. Minor Modifications to Flavones Alter their Antibiotic Mechanism of Action. Manuscript in preparation.

FIELDS OF STUDY

Major Field: Biology

Studies in Microbiology
Professor Kit Pogliano

ABSTRACT OF THE DISSERTATION

Activity of Antibiotic Molecules Present in the Eukaryotic/Prokaryotic Interface

by

Roland B. Liu

Doctor of Philosophy in Biology

Professor Kit Pogliano, Chair
Professor Eric Schmelz, Co-Chair

Antibiotic metabolites play a major role in the interactions between prokaryotes and eukaryotes. The exact effect of these antibiotics can be difficult to study due to the complexity of microbial communities and dynamics, as well as environmental conditions that differ from laboratory ones. Here, I employ Bacterial Cytological Profiling, an unbiased microscopy-based technique able to determine the mechanism of action of an antibiotic within hours. In Chapter 1, I have discovered using BCP that a family of plant defense metabolites called the flavones exhibits nontraditional structure-activity relationships, where minor modifications

made to the flavone backbone alter their antibiotic mechanism of action, as well as discover new antibiotic MOAs previous unattributed to flavones. I also employ BCP in Chapter 2 to study fungal-bacterial interactions on Cheese Curd Agar, and identify the nature of fungal inhibition of bacterial growth in microbial cheese communities. Finally, in Chapter 3, I use BCP to analyze the drug SCH79797, to show a dual effect of boosting neutrophil killing *in vivo* as well as having direct antibacterial activity, highlighting the complexity of studying the effects of molecules in eukaryotic environments. Overall, these studies provide insight into the prokaryotic-eukaryotic interface, as well as provide proof-of-concept studies for the development of *in situ* techniques to analyze antibiotic activities in non-laboratory settings.

INTRODUCTION

There are an estimated more than 1 trillion species of microorganisms on our Earth[1]. While significant advances have been made towards the high-throughput identification and classification of large clades of microbes as well as their metabolic potentials[2], we have only begun to scratch the surface of understanding all of these organisms' ecological importance, and the ways that they influence each other on a micro and a macro scale. Part of the barrier towards a holistic understanding of microbial ecology is the "Great Plate Count" anomaly[2,3], which estimates that only 1 out of 100 species of microbes can be cultured in the laboratory using current techniques – a proportion that may truly be even orders of magnitude lower for microbes inhabiting novel or understudied environments[2,4].

Microbial interactions – or symbioses – with other organisms are classified into six different categories: mutualism, in which both organisms benefit; commensalism, where one organism benefits and the other is unharmed; parasitism, where one organism benefits at the expense of the other; neutralism, in which neither organism is affected positively or negatively; amensalism, where one organism is unaffected while the other is harmed; and competition, where the fitness of both two organisms are harmed by the other's presence[5,6]. Of these, mutualism, commensalism,

parasitism, and competition are the most studied, although amensalism is ecologically frequent and important[6].

Many of these microbial interactions are regulated or actualized through the production or secretion of metabolites. These metabolites can range from being generally produced to being induced only under specific circumstances, and can embody all forms of symbioses. For example, mutualistic species living in microbial biofilms may cycle carbon and nitrogen-containing nutrients between each other, allowing for streamlined and thereby more efficient metabolisms[7]. Conversely, bacteria that sense the presence of other organisms may increase siderophore production, chelating valuable iron atoms away from the other organisms[8,9]. In turn, some organisms have developed specialized siderophore uptake channels for their competitor's siderophores, allowing them to 'steal' both the iron atom and the siderophore produced by the original bacteria[9].

Perhaps one of the most well-known examples of metabolic warfare are antibiotics. The growth of the antibiotic discovery field in the modern era is largely attributed to the discoveries of Paul Ehrlich and Alexander Fleming. At the beginning of the 20th century, Paul Ehrlich noticed that certain dyes were able to selectively stain some bacteria but not others, and extrapolated that therefore, there should exist chemicals

that are able to selectively kill some bacteria while leaving others unharmed. In 1909, Ehrlich the compound arsphenamine, an arsenic-based compound that was able to kill the *Treponema pallidum,* the causative bacterium for syphilis. The late 1920's and 1930's saw the discovery of the sulfadrugs at Bayer, and the serendipitous discovery of penicillin by Alexander Fleming. Fleming noted that a fungal contaminant on a petri dish prevented the growth of *Staphylococcus* bacteria in a radius around the fungal colonies, implying the secretion of a potent antibiotic molecule.

The discovery of penicillin engendered the discovery of many new families of antibiotics in the next few decades, especially in the 1940's through the 1960's, where more than half of the antibiotics used in clinics today were discovered[10]. Researchers capitalized on the fact that many organisms in ecological settings produce antibiotic molecules in order to compete with or protect themselves against the milieu of microorganisms surrounding them. Indeed, many modern antibiotics were originally isolated from *Streptomyces*, an actinobacterium ubiquitous in soil that is rich with biosynthetic gene clusters. Scientists are exploring links between microbial diversity and specific nutrient limitations of environmental niches and the antibiotic biosynthetic potential of the organisms in these niches with the end goal of discovering new antibiotics[11]. However, a major

roadblock to the clinical effectiveness of these new potential antibiotics the resistance mechanisms that bacteria have evolved, which can be via nonspecific mechanisms (expression of drug efflux pumps or increasing physical barriers to antibiotic entry)[12-14], or specific ones (mutations in the target molecule of the antibiotic, or expression of enzymes able to cleave the antibiotic molecule, rendering them ineffective)[14, 15]. Emergence of antibiotic-resistant bacteria in hospitals occurred immediately after the adoption of antibiotics into clinical use in the 1940's; however, initial rates of antibiotic discovery were high, so newer antibiotics could be used in lieu of the previous, now-ineffective ones. Thus, an "arms race" was created between antibiotic discovery and antibiotic-resistant pathogens.

As sources of novel antibiotics from screening natural metabolic products started to dwindle in the 1970's and 1980's, researchers developed more streamlined drug discovery pipelines, incorporating both natural, synthetic, and semi-synthetic chemical scaffolds for screening[16]. Modern drug discovery pipelines comprise several steps, including chemical library screens, *in silico* filtering steps, mechanism of action (MOA) determination, synthetic analog generation, and verification/optimization of candidate molecules to be sent to clinical trials.

In drug discovery, researchers often first compile large libraries of compounds, from either natural product libraries, synthetic chemical libraries, or a combination of both. These libraries are screened for potency against test strains of bacteria. The minimum inhibitory concentration (MIC) of molecules are then often determined either by disk-diffusion, where disks are infused with the antibiotic and placed on a plate where bacteria grown in a lawn and zones of clearing around the antibiotic-containing disks are measured; or by microbroth-dilution, where the antibiotic is serially diluted across media-containing wells in a multi-well plate, and the lowest dilution of antibiotic able to prevent bacterial growth is recorded.

After the efficacy and MICs of molecules in the libraries are established, molecules are studied for their mechanism of action (MOA); essentially, which component of the cell the antibiotic targets. Antibiotics can be categorized into broad categories based on which essential cellular process they inhibit; these include DNA replication, RNA transcription, nucleotide synthesis, protein translation, lipid biosynthesis, cell wall biosynthesis, and direct membrane activity as well as surfactant-like activity[17]. The MOAs of novel or unknown antibiotics can be determined through several methods, including resistant mutant generation, macromolecular synthesis assays, and newer -omics-level

approaches such as transcriptomics and proteomics to conduct surveys of cellular response to treatment[18-20]. Resistant mutant generation often involves the serial passaging on agar plates or in liquid medium containing increasing concentrations of antibiotics. Once mutants with several-fold resistance to the antibiotic have been isolated, they are sequenced and analyzed for deviations from the sensitive parent strain. Sequence differences between mutants and the parent strain may indicate mutations in the target binding site of the antibiotic, or could represent regulatory alterations in homeostasis that are able to suppress the effects of the antibiotic, providing information as to potential cellular targets. Meanwhile, macromolecular synthesis assays directly measure the levels of essential macromolecules (such as nucleotides, proteins, or cell wall or membrane precursors) being newly produced. Treatment with most antibiotics will result in one or more of these essential biosynthetic pathways being affected, which can be detected with the assay. An antibiotic's MOA can often be inferred from this information.

While mutant generation screens and macromolecular synthesis assays have been invaluable for determining antibiotic MOAs, they have several weaknesses. While mutant generation screens often identify the exact target of an antibiotic, it can take weeks to months for a mutant to appear, and whole genome sequencing (WGS) to identify single

nucleotide polymorphisms (SNPs) is expensive and low-throughput. These SNPs need to be verified as well by backcrossing into the parent strain, which takes additional time and resources. Furthermore, there is a potential for suppressor mutations in related but non-target genes to arise, giving false information as to the molecular target of the antibiotic[21]. Macromolecular synthesis assays, while much faster than mutant generation, are not able to determine the exact target of an antibiotic, and the interconnectedness of biological pathways can confuse the interpretation of MSA results, requiring a panel of assays to be performed for each antibiotic[18]. For example, a transcription inhibitor would likely reduce the rates of protein translation due to the reduced levels of mRNA; therefore, both mRNA synthesis assays and protein synthesis assays must be performed to be able to delineate between inhibitors of the two pathways[18]. Furthermore, many strains have a stringent response, which causes cells to alter the regulation of many basic cellular processes such as DNA replication, transcription, and translation in response to different stress conditions including amino acid deprivation or antibiotic treatment, which can further obfuscate the analysis of MSA panels[22].

The weaknesses of such *in vitro* assays coupled with improvements in bioinformatic techniques have led to the popularization of *in silico* methods in drug discovery. Two such methods include docking studies

and algorithmic prediction of molecule potency based on molecular bond characteristics[23-25]. Docking studies predict the fit of candidate molecules to a target of interest. For example, if a candidate molecule appears to inhibit protein A, and the crystal structure of protein A has been solved, structural biologists can import chemical structure of hundreds of analogs of the candidate, and computationally predict the binding affinity of these analogs to protein A. This has the obvious upside of cost and through-put, where thousands of chemicals can be screened with only the capital investment of computer processing power. Furthermore, these docking studies can infer activity against a specific target, as opposed to merely obtaining information as to the general cellular pathway targeted by the antibiotic[23,24]. Another *in silico* method of drug candidate screening involves algorithmic prediction of molecules' efficacy against a target. For this, *in vitro* studies must have already been performed against a target for a variety of chemical analogs[25]. With these data, algorithms can take chemical bond parameters (bond length, type, angle, and atomic members) and determine which combination of parameters are most predictive of inhibitory activity. This parameter matrix can then be used to predict the activity of other structurally similar compounds, allowing for faster predictive capabilities than docking

studies once the algorithm has been developed, at the cost of requiring *in vitro* data from a training library of compounds[25].

While *in silico* screens have major advantages in cost and throughput versus *in vivo* and *in vitro* methods of determining MOA, they rely on the assumption of a predetermined target molecule, as assaying for binding affinity against a large panel of possible targets becomes multiplicatively unwieldy computationally. Therefore, they rely on the assumption of structure-activity relationship (SAR): essentially, the assumption that molecules with similar core structures will likely have the same activity[23-26]. While this assumption greatly simplifies screening in terms of computing power and analysis, it is unable to detect when a molecule could have a secondary or alternate primary MOA. For example, if a candidate molecule was shown to inhibit protein A, but an analog to the candidate molecule is a potent protein B inhibitor but has less affinity to protein A, it may be filtered out in an *in silico* screen due to the assumption of a molecular target, biasing the screen results.

Recent years have seen the development of more unbiased MOA determination methods that can be any combination of cheaper, faster, or more descriptive than the mutant generation, *in vitro*, and *in silico* procedures previously outlined. One such technique, developed by previous members of the lab, is called Bacterial Cytological Profiling

(BCP)[27-29]. BCP is a fluorescence microscopy-based technique that interprets morphological changes to cells in response to antibiotic treatment, based on the finding that treatment of cells with antibiotics that target different essential cellular processes result in distinct cytological profiles. In the flagship study[27], the authors treated *E. coli* cells with antibiotics that inhibit protein synthesis, RNA transcription, DNA replication, lipid biosynthesis, DNA replication, cell wall biosynthesis, proton-motive force, or are directly membrane active. They showed that quantifiable morphological differences can be observed between cells treated with antibiotics that target different cellular pathways, and even between cells treated with antibiotics that have different targets within the same cellular pathway. With this, the authors constructed an algorithm based on a training set of known, control antibiotics wherein new drugs with unknown MOAs can be compared[27].

BCP has many advantages when compared to traditional methods of MOA determination. As it is an observation-based method, it is unbiased, with no prior knowledge of an assumed target needed. Additionally, it is cost-effective, requiring only dyes, the antibiotic itself and media components after the capital investment of a fluorescent microscope. And importantly, it is rapid, as these distinct morphological changes can be observed within 1 to 2 hours, and as possibly as quickly

as within 10 minutes. While not as high-throughput as *in silico* screens, dozens of molecules can be analyzed daily per person due to the rapidity of the test. After the initial work with *E. coli*, BCP has been developed for many organisms, including other Gram-negatives such as *Pseudomonas aeruginosa* and *Acinetobacter baumanii*, as well as Gram-positives such as *Staphylococcus aureus*[28] and *Bacillus subtilis*[29].

Because of these advantages, BCP has been used for the screening and identification of bioactive natural products. As mentioned previously, natural products have been a rich source for potent clinical antibiotics. Traditional drug discovery pipelines that screen natural products are predisposed to select molecules that are stable, potent, and highly specific to their cellular target with low toxicity – all very desirable qualities for an antibiotic[16,17]. However, many bioactive natural products are less stable, less potent, more toxic, and can have multiple targets, but still serve important ecological functions[30,31].

This is likely the case with plant defense metabolites. Over the past century of antibiotic discovery, no clinically used antibiotic has been isolated from a plant, despite many attempts and the fact that plants produce a wealth of antibiotic metabolites[31]. Plant antibiotics that are produced locally on demand following microbial stress are termed phytoalexins. Phytoalexins comprise several chemical classes including

terpenoids, glycosteroids, alkaloids, and flavonoids[31,32]. As phytoalexins play a major role in plant defense and subsequently plant health, understanding the induction, production, and functions of phytoalexins has major implications for both agriculture and plant ecology. However, despite the wealth of past and ongoing research on phytoalexins, many aspects of phytoalexins remain to be fully characterized or understood.

One well-known group of plant metabolites are the flavonoids[31,33-35]. Flavonoids are polyphenolic molecules that can be found in nearly all parts of plant anatomy, including the bark, root, stems, leaves, flowers, fruit, and seeds. The term flavonoids comprise the anthocyanidin, flavone, flavonol, flavanone, flavanonol, flavan, flavanol, and respective isoflavonoid groups[33]. They are often synthesized via the cyclization of chalcones, which are themselves formed via the combination of malonyl-CoA with 4-coumaryl-CoA derived from phenylalanine[36]. They have been shown to have a wide variety of biological functions *in planta* and medicinally, including pigmentation and UV filtration, as well as having antioxidant, anti-inflammatory, anti-mutagenic, and anti-carcinogenic activities[33-35]. Additionally, certain flavonoids have been shown to have antibiotic activity, classifying them as antimicrobial defenses. However, flavonoids are often unstable in aqueous solution and when exposed to light, making longer-term studies of the antibiotic effects or MOAs difficult

to study *in vivo*[34-35]. Furthermore, many flavonoid phytoalexins have relatively low solubility and potency, diminishing their possible clinical relevance.

Nevertheless, much research has been conducted on the antibiotic activities of flavonoids, most often as DNA replication inhibitors by either inhibiting enzymes required for DNA replication or segregation or by direct intercalation within the DNA. The flavone and flavonol subgroups of flavonoids appear to be particularly prolific DNA replication inhibitors, with a large body of literature supporting their anti-DNA antibiotic activity[37-39]. For example, apigenin has been demonstrated to inhibit bacterial DNA Gyrase *in vivo*, *in vitro*, and *in silico*[38,39]. Flavonoids have also been demonstrated to have direct membrane activity, likely due to their lipophilicity and therefore their ability to integrate directly within the bacterial cell membrane[34,35].

Furthermore, it has been suggested through *in vitro* assays and *in silico* docking studies that flavones may inhibit other cellular pathways. For example, some studies have shown binding affinity between flavones and *fabZ* and penicillin binding proteins[40,41]. However, *in vivo* studies of these MOAs are lacking, likely due to the low potency and instability of the flavones. The ability to examine flavonoid phytoalexin antibiotic MOA *in vivo* would impact our understanding of the plant microbiome and the

mechanism by which plant defense metabolites are able to inhibit the growth of pathogenic bacteria. In this dissertation, I outline my research on how the use of BCP allows us to gain new *in vivo* information on how plant defense metabolites – specifically the flavones – inhibit bacteria through mechanisms previously unshown, and show the power of unbiased *in vivo* MOA determination techniques when compared to *in vitro* assays or *in silico* docking studies. The direct analysis of these antibiotic effects also allows us to gain more understanding to how specialized metabolites affect the ecological dynamics between plants and bacteria within the plant microbiome environment.

Here, we also briefly expand our use of BCP into other microbiomes. One microbial community that has garnered recent interest is the cheese microbiome[42]. Unlike environmental microbiomes such as the marine microbiome or soil microbiome which contain thousands of species of bacteria simultaneously interacting, cheeses contain a much smaller and manageable number of species – on the order of ten – allowing for an intermediate between studying bacteria in isolation and surveying extremely complex microbial interactions. Previous research on cheese communities saw repeatable patterns of succession in community member abundance over the age of the cheese[42], and were replicable in laboratory settings when the community was reconstructed *in vitro*.

While the exact molecular mechanisms behind the robustness of this pattern of succession are still being elucidated, this "just-enough" level of species diversity allows researchers to study more than just -omic-level interactions between community members, and begin to dive into more detailed mechanisms of interaction and symbioses due to the finite number of cross-species interactions.

These mechanisms include the metabolic communication and interactions between species that were previously described, such nutrient sharing and competition, the triggering of molecular signaling pathways by metabolites from different species, as well as the secretion of antibiotic molecules. The development of *in vivo* techniques such as BCP for use in ecologically relevant samples can allow us to better understand the molecular mechanisms underlying competition between species by observing them in co-culture or in a community, as opposed to in isolation in laboratories, which often results in a completely different metabolic profile for organisms than when grown in co-culture.

In this dissertation, I outline my research exploring how bacteria respond to antibiotic molecules produced by plants and cheese microorganisms. With respect to the former, I explore a family of plant metabolites called the flavones, and show that antibiotic flavones can have different MOAs that are based off their minor modifications –

hydroxylations and methoxylations – to the flavone backbone, and not the backbone itself. These results are obtained through *in vivo* observation of cellular morphological changes as a result to flavone exposure in *E. coli* via Bacterial Cytological Profiling, and are contrasted with *in vivo* experiments and *in silico* research performed by other groups. The finding that antibiotic flavones have different *in vivo* antibiotic MOAs based on modifications runs counter to the backbone-based SAR assumption widely used in drug discovery pipelines and provides insight into the ecological importance and mechanism of phytoalexins in plant pathogen defense. In the latter, we explore pairwise interactions between fungal and bacterial species found in the cheese microbial community, and identify certain genes and antimicrobial peptides that impact fitness specifically when these fungal and bacterial strains are grown in co-culture, highlighting their importance in the metabolic warfare present within cheese. Finally, we include a study on an antibiotic molecule that both boosts neutrophil killing and exhibits direct antibiotic activity, which further exemplifies the complexity of studying antibiotic molecules in the context of a eukaryotic-based environment. Overall, my research provides insight into the role of antibiotic metabolites in the symbiosis between eukaryotic and prokaryotic species.

REFERENCES

1. Locey, K.J. & Lennon, J.T. Scaling Laws predict global microbial diversity. *PNAS* 113, 5970 (2016)

2. Tanyaradzwa Rodgers Ngara, Houjin Zhang. Recent Advances in Function-based Metagenomic Screening. *Genomics, Proteomics & Bioinformatics.* 16:6, p.405-415 (2018)

3. Harwani, Dharmesh. (2012). The Great Plate Count Anomaly and the Unculturable Bacteria. International Journal of Scientific Research. 2. 350-351. 10.15373/22778179/SEP2013/122.

4. Sonia R. Vartoukian, Richard M. Palmer, William G. Wade, Strategies for culture of 'unculturable' bacteria, *FEMS Microbiology Letters*, 309:1, p.1–7 (2010)

5. Martin, Bradford & Schwab, Ernest. (2012). Symbiosis: "Living together" in Chaos. Studies in history of biology. 4. 7-25.

6. R.L. Kitching, R. Harmsen. Amensalism. Editor(s): Sven Erik Jørgensen, Brian D. Fath. *Encyclopedia of Ecology*, Academic Press (2008)

7. Hubas C., Boeuf D., Jesus B., Thiney N., Bozec Y., Jeanthon C. A Nanoscale Study of Carbon and Nitrogen Fluxes in Mats of Purple Sulfur Bacteria: Implications for Carbon Cycling at the Surface of Coastal Sediments. *Frontiers in Microbiology,* Volume 8 (2017).

8. Jin, B. Newton S., Shao Y., Jiang X, Charbit A., Klebba P. Iron acquisition systems for ferric hydroxamates, haemin and haemoglobin in *Listeria monocytogenes*. *Mol. Microbiol.* 59, 1185–1198 (2006).

9. Heymann, P., Ernst, J. F. & Winkelmann, G. A gene of the major facilitator superfamily encodes a transporter for enterobactin (Enb1p) in *Saccharomyces cerevisiae*. *Biometals* 13, 65–72 (2000).

10. Matthew I Hutchings, Andrew W Truman, Barrie Wilkinson. Antibiotics: past, present and future. Current Opinion in Microbiology. Volume 51, Pages 72-80 (2019)

11. Allison M. Sharrar, Alexander Crits-Christoph, Raphaël Méheust, Spencer Diamond, Evan P. Starr, Jillian F. Banfield. Bacterial Secondary Metabolite Biosynthetic Potential in Soil Varies with Phylum, Depth, and Vegetation Type. mBio Jun 2020 11(3).

12. Husain, F., M. Humbard, and R. Misra, *Interaction between the TolC and AcrA proteins of a multidrug efflux system of Escherichia coli.* J Bacteriol, 2004. 186(24): p. 8533-6.

13. Bay DC, Stremick CA, Slipski CJ, Turner RJ. Secondary multidrug efflux pump mutants alter Escherichia coli biofilm growth in the presence of cationic antimicrobial compounds. Res Microbiol. 2017 Apr;168(3):208-221

14. Reygaert, Wanda C. "An overview of the antimicrobial resistance mechanisms of bacteria." *AIMS microbiology* vol. 4,3 482-501. 26 Jun. 2018

15. Dever LA, Dermody TS. Mechanisms of Bacterial Resistance to Antibiotics. *Arch Intern Med.* 1991;151(5):886–895.

16. Theuretzbacher, U., Outterson K., Engel A., Karlen A., *The global preclinical antibacterial pipeline.* Nat Rev Microbiol, 2020. 18(5): p. 275-285.

17. Kapoor, Garima, Saigal S., Elongavan A. "Action and resistance mechanisms of antibiotics: A guide for clinicians." *Journal of anaesthesiology, clinical pharmacology* vol. 33,3 (2017): 300-305. doi:10.4103/joacp.JOACP_349_15

18. Cotsonas King, A. and L. Wu, *Macromolecular synthesis and membrane perturbation assays for mechanisms of action studies of antimicrobial agents.* Curr Protoc Pharmacol, 2009. Chapter 13: p. Unit 13A 7.

19. Aubrie O'Rourke, Sinem Beyhan, Yongwook Choi, Pavel Morales, Agnes P. Chan, Josh L. Espinoza, Chris L. Dupont, Kirsten J. Meyer, Amy

Spoering, Kim Lewis, William C. Nierman, Karen E. Nelson. Mechanism-of-Action Classification of Antibiotics by Global Transcriptome Profiling Antimicrobial Agents and Chemotherapy Feb 2020, 64 (3)

20. Franken, H., Mathieson, T., Childs, D. Sweetman G., Werner T., Togel I., Doce C., Gade S., Bantscheff M., Drewes G., Reinhard F., Huber W., Savitski M. Thermal proteome profiling for unbiased identification of direct and indirect drug targets using multiplexed quantitative mass spectrometry. *Nat Protoc* 10, 1567–1593 (2015).

21. Zeng, D., Zhao J., Chung H., Guan Z., Raetz C., Zou P. "Mutants resistant to LpxC inhibitors by rebalancing cellular homeostasis." *The Journal of biological chemistry* vol. 288,8 (2013)

22. Joanne K. Hobbs and Alisdair B. Boraston (p)ppGpp and the Stringent Response: An Emerging Threat to Antibiotic Therapy. *ACS Infectious Diseases* 2019 *5* (9), 1505-1517

23. Moulishankar, A. and K. Lakshmanan, *Data on molecular docking of naturally occurring flavonoids with biologically important targets.* Data Brief, 2020. 29: p. 105243.

24. Bhattacharjee K, Kumar S, Palepu NR, Patra PK, Rao KM, Joshi SR. Structure elucidation and in silico docking studies of a novel furopyrimidine antibiotics synthesized by endolithic bacterium *Actinomadura* sp. AL2. World J Microbiol Biotechnol. 2017 Sep 20;33(10):178.

25. Durrant, Jacob D, and Rommie E Amaro. "Machine-learning techniques applied to antibacterial drug discovery." *Chemical biology & drug design* vol. 85,1 (2015):

26. Bryskier, A., *Antimicrobial agents : antibacterials and antifungals*. 2005, Washington, D.C.: ASM Press. xxx, 1426 p.

27.Nonejuie, P., Burkhart M., Pogliano K., Pogliano J., *Bacterial cytological profiling rapidly identifies the cellular pathways targeted by antibacterial molecules.* Proc Natl Acad Sci U S A, 2013. 110(40): p. 16169-74.

28. Quach, D., Sakoulas G., Nizet V., Pogliano J., Pogliano K. "Bacterial Cytological Profiling (BCP) as a Rapid and Accurate Antimicrobial Susceptibility Testing Method for Staphylococcus aureus." *EBioMedicine* vol. 4 95-103. 18 Jan. 2016

29. Lamsa, A., Lopez-Garrido J., Quach D., Riley E., Pogliano J., Pogliano K. *Rapid Inhibition Profiling in Bacillus subtilis to Identify the Mechanism of Action of New Antimicrobials.* ACS Chem Biol, 2016. 11(8): p. 2222-31.

30. Cowan, M.M., *Plant products as antimicrobial agents.* Clin Microbiol Rev, 1999. 12(4): p. 564-82.

31. Andersen, E.J., Ali S., Byamukama E., Yen Y., Nepal M. *Disease Resistance Mechanisms in Plants.* Genes (Basel), 2018. 9(7).

32. Ahuja, I., R. Kissen, and A.M. Bones, *Phytoalexins in defense against pathogens.* Trends Plant Sci, 2012. 17(2): p. 73-90.

33. Kumar, S. and A.K. Pandey, *Chemistry and biological activities of flavonoids: an overview.* ScientificWorldJournal, 2013. 2013: p. 162750.

34. Cushnie, T.P. and A.J. Lamb, *Antimicrobial activity of flavonoids.* Int J Antimicrob Agents, 2005. 26(5): p. 343-56.

35. Cushnie, T.P. and A.J. Lamb, *Recent advances in understanding the antibacterial properties of flavonoids.* Int J Antimicrob Agents, 2011. 38(2): p. 99-107.

36. Ververidis F, Trantas E, Douglas C, Vollmer G, Kretzschmar G, Panopoulos N. Biotechnology of flavonoids and other phenylpropanoid-derived natural products. Part I: Chemical diversity, impacts on plant biology and human health. Biotechnol J. 2007 Oct;2(10):1214-34.

37. Kanakis, C.D., Tarantilis P., Polissiou M., Tamjir-Riahi H. *Interaction of antioxidant flavonoids with tRNA: intercalation or external binding and comparison with flavonoid-DNA adducts.* DNA Cell Biol, 2006. 25(2): p. 116-23.

38. Morimoto, Y., Baba T., Sasaki T., Hiramitsu K. *Apigenin as an anti-quinolone-resistance antibiotic.* Int J Antimicrob Agents, 2015. 46(6): p. 666-73.

39. Verghese, J., Nguyen T., Oppegard L, Seivert L, Hiasi H, Ellis K. *Flavone-based analogues inspired by the natural product simocyclinone D8 as DNA gyrase inhibitors.* Bioorg Med Chem Lett, 2013. 23(21): p. 5874-7.

40. Geethalakshmi, R., J.C. Sundaramurthi, and D.V.L. Sarada, *Antibacterial activity of flavonoid isolated from Trianthema decandra against Pseudomonas aeruginosa and molecular docking study of FabZ.* Microb Pathog, 2018. 121: p. 87-92.

41. Alhadrami, H., Hamed A., Hassan H., Belbahri L., Rateb M., Sayed A. "Flavonoids as Potential anti-MRSA Agents through Modulation of PBP2a: A Computational and Experimental Study." *Antibiotics (Basel, Switzerland)* vol. 9,9 562. 31 Aug. 2020.

42. Wolfe, B. E., Button, J. E., Santarelli, M. & Dutton, R. J. Cheese rind communities provide tractable systems for in situ and in vitro studies of microbial diversity. *Cell* 158, 422–433 (2014).

CHAPTER 1: MINOR MODIFICATIONS TO FLAVONES ALTER THEIR *in vivo* ANTIBIOTIC MECHANISM OF ACTION

1.1 Abstract

Flavones are important molecules in plant pigmentation, UV filtration, communication, and pathogen defense. Their antibiotic activities have previously been studied using traditional in vitro and in silico drug discovery methods such as enzymatic activity assays and docking studies. By using Bacterial Cytological Profiling, an in vivo method able to determine the cellular pathway affected by antibiotics within two hours, we have observed at least four distinct antibiotic mechanisms of action among flavones that differ only by minor modifications, namely hydroxylations and methoxylations. Among these, we identified at least two antibiotic MOAs not previously confirmed either in vivo or in vitro within the flavone family, specifically inhibition of outer membrane biosynthesis by tetramethyl-O-Scutellarein and inhibition of cell division by tamarixetin. Most flavones that exhibited primary antibiotic mechanisms of action other than inhibition of DNA replication/segregation in vivo still demonstrated significant in vitro inhibition of DNA Gyrase and Topoisomerase as well as DNA intercalation. The modification-based antibiotic MOA of flavones provides an example of a class of molecules that fall outside of the traditional structure-activity relationship paradigms,

where analogs built from a common scaffold frequently have a similar MOA. Furthermore, we highlight the importance of using both an in vivo MOA assay together with an in vitro assay for antibiotic mechanism of action determination of chemical analogs even if a cellular target of a starting molecule has been identified. These results also provide insight into plant metabolite defenses against bacteria, which take a "shotgun" approach to pathogen defense with structurally related molecules providing inhibition of multiple bacterial cellular pathways.

1.2 Introduction

A key bottleneck in antibiotic drug discovery is determining the molecules' mechanism of action (MOA), the means by which an antibiotic either inhibits the growth of or kills bacteria[1, 2]. Traditional methods of MOA determination involve the use of macromolecular synthesis assays or resistant mutant generation and sequencing, both of which are low-throughput and can have difficulties identifying the MOA of many classes of drugs, especially those with direct membrane activity or other non-protein-level effects[1-3]. More recently, transcriptomics has been used to investigate antibiotic MOA by identifying the transcriptional response to antibiotic treatment. However, many antibiotics with distinct MOAs can cause similar transcriptional responses in marker genes,

especially in bacteria with stringent responses or other generalized response pathways to antibiotics[4] . Another recent development in MOA determination is Thermal Proteome Profiling, which utilizes shifts in protein melting temperatures when bound to a ligand to conduct an unbiased survey of potential protein targets of drugs, but this method can be costly, low-throughput, and restricted to drugs with protein targets[5].

Central to the field of antibiotic discovery is the concept of structure-activity relationship (SAR), where a molecules' efficacy is often linked a pharmacophore present within the backbone structure[6]. Minor modifications to the backbones can alter various characteristics of the drug, such as potency, solubility, stability, and bioavailability, but these chemical analogs are often assumed to have similar MOAs to the parent molecule[6]. As such, drug discovery pipelines often identify the MOA of candidate molecules identified from screens, and then synthesize chemical analogs to improve upon these candidates. The activity of these analogs is often measured by killing assays or inferred via in vitro or in silico target-molecule interactions[2, 7, 8]; rarely are analogs re-screened in vivo for MOA.

An interesting parallel to the chemical synthesis of antibiotic analogues can be seen in plant defense metabolic pathways. A key component of plant defense pathways are phytoalexins, which are

specialized metabolites produced in response to pathogen infection that include many chemically diverse families of molecules[9-12]. Plants are known to express an abundance of hydroxyl-, methyl- and acetyl-transferases that allow plants to produce large libraries of defense metabolites that have identical backbone structures with differing modifications[9, 10, 13], similar to the results of chemical analog synthesis during drug discovery. The natural plant metabolome thus provides a wealth of pre-existing molecules to study for bioactivity and structure-activity relationship.

The flavonoids are a large family of phenylpropanoid derivatives containing two phenyl rings and a third heterocyclic ring, and comprise over 5000 characterized representatives found throughout plants and some fungi[14-17]. Flavonoids have been previously studied for their antibiotic effects, but these studies are sometimes hindered by the molecules' low solubility, poor stability in aqueous solution and when exposed to light, relatively low potency, and their sometimes pleotropic or unclear effects[14, 16, 18]. Nevertheless, a large body of research exists characterizing the flavonoids as DNA replication inhibitors, either by inhibiting topoisomerases or by acting as DNA intercalators[7, 15, 19-21]. Specifically, the flavone (Figure 1.1A) and flavonol subgroups of flavonoids have demonstrated strong in vitro anti-topoisomerase or

intercalative activities, the efficacy of which has been attributed to the planarity of the molecules' backbone due to the double bond between C2 and C3 [7, 18]. For the purposes of this study, we will refer to flavonols as within the "flavone" group for brevity, as flavonols refer to 3-hydroxylated flavones. Flavones have also been shown to have direct membrane active effects, due to their lipophilicity and ability to integrate within cell membranes[15]. Other potential antibiotic MOAs of flavones have been proposed and studied in vitro and in silico[22], but in vivo demonstrations of these MOAs are lacking.

Due to the difficulties of understanding the in vivo effect of flavones, much recent work has focused on further characterizing their anti-DNA replication effects in vitro or in silico, based on the assumption of SAR[7, 15, 23]. In this study, we instead look at the in vivo antibiotic effects of flavones using Bacterial Cytological Profiling (BCP), a microscopy-based technique that can identify the primary cellular pathway inhibited by molecules within two hours by examining morphological changes in response to treatment at or near the molecules' minimum inhibitory concentration (MIC)[24-26]. Unlike most in vitro and in silico studies, BCP does not require the prior assumption of a target, allowing for unbiased determination of the MOA of antibiotic molecules[25]. Furthermore, the rapid timeline of BCP allows us to circumvent the traditional challenges

associated with working with unstable plant-derived metabolites and requires orders of magnitude fewer amounts of material than traditional resistant mutant-generation-based MOA determination methods.

Surprisingly, our analysis of thirteen flavones using BCP suggests that flavones can primarily impact at least four distinct cellular pathways, including two that to our knowledge have not been previously confirmed in flavones in vivo. Specifically, we found that some flavones can inhibit DNA replication and others directly impact the membrane, activities that have previously been described[14], while others can inhibit cell division and outer membrane biosynthesis, activities that have not previously been identified in vivo. These results showcase the importance of in vivo MOA studies and the potential pitfalls of assuming SAR between two structurally similar molecules, and provides us with insight as to how minor enzymatic modifications such as hydroxylations and methoxylations may result in broad-spectrum pathogen defense within a single family of molecules.

1.3 Results

We assayed a library of 31 flavones for activity against E. coli Δ*tolC*, a drug efflux pump knockout strain, to determine the minimum inhibitory concentration (MIC) of these compounds (Table 1.1). Of these, 18 had

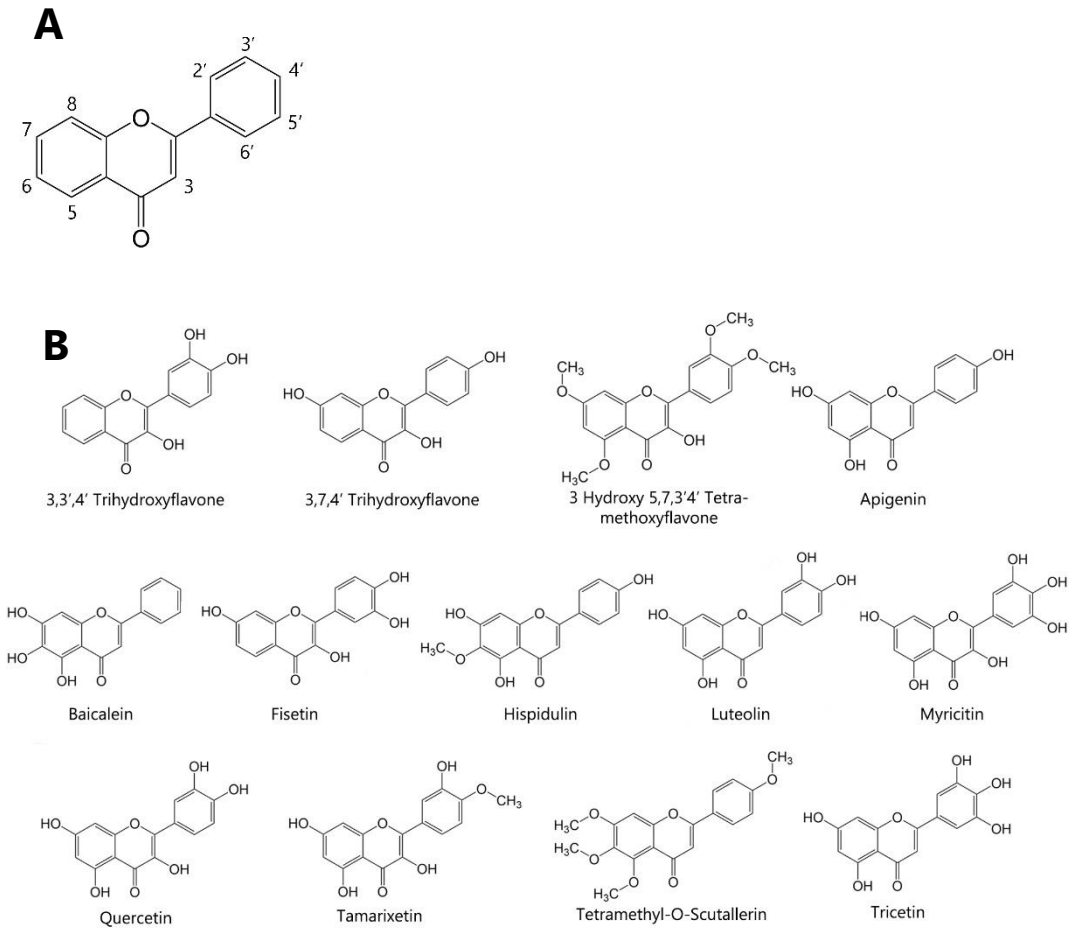

Figure 1.1. Chemical structures of (A) the flavone backbone, and (B) flavones and flavonols examined in this study.

measurable (<200µg/mL) inhibitory effects. We then selected 13 of the flavones and flavonols (Figure 1.1B) with the lowest MICs to perform in vitro DNA gyrase/topoisomerase assays as well as Bacterial Cytological Profiling to determine their antibiotic mechanism of action. While several flavones exhibited significant (<20µg/mL) activity against the E. coli ΔtolC strain, none of the flavones had a measurable (<200µg/mL) MIC against wild-type strains of E. coli, suggesting that all of these molecules are substrates for efflux and highlighting the importance of the efflux pump knockout strain in studying the effect of these molecules.

In vitro Gyrase and Topoisomerase IV assays of flavones and flavonols show strong inhibitory activity

Previous research regarding the antibacterial activity of flavones has centered around their anti-DNA replication activities, either by inhibiting topoisomerases themselves by direct binding, or by intercalating within DNA, preventing the progression of topoisomerases[7, 14, 15, 19, 20, 27]. These anti-DNA replication activities and the differences between enzymatic binding and DNA intercalation can be resolved by in vitro topoisomerase assays. To confirm the in vitro activity of the flavones in our study, we assayed for anti- E. coli gyrase and topoisomerase IV activity using the TopoGEN kits TG2000G and TG1007 respectively (Figure 1.2A-E).

Table 1.1. Flavones tested for antibiotic activity, and associated modifications to the positions shown in Figure 1.1A and minimum inhibitory concentrations (MIC) against *E. coli* Δ*tolC*.

Flavone	3	5	6	7	8	2'	3'	4'	5'	6'	MIC (μg/mL)
2'-Hydroxyflavone	-	-	-	-	-	-OH	-	-	-	-	>200
3H-5,7,3'4'-TMF	-OH	-OMe	-	-OMe	-	-	-OMe	-OMe	-	-	70.5
3,3',4'-THF	-OH	-	-	-	-	-	-OH	-OH	-	-	12.5
3',4'-DHF	-	-	-	-	-	-	-OH	-OH	-	-	50
3,7,4'-THF	-OH	-	-	-OH	-	-	-	-OH	-	-	17.7
7,8-DHF	-	-	-	-OH	-OH	-	-	-	-	-	70
7-Hydroxyflavone	-	-	-	-OH	-	-	-	-	-	-	>200
8-H-7-Methoxyflavone	-	-	-	-OMe	-OH	-	-	-	-	-	>200
Apigenin	-	-OH	-	-OH	-	-	-	-OH	-	-	8.8
Baicalein	-	-OH	-OH	-OH	-	-	-	-	-	-	70
Cirsiliol	-	-OH	-OMe	-OMe	-	-	-OH	-OH	-	-	>200
Diosmetin	-	-OH	-	-OH	-	-	-OH	-OMe	-	-	>200
Eupatilin	-	-OH	-OMe	-OH	-	-	-OMe	-OMe	-	-	>200
Fisetin	-OH	-	-	-OH	-	-	-OH	-OH	-	-	25
Gossypetin	-OH	-OH	-	-OH	-OH	-	-OH	-OH	-	-	100
Herbacetin	-OH	-OH	-	-OH	-OH	-	-	-OH	-	-	141
Hispidulin	-	-OH	-OMe	-OH	-	-	-	-OH	-	-	12.5
Isorhamnetin	-OH	-OH	-	-OH	-	-	-OMe	-OH	-	-	>200
Kaempferide	-OH	-OH	-	-OH	-	-	-	-OMe	-	-	>200
Luteolin	-	-OH	-	-OH	-	-	-OH	-OH	-	-	17.7
Myricetin	-OH	-OH	-	-OH	-	-	-OH	-OH	-OH	-	141
Nobiletin	-	-OMe	-OMe	-OMe	-OMe	-	-OMe	-OMe	-	-	>200
Primuletin	-	-OH	-	-	-	-	-	-	-	-	>200
Quercetagetin	-OH	-OH	-OH	-OH	-	-	-OH	-OH	-	-	100
Quercetin	-OH	-OH	-	-OH	-	-	-OH	-OH	-	-	25
Rhamnazin	-OH	-OH	-	-OMe	-	-	-OMe	-OH	-	-	>200
Tamarixetin	-OH	-OH	-	-OH	-	-	-OH	-OMe	-	-	8.8
Tangeretin	-	-OMe	-OMe	-OMe	-OMe	-	-	-OMe	-	-	>200
TMOS	-	-OMe	-OMe	-OMe	-	-	-	-OMe	-	-	17.7
Tricetin	-	-OH	-	-OH	-	-	-OH	-OH	-OH	-	50
Wogonin	-	-OH	-	-OH	-OMe	-	-	-	-	-	>200

MICs were measured as MIC_{10} after 24 hours using the microbroth dilution method in LB media grown at 30°C. MICs were conducted in triplicate with all triplicates resulting in the shown values. Column header numbers indicate carbon backbone positions (see Figure 1.1A).

All flavones were assayed at 100µg mL^{-1}, except for Luteolin which was assayed at 25µg mL^{-1} due to solubility limitations and to keep the 0.5% DMSO solvent concentration consistent with all samples.

We measured DNA Gyrase activity by providing a relaxed plasmid substrate and measuring the relative amount of supercoiled plasmid product compared to the DNA gyrase and solvent control (Figure 1.2A, 0.5% DMSO). Lower relative amounts of supercoiled product correspond to a stronger inhibitory effect (Figure 1.2C). Ciprofloxacin was measured on a separate gel with control antibiotics and, as expected, treatment with ciprofloxacin resulted in no visible supercoiled DNA band (Figure 1.3). Among the flavones, treatment with Myricetin and Quercetin appeared to have the strongest inhibitory effect, with no detectable supercoiled product. Tetramethyl-O-Scutallerin (TMOS) and 3,3',4' Trihydroxyflavone (33'4'THF) had the least inhibitory effect on DNA Gyrase, with 100µg/mL only reducing supercoiled DNA amounts by two-fold (Figure 1.2B).

The Topo IV assay utilizes a supercoiled plasmid substrate that is processed into a relaxed product by active topoisomerase IV. Topo IV inhibitors reduce the accumulation of relaxed product, resulting in either the supercoiled plasmid substrate, or a linear DNA product that is accumulated by inhibitors that cause DNA cleavage.

We then quantified the relative amount of linear DNA that was produced on these gels when resolved on a gel containing ethidium bromide (Figure 1.2B, EtBr). Linear DNA results from inhibition of TopoIV subunit A after making a double-stranded break in the plasmid, as seen with subunit A inhibitors such as the quinolones. As expected, treatment with ciprofloxacin resulted in a strong linear DNA signal (Figure 1.2B, D). This assay showed that 3,7,4' Trihydroxyflavone (374'THF), 3-Hydroxy, 5,7,3',4' Tetramethoxyflavone (3H573'4'TMF), Apigenin, Fisetin, Myricetin, and Quercetin accumulated the most linear plasmid DNA, and were the strongest Topo IV inhibitors, while TMOS showed almost no inhibition of Topo IV (Figure 1.2C-D).

We then measured the ability of the flavones and flavonols to intercalate into DNA intercalation with the Topoisomerase IV assay based on the amount of supercoiled plasmid present when resolved on a gel without ethidium bromide. As shown with treatment with daunorubicin, DNA intercalation activity mimics samples where no topoisomerase has been added (Figure 1.3). We found Apigenin, Fisetin, Myricetin, Quercetin, and Tamarixetin to have a strong intercalative effect, with little to no intercalative activity found with the other flavones (Figure 1.2B No EtBr, Figure 1.2E).

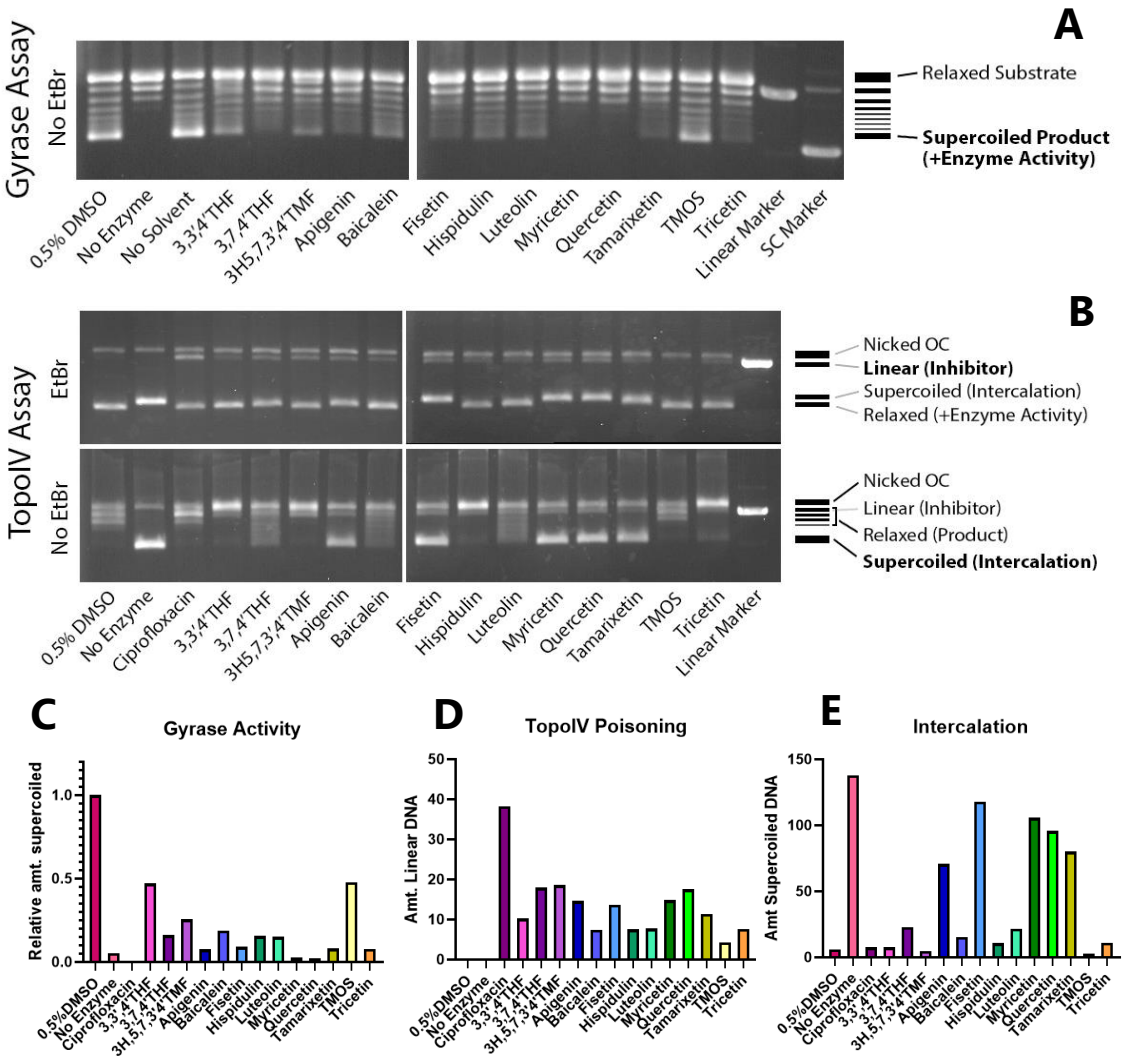

Figure 1.2. *in vitro a*nti-DNA replication assays. (A) Anti-Gyrase assay resolved on a non-EtBr 1% Agarose gel. (B) Anti-TopoIV assay resolved on 1% Agarose gel with and without 0.2µg mL^{-1} EtBr; flavones were tested at 100µgmL and Ciprofloxacin at 10µgmL for both assays with 0.5% DMSO solvent concentration. (C) Quantitation of gyrase activity when in presence of various flavones measured by intensity of supercoiled plasmid band; (D) Quantitation of Topo IV inhibition by various flavones measured by intensity of linear DNA band on EtBr gel; (E) Quantitation of intercalative activity of various flavones measured by intensity of supercoiled DNA band on the gel lacking EtBr.

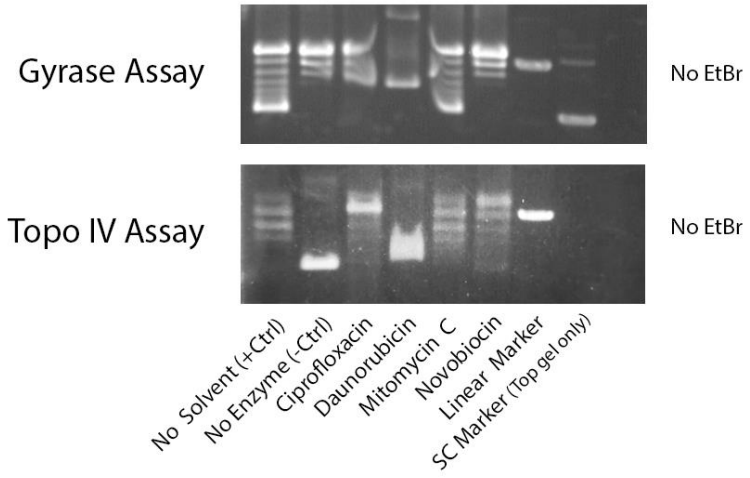

Figure 1.3. Gyrase and TopoIV assay antibiotic controls. Antibiotics were added at 10µg mL^{-1}. No Enzyme ctrl contains 0.5% DMSO solvent. Both assays resolved on a 1% Agarose gel without Ethidum Bromide.

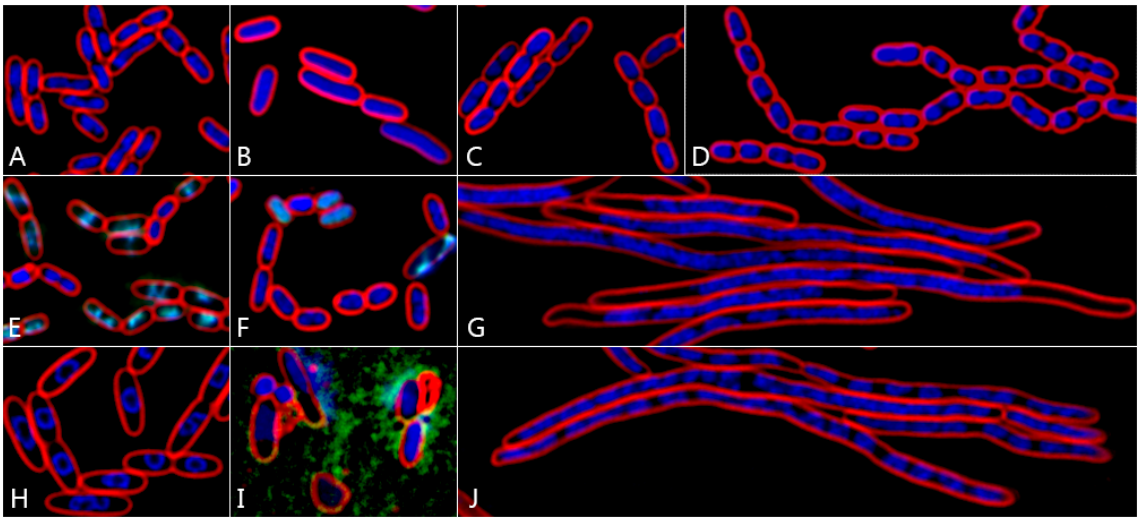

Figure 1.4. Bacterial cytological profiling of control antibiotics after 2 hours of treatment. (A) untreated cells; (B) Rifampicin; (C) Cerulenin; (D) CHIR-0900; (E) Triton-X; (F) Polymyxin B; (G) Ciprofloxacin; (H) Chloramphenicol; (I) D-Cycloserine; (J) Ampicillin. Cell membranes stained with FM4-64 (red); DNA with DAPI (Blue); and cell permeability indicated by SYTOX Green (green).

Overall, with the notable exceptions of TMOS and to a lesser extent 33'4'THF, the flavones demonstrated various combinations of inhibition of DNA gyrase and Topoisomerase IV, and/or direct intercalation into the DNA. These results agree well with the previous research of other groups, which have shown that flavones have both intercalative[7, 19] and anti-topoisomerase[7, 20] activities. However, our following results indicate that while some of these flavones and flavonols exhibit inhibition of these enzymes required for DNA segregation and replication in in living cells, many exhibit different primary antibiotic mechanisms of action in vivo.

Bacterial Cytological Profiling of control antibiotics against E. coli ΔtolC

Bacterial Cytological Profiling (BCP) has been previously developed for many bacteria, where it provides rapid insight into the in vivo mechanism of action[24-26], which can differ from the mechanisms that are observed in vitro[24].For molecules with very high MICs such as the flavones and other flavonoids, BCP often uses sensitized strains, such as the *imp* mutant strain of E. coli[25], which has defects in the *imp* gene involved in outer membrane biogenesis. For these studies we decided to switch to strains lacking the TolC protein that is required for antibiotic efflux, to avoid potential synergistic effects with the *imp* strain, which necessitated the creation of a control compound training set for E. coli

ΔtolC. We performed BCP of 32 antibiotics (Figure 1.4, Table 1.2) with known mechanisms of action against ΔtolC, broadly classifying the antibiotics into the categories of translation, transcription, DNA replication, lipid synthesis, outer membrane synthesis, nucleotide synthesis, cell wall synthesis, and cell division inhibitors, as well as membrane-active and detergent-like activities (Table 1.2). Exponentially growing cells were treated with control antibiotics for 2 hours, then stained with FM4-64, a membrane dye; DAPI, a membrane-permeable DNA dye; and SYTOX-Green, a membrane-impermeable DNA dye that will only stain cells whose membrane integrity has been compromised[25].

We found that many of the phenotypes seen in the imp strain are identical or similar to those in the ΔtolC strain: transcription inhibitors cause slightly larger cells with decondensed DNA (Figure 1.4B); DNA replication and segregation inhibitors cause elongated cells with a single central, mis-located, or absent chromosome (Figure 1.4G), translation inhibitors cause toroidal DNA due to the lack of structural proteins (Figure 1.4H), cell division inhibitors cause elongated cells with many chromosomes spread throughout the cell or rounded cells with lysis (Figure 1.4I-J), and surfactants and membrane active compounds cause the cell to become permeable to SYTOX-Green, appearing as cyan when merged with the

Table 1.2. Control antibiotics analyzed using BCP to create a reference compound database, associated cellular targets, and MIC_{10} values at 24 hours observed via microbroth dilution in LB.

Antibiotic	Cellular Pathway Targeted	MIC (ΔtolC, μg/mL)	xMIC for microscopy
Adriamycin	DNA intercalation	1.3021	2
Amikacin	Protein synthesis	1.1563	2
Amoxicillin	Cell wall biosynthesis (1)	3.9583	0.5
Bactobolin	Protein synthesis	2.3438	0.5
CCCP	Membrane active	1.00	2
Cefoxitin	Cell wall biosynthesis (1)	1.9531	10
Ceftazidime	Cell wall biosynthesis (1)	0.5625	0.5
Cerulenin	Lipid biosynthesis	3.125	10
Chloramphenicol	Protein synthesis	0.8464	5
Ciprofloxacin	DNA replication	0.0025	1
Clindamycin	Protein synthesis	5.9896	5
Doxycycline	Protein synthesis	0.1842	5
Epirubicin	DNA replication	1.3073	2
Erythromycin	Protein synthesis	2.5	5
Gentamicin	Protein synthesis	1.1719	2
Imipenem	Cell wall biosynthesis (2)	0.3-0.4	0.3 μg/mL (~1x)
Kanamycin	Protein synthesis	1.9792	2
Levofloxacin	DNA replication	0.0057	1
Mecillinam	Cell wall biosynthesis (2)	0.0438	2
Meropenem	Cell wall biosynthesis (2)	0.0292	0.8
Mitomycin C	DNA crosslinking	0.625	0.5
Mupirocin	Protein synthesis	0.25	2
Penicillin V	Cell wall biosynthesis (1)	13.021	0.5
Polymyxin B	Outer membrane active	0.2214	2
Puromycin	Protein synthesis	2.8646	5
Rifampicin	RNA synthesis	7.5521	2
SDS	Detergent	17.708	5
Streptonigrin	DNA replication	0.2031	0.5
Tetracycline	Protein synthesis	0.3646	5
Triclosan	Lipid biosynthesis	0.0146	5
Trimethoprim	Nucleotide synthesis	0.28125	2
Triton X-100	Detergent	0.0146 (MIC in %)	10

DAPI channel (Figure 1.4E-F)[25]. Thus, many BCP phenotypes were consistent between the ΔtolC and imp strains.

However, we found that there were several key differences in the BCP phenotypes of the ΔtolC and imp strains after treatment with molecules that inhibit lipid and outer membrane biogenesis. For example, treatment with triclosan and cerulenin reproducibly produced chains of three small, unevenly sized cells in the imp strain, but produced chains of four evenly-sized cells in ΔtolC (Figure 1.4C). Additionally, the outer membrane inhibitor CHIR-090, which was not tested in the imp mutant database, resulted in long chains of from eight to sixteen cells in ΔtolC, caused by the inability for the cells to septate fully due to the decoupling of outer and inner membrane synthesis (Figure 1.4D)[28]. The differences in these membrane-associated phenotypes is likely due to the different mechanisms by which the imp and tolC strains are sensitized to antibiotics, which the imp strain showing defects in outer membrane assembly, and the tolC strain more precisely defective in the efflux of antibiotics.

Bacterial Cytological Profiling of bioactive flavones

We then performed BCP on the thirteen flavones (Figure 1.5A-B) at various concentrations ranging from slightly above (2X) or slightly below (0.5X) their MIC (Table 1.1). Remarkably, among the thirteen compounds

tested, we found at least four distinct antibiotic mechanisms of action. First, as expected based on previous publications[7, 14, 21, 27] and our in vitro data, 3,7,4'THF, Apigenin, Fisetin, Hispidulin, and Quercetin exhibited clear phenotypes associated with the inhibition of DNA replication and segregation, with centrally-located chromosomes inside of elongated cells similar to ciprofloxacin (Figure 1.5A). Second, Tetramethyl-O-Scutallerin (TMOS) and 3H573'4'TMF inhibited outer membrane synthesis, with long chains of eight or more cells (Figure 1.5B) similar to treatment with the LpxC inhibitor CHIR-090[28] (Figure 1.4D). Third, Tamarixetin and Tricetin inhibited cell septation, with elongated cells with multiple chromosomes spread throughout the cell. Fourth, several compounds (myricetin, baicalein) were primarily membrane-active. Myricetin showed FM4-64 staining intensity that was twice that of untreated cells, indicating that the molecule was able to permeabilize the outer membrane, whereas baicalein permeabilized the cells to SYTOX-Green. Finally, two flavones exhibited unknown, novel, or possible combinatorial antibiotic mechanisms of action. 3,3',4'THF treatment resulted in chains of four cells but was morphologically distinct from treatment with the known lipid synthesis inhibitors Triclosan and Cerulenin (Figure 1.4C). Treatment with luteolin resulted in a curled-cell shape with one or two compacted nucleoids, which we have never observed with this strain in response to

treatment with any antibiotic. Thus, the flavones appear to kill cells via an array of distinct mechanisms. While some molecules that strongly inhibit DNA gyrase in vitro showed a BCP phenotype consistent with a DNA segregation/replication defect, others did not. For example, Tamarixetin showed 90% inhibition of DNA gyrase activity, but failed to show a DNA segregation phenotype, instead accumulating long multinucleate cells.

To further study the in vivo mechanism of action of these molecules, we attempted to isolate resistant mutants for some of the molecules that had novel phenotypes: TMOS, Tamarixetin, and Luteolin. Isolating resistant mutants proved challenging for all of these molecules, and required that we resort to serial passaging of the strains in medium with concentrations slightly above the MIC. We were unable to isolate mutants with a significant (more than 2-fold greater than ΔtolC E. coli) level of resistance for Tamarixetin and Luteolin, but succeeded in isolating and characterizing mutants resistant to TMOS.

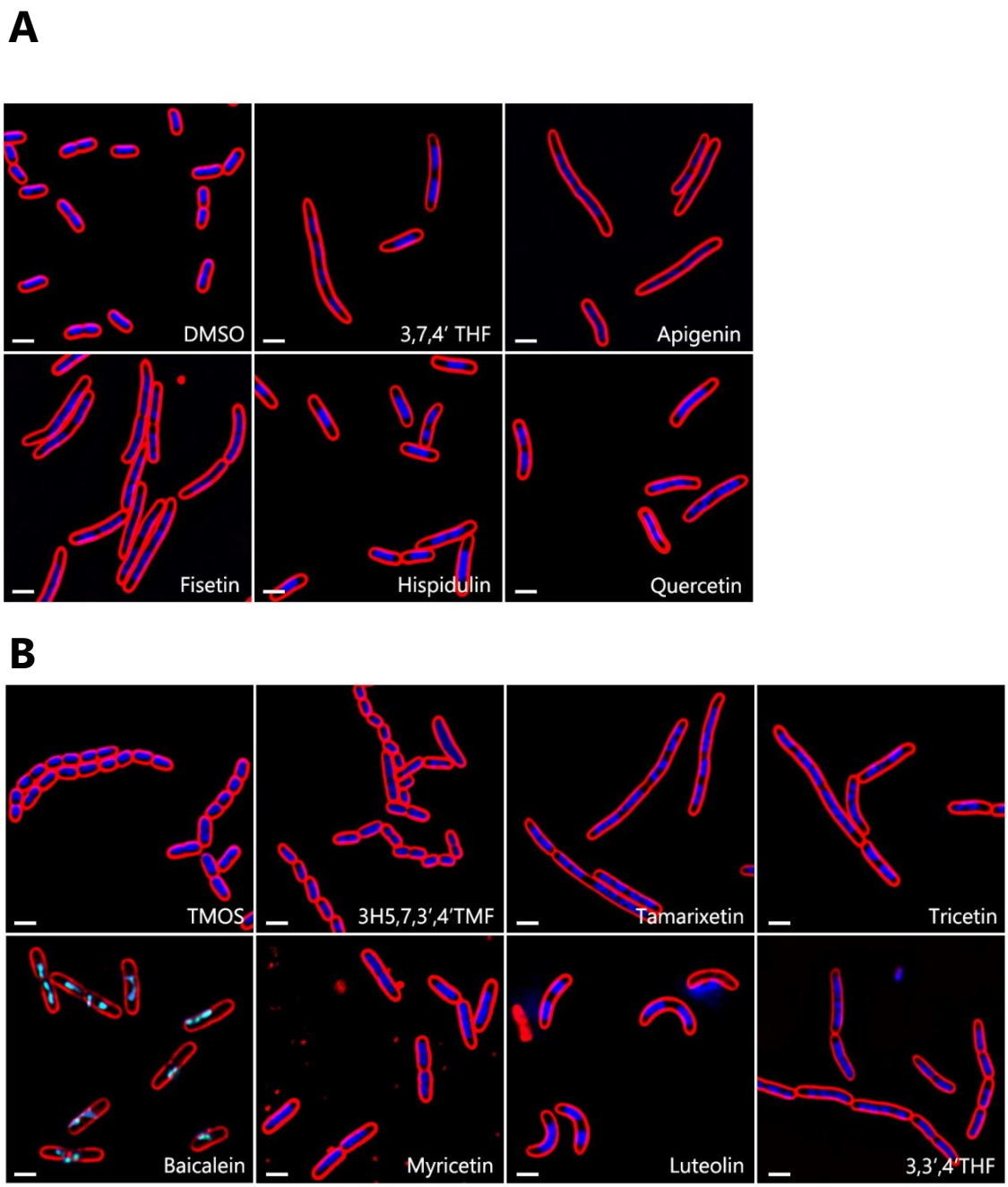

Figure 1.5. BCP profiles of antibiotic flavones. (A) Solvent control and flavones with an anti-DNA replication phenotype. (B) Flavones that exhibit non-anti-DNA replication phenotypes. Cells were imaged at 2 hours of treatment with 0.5X to 2X MIC. Scale bars represent 2μm. Red: FM4-64. Blue: DAPI. Green: SYTOX Green.

Tetramethyl-O-Scutallerin (TMOS) inhibits outer membrane (LPS) biosynthesis

The BCP results suggest that TMOS inhibits outer membrane biosynthesis, as it produces chains of eight or more cells after two hours of treatment, similar to the known LpxC inhibitor CHIR-090 (Figure 1.6A-C). To confirm this result and gain more insight into the cellular target of TMOS, we generated mutants of E. coli ΔtolC that were resistant to TMOS after serial passaging (as described in the Materials and Methods). We isolated three strains that originated from separate colonies of E. coli ΔtolC showed a >4-fold increase in the MIC of TMOS, and subjected the strains to whole genome sequencing. All three strains had different mutations in the fabZ gene (Table 1.3), which is involved in phospholipid synthesis[29-31]. Mutations in fabZ are known to suppress antibiotics that target the Lpx pathway[29, 30], so we tested additional strains with mutations in lpxA and accB originally identified by generating mutations resistant to other outer-membrane compounds (described in Materials and Methods) against TMOS (Table 1.4) and CHIR-090 (Table 1.5). We found that while fabZ mutations were able to confer resistance to both TMOS and CHIR-090, lpxA and accB mutations were only able to confer significant (>2-fold) resistance to TMOS. These results indicate that while it is likely that TMOS inhibits the Lpx pathway, it likely does not inhibit LpxC specifically, as

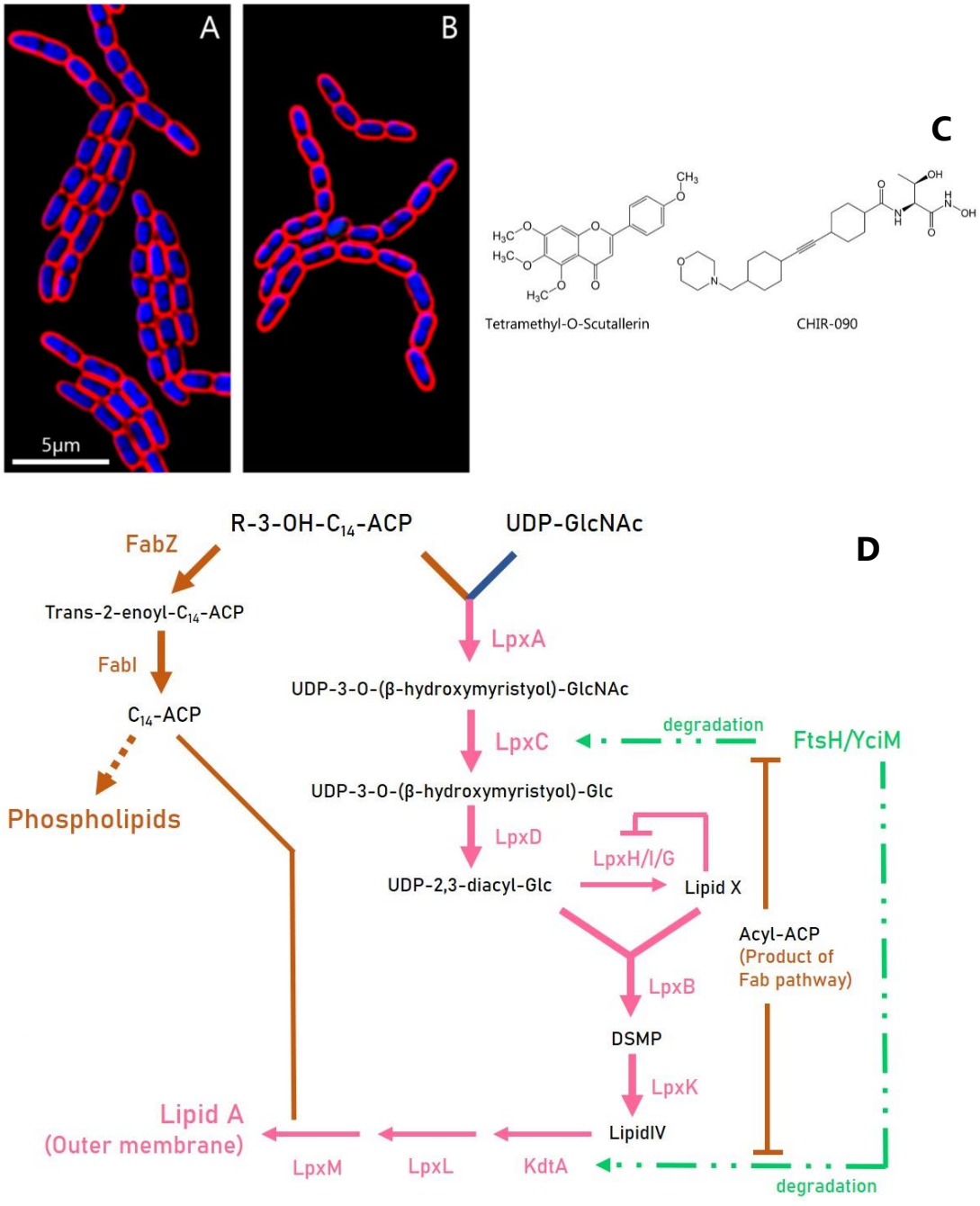

Figure 1.6. Bacterial Cytological Profile of TMOS (A) and CHIR-090 (B). (C) Chemical structures of TMOS and CHIR-090. (D) LPS biosynthesis pathway of *E. coli*(adapted from Zhou et al 2017).

Table 1.3. TMOS Resistant mutants generated via serial passaging from three separate colonies of the parent strain AD3644.

Strain	Gene	Mutation & Effect
ATJ029	*fabZ*	C64A: Phe22Thr
ATJ030	*fabZ*	C206T: Ala69Val
	ydaC	Nucleotides 34-51 deleted: 6 amino acids (LSGLLL) deleted, in frame
ATJ031	*fabZ*	G165C: Phe55Leu
	motB	G176A: Ala58Ala (silent)
	Between *rrlA* rRNA and *alaT* tRNA	2742600: TTGCGATCCATCATCGT-> ACTTCAGA, unknown effect
	yqgD	Base 129 (T) deleted - premature termination

Strain genomes were sequenced via Illumina sequencing, and compared to the AD3644 genome using Geneious. Mutations in the above table reflect all deviations from AD3644 found in each strain.

Table 1.4. Mutations in genes related to outer membrane and fatty acid biosynthesis confer resistance to TMOS.

Strain	Genotype	Fold change in TMOS MIC vs. *ΔtolC*
ATJ029	*fabZ* Phe22Thr	>4x
ATJ030	*fabZ* Ala69Val*	4x
ATJ031	*fabZ* Phe55Leu*	>4x
PTM21	*accB* Gly133Ala	2.8x
PTM23	*accB* Asp149Tyr	2.8x
PTM28	*lpxA* Arg100Pro	4x
PTM30	*lpxA* Val159Phe	4x
PTM31	*lpxA* Gly196Cys	1.4x
PTM34	*accB* Cys116Tyr	2x
PTM35	*accB* -16 A>T	2x
AD3644	WT *ΔtolC*	1x (17.7-25µg/mL)

* represents strains with mutations elsewhere in additional genes (see Table 1.3). WT MIC was considered as 17.7µg/mL for purposes of fold calculations. >4x represents resistance at the limit of solubility of TMOS (~70µg/mL)

Table 1.5. Efficacy of CHIR-090 against strains resistant to TMOS as compared to AD3644.

Strain	Genotype	Fold change in CHIR-090 MIC vs. *ΔtolC*
ATJ029	*fabZ* Phe22Thr	5.6x
ATJ030	*fabZ* Ala69Val*	5.6x
PTM28	*lpxA* Arg100Pro	1x
PTM30	*lpxA* Val159Phe	1x
PTM23	*accB* Asp149Tyr	1x
PTM34	*accB* Cys116Tyr	1x
AD3644	WT *ΔtolC*	1x (0.016μg/mL)

Table 1.6. Resistance of *fabZ* mutant strains with WT *fabZ* locus transduced via P1 phage as compared to AD3644.

Strain	*fabZ* locus	Fold change in TMOS MIC vs. *ΔtolC*
ATJ029-2	WT	2x
ATJ029-4	WT	1x
ATJ030-1	Ala69Val	4x
ATJ030-4	WT	1x
ATJ031-1	WT	1x
ATJ031-2	WT	1x
ATJ031-3	WT	1x
ATJ031-4	Phe55Leu	4x
ATJ031-5	WT	1x
AD3644	WT	1x (17.7-25μg/mL)

mutations in LpxA, the enzyme directly upstream of LpxC in the lipopolysaccharide synthesis pathway (Figure 1.6D), do not confer resistance to CHIR-090, an LpxC inhibitor. While previous groups have documented flavonoid interactions with the FabZ protein in vitro and in silico[23, 31, 32], we do not believe that the FabZ is the in vivo target of TMOS, as the specific morphological phenotype of four-chained cells resulting from inhibition of the Fab proteins (Figure 1.4C) is distinct from the phenotype of eight- to sixteen-chained cells resulting from specific outer membrane biosynthesis inhibition Figure 1.4D).

FtsZ-GFP studies reveal that tamarixetin primarily inhibits cell septation

While tamarixetin exhibited strong in vitro anti-topoisomerase and DNA intercalation activity (Figure 1.2C-E), the cellular morphologies resulting from tamarixetin treatment (Figure 1.5B) did not match those of other molecules that inhibit DNA replication or segregation (Figure 1.5A; 1.4G). Rather, cells treated with tamarixetin were elongated, contained multiple chromosomes, and were occasionally pinched at septation sites, reminiscent of molecules that inhibit peptidoglycan biosynthesis and cell division such as Cephalexin, which inhibits FtsI (Figure 1.7A)[33]. Furthermore, while we were unable to generate any mutants that conferred more than a 2-fold increase in resistance to tamarixetin, we

isolated a strain with a reproducible, 1.5-fold increased resistance that contained a mutation in ftsA. In order to determine whether tamarixetin indeed affected cell septation, we transduced a chromosomally-integrated, IPTG-inducible GFP-tagged FtsZ (FtsZ-GFP) into E. coli ΔtolC (ERL100) at the lamda attachment site (att^{lambda})[34]. We induced FtsZ-GFP with 30 μM of IPTG one hour before antibiotic treatment, allowing for the visualization of Z-ring formation and dynamics. Induced but untreated cells did not exhibit any significant morphological defects at either timepoint corresponding to those of treated cells (1.5 and 3 hours of induction). (Figure 1.7B).

We treated the FtsZ-GFP strain with either tamarixetin, apigenin (flavone gyrase/intercalator control), cephalexin (FtsI inhibitor), or daunorubicin (DNA intercalator) at 0.25X, 0.5X, 1X, and 2X MIC and observed cellular morphology, septation status, and Z-ring formation and location. We then classified and counted cells under each treatment as belonging to the five following categories: multiple Z-rings, 1 Z-ring with constriction, 1 Z-ring without constriction, No Z-ring with a central chromosome, and No Z-ring with separate chromosomes (Figure 1.7C, D). We found that after 30 minutes of treatment with tamarixetin and cephalexin cells had properly formed Z-rings between chromosomes that had properly replicated, but fewer cells were undergoing active septation

than compared to control cells. This effect was dose-dependent, with 2X-MIC treatment of cephalexin and tamarixetin resulting in almost no (<5%) cells with active septation compared to the controls (31%) and cells treated below the MIC (Figure 1.7E). No clear dose dependency on the population of cells with 1 Z-ring undergoing constriction was found in the apigenin or Daunorubicin-treated samples. On the contrary, cell treated with daunorubicin had centrally-located chromosomes hallmark of DNA replication inhibitors[25], resulting in a significant proportion (42-69%) of cells that were completely unable to correctly assemble a Z-ring (Figure 1.7F). Cells treated with apigenin exhibited a dose-dependent response similar to daunorubicin, with increasing concentrations of apigenin causing higher proportions of cells without an assembled Z-ring (4-30%) due to the centrally located chromosome. At 2 hours, all cells appeared elongated, but tamarixetin and cephalexin-treated cells had multiple chromosomes along the length of the cell punctuated by many properly-assembled or spiral-shaped Z-rings, while daunorubicin-treated cells contained a single large chromosome, often flanked by two Z-rings (Fig 1.7A).

Figure 1.7 (Opposite page): Fluorescence microscopy of GFP-FtsZ-tagged *E. coli* under treatment with DMSO, Tamarixetin, Cloxacillin/Tazobactam, or Daunorubicin at 30 minute and 2 hours of treatment. Cells were induced for expression of FtsZ-GFP with 30μM IPTG 1 hour before addition of antibiotic. Red: FM4-64. Blue: DAPI. Green: SYTOX Green. Treatments were conducted at 1x MIC (see Tables 1.1 and 1.2).

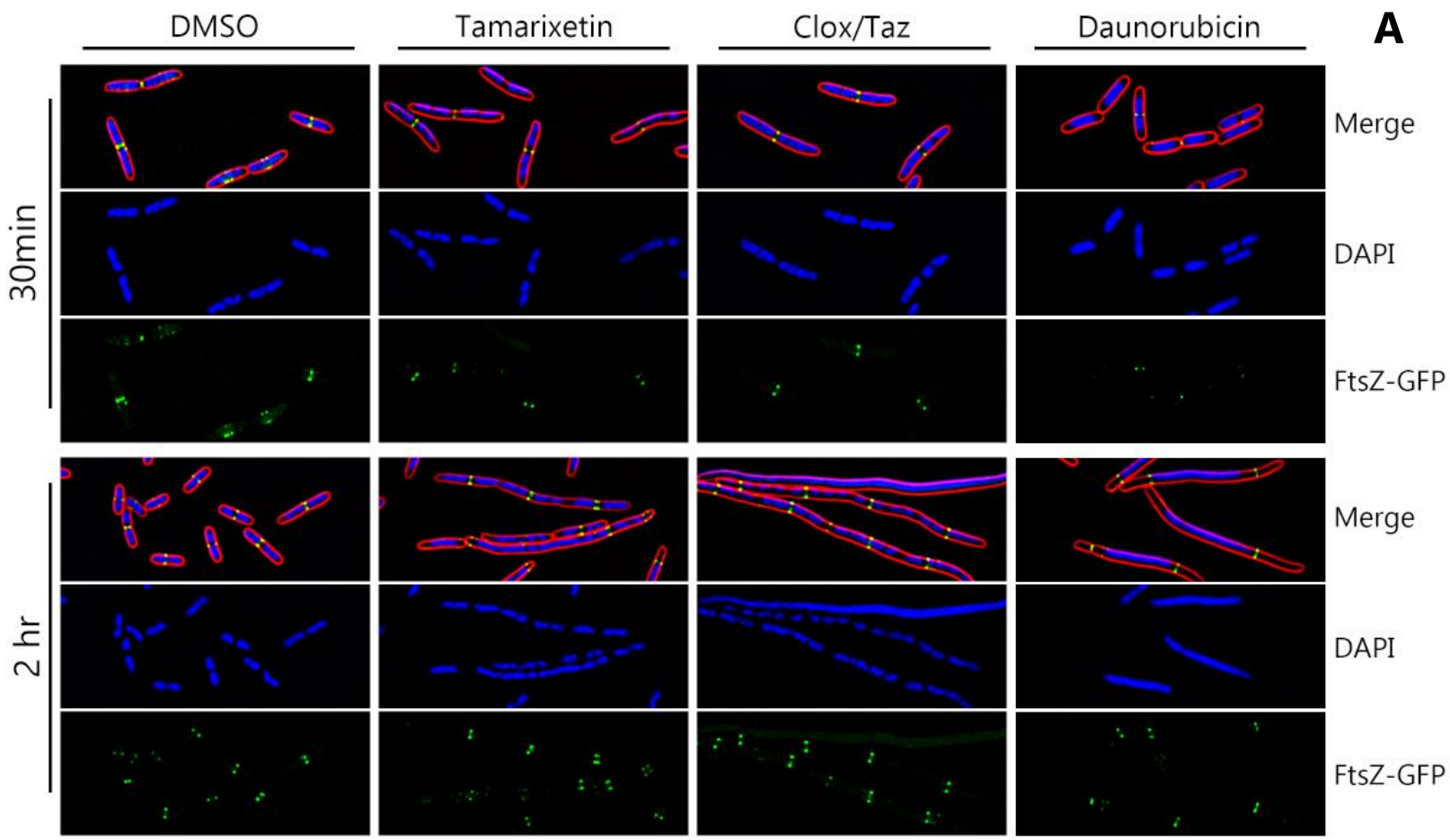
DMSO
Tamarixetin
Clox/Taz
Daunorubicin
A
30min
2 hr
Merge
DAPI
FtsZ-GFP
Merge
DAPI
FtsZ-GFP

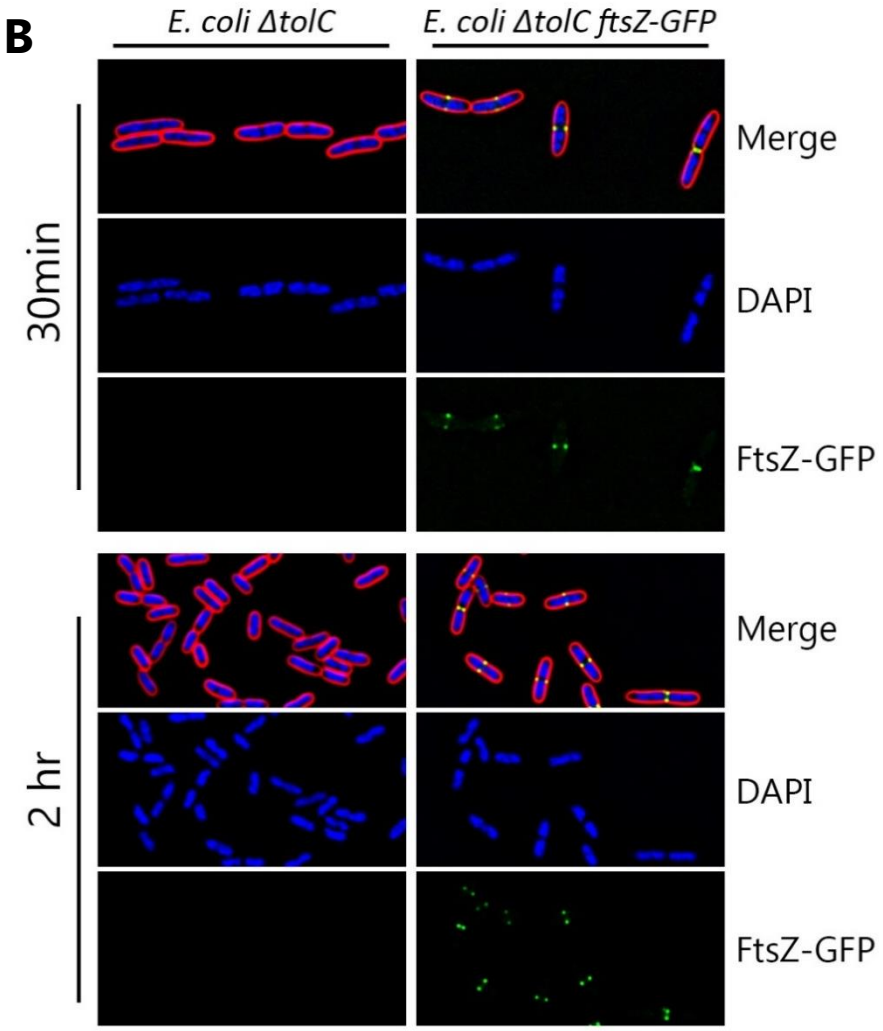

Figure 1.7 (continued) . Induction of GFP-tagged FtsZ does not incur significant morphological defects. AD3644 (left) and ERL100 (right) cells were induced with 30μM IPTG 1 hour before "T0" to mimic antibiotic treatment timeline. Red: FM4-64. Blue: DAPI. Green: SYTOX Green.

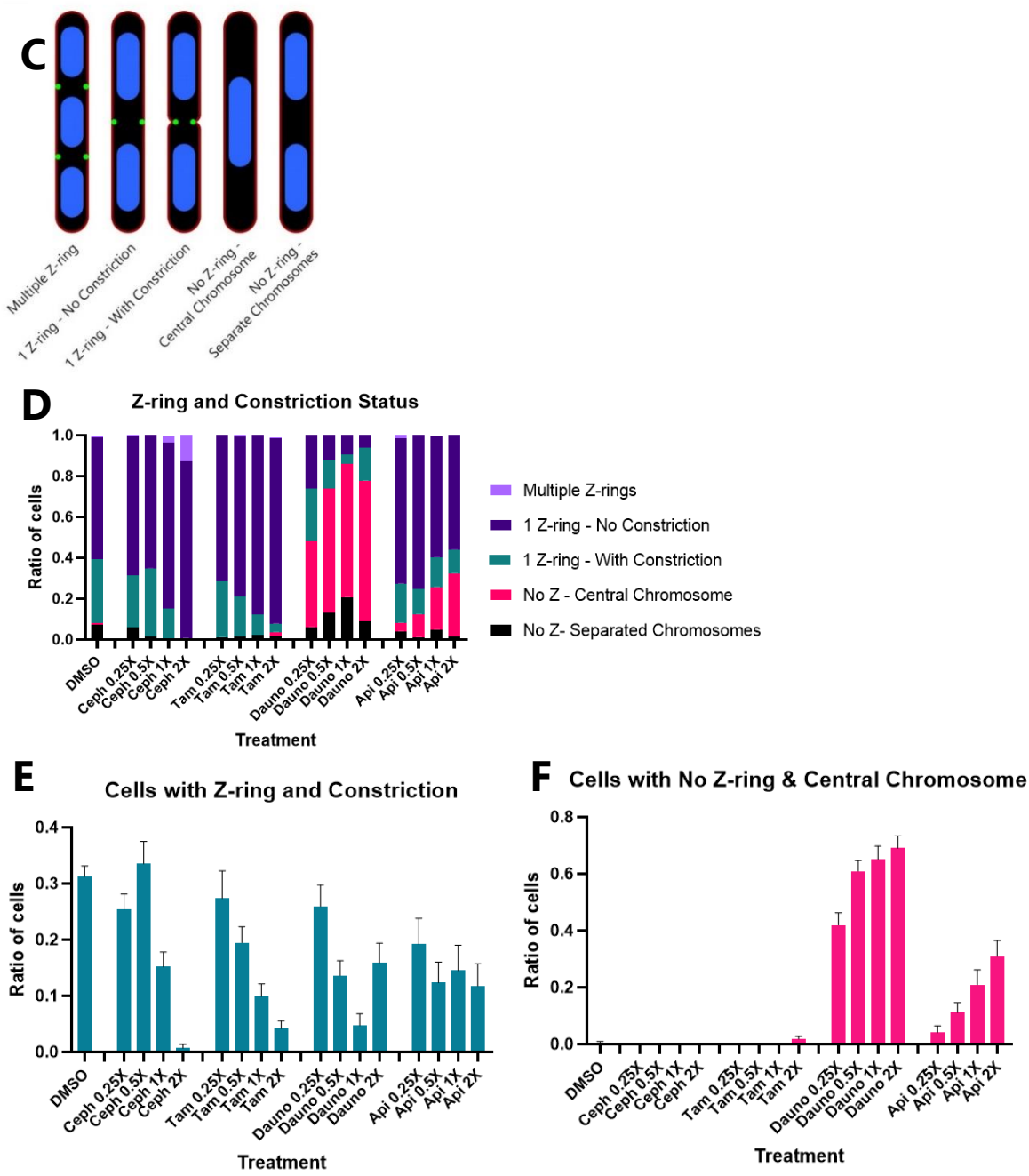

Figure 1.7 (continued). Quantification of cell septation status with and without treatment with various concentrations of antibiotics and flavones. (B) Classification of septation statuses. (C) Overall population of cell septation status in response to antibiotic treatment. (D) Ratio of cells actively constricting for each treatment. (E) Ratio of cells without a properly formed Z-ring and central chromosome.

Luteolin impacts cell shape by an unknown, potentially novel mechanism.

We found that treatment with concentrations near the MIC (17.7µg/mL) of Luteolin resulted in a significant portion of curled cells (Figure 1.5B). This effect was dose-specific, centered around the MIC (16-20 µg/mL), as treatment with lower concentrations resulted in straight, longer cells, and treatment with higher concentrations resulted in straight, slightly elongated cells with compacted DNA typical of DNA replication inhibitors (Figure 1.8A). The curvature of cells was determined by measuring the angle (θ) between lines drawn orthogonal to each pole (Figure 1.8D) for cells treated with varying concentrations of Luteolin. Angle of curvature was defined as 180- θ, such that a completely straight cell (θ = 180) would be defined as having 0 curvature. Only cells that had at least one pole not in contact with another cell were quantified, to avoid curvature due to spatial restrictions on growth. Treatment with 20µg/mL of Luteolin resulted in the highest average curvature of cells (54.8°), compared to the average curvature of 7.1° for untreated cells (Figure 1.8B). We defined "curled" cells as cells that had an angle of curvature greater than three standard deviations from the mean of untreated cells (>22.7°). 82.2% of cells were curled in the 20µg/mL treatment (Figure 1.8C). Cells treated with 16µg/mL of Luteolin also displayed significant curvature and proportions of curved

Figure 1.8 (Opposite page): Characterization of cell curvature resulting from treatment with Luteolin. A) Fluorescence microscopy of *E. coli* Δ*tolC* cells treated with increasing concentrations of Luteolin. B) Single-cell quantification of cell curvature with increasing concentrations of Luteolin. Red lines indicate average values. C) Proportion of cells with an angle of curvature significantly higher (>3 standard deviations) than control cells. Error bars denote SEM. D) Schematic of how angle of curvature of cells is quantified. ***: P≤0.001; ****: P≤0.0001. Scale bars represent 2μm.

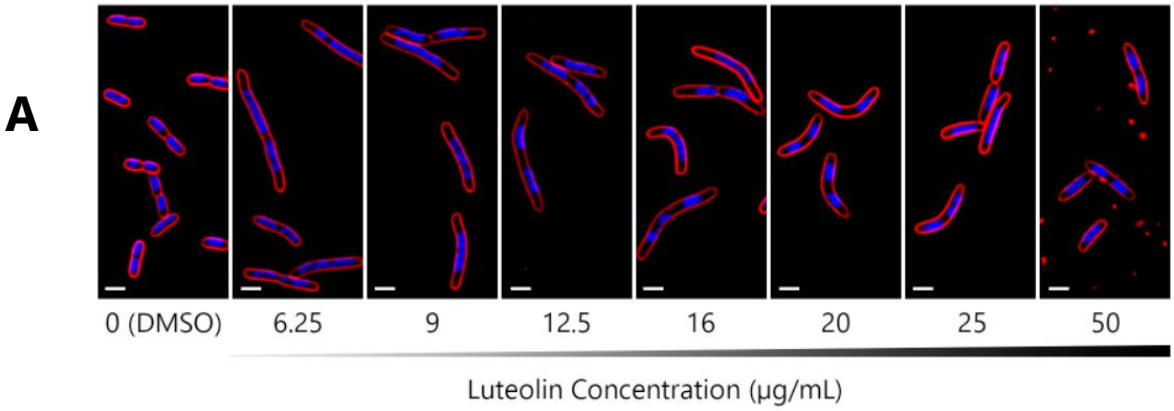

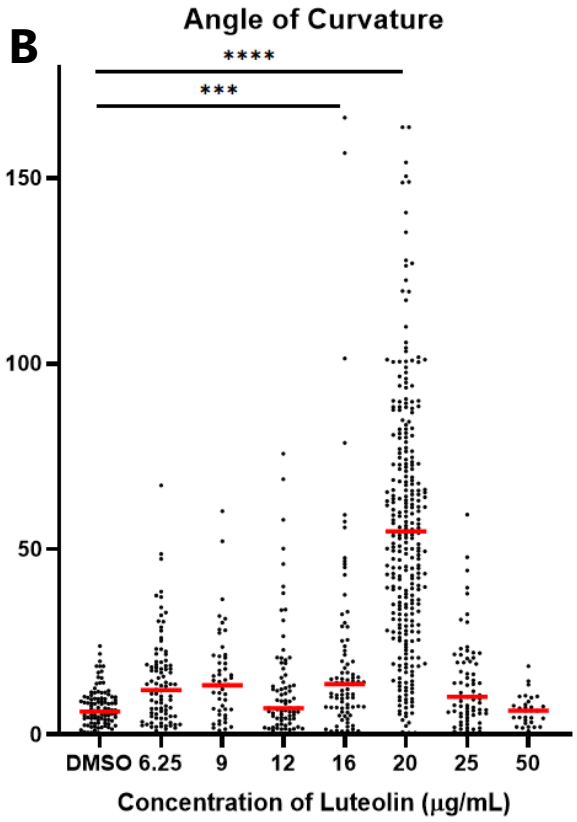

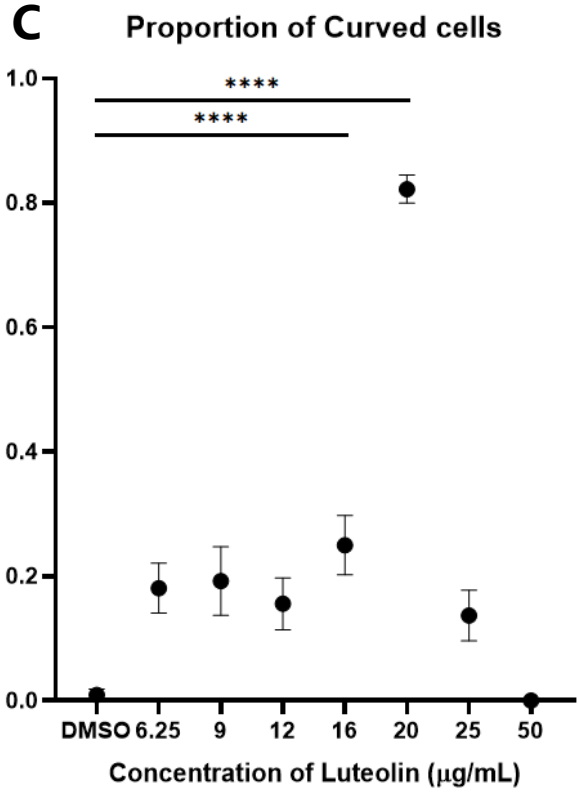

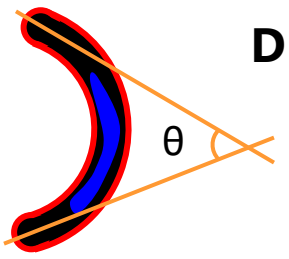

Angle of Curvature = 180-θ

cells, although to a lesser extent than cells treated with 20µg/mL of Luteolin.

The mechanism by which Luteolin causes curvature of cells is still unknown. None of the 32 control antibiotics spanning the major antibiotic MOAs (DNA replication, cell wall biosynthesis, lipid biosynthesis, outer membrane biosynthesis, protein synthesis, RNA synthesis, membrane active, and surfactant) tested to generate the cytological profile database result in curled cells. Multiple series of mutant generation by serial passaging over several months were unable to generate mutants resistant to more than 1.25X MIC. All of the resistant mutants had multiple indels in a variety of genes. While 4 of the 6 mutants did have frameshift mutations likely causing LOF in eda, biochemical studies with Eda did not reveal any interaction with Luteolin, indicating it is likely not being converted by Eda into a toxic product. The high frequency of indels in these mutants may suggest that Luteolin may cause DNA damage that is subsequently repaired by DNA repair mechanisms such as NER, which can repair damage caused by DNA intercalators but can result in the accumulation of indels. However, molecules that cause DNA damage such as DNA intercalators (daunorubicin) and crosslinkers (mitomycin C) do not result in curled cells (REF mike paper); thus, this activity alone cannot explain the BCP phenotype resulting from treatment with Luteolin.

Additionally, it is possible that Luteolin interferes with cell shape determining proteins such as MreB to mimic the effects of proteins like crescentin, or affects cell wall biosynthesis in an asymmetric fashion. As morphological responses such as compacted DNA indicative of DNA replication or segregation inhibition are clearly visible with Luteolin treatment, the curled-cell phenotype may also be an effect of Luteolin exhibiting a combination of antibiotic MOAs. These multiple MOAs could possibly be elucidated by performing combinatorial screens of antibiotics with different MOAs with BCP[26].

Synergy and Efficacy of Flavone Cocktails

An ecological impact of the varied antibiotic MOAs of flavones resides in the diverse profile of specialized metabolites produced by plants upon pathogen challenge[9, 10, 13]. Theoretically, production of a panel of molecules that target different cellular pathways would guard against the evolution of bacterial mutations that grant resistance to antibiotics with a single mechanism of action, as other molecules would remain effective against the mutant bacteria. In other words, plants may employ a "shotgun" approach to pathogen defense reminiscent of combination therapy used in clinics for multidrug-resistant infections[35],

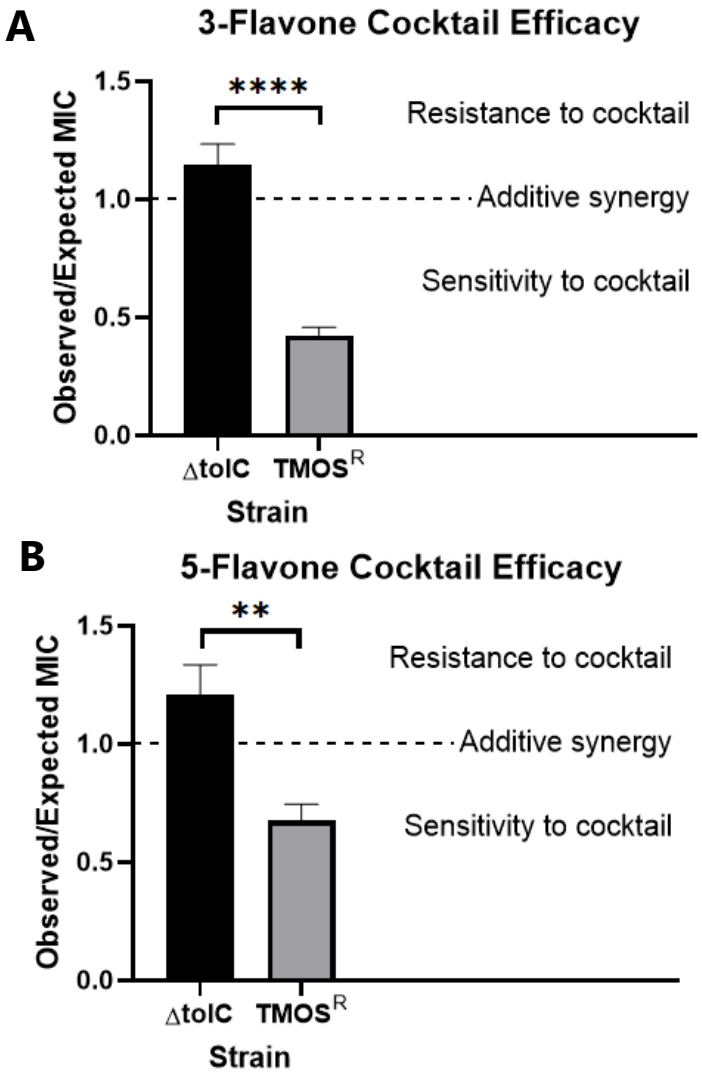

Figure 1.9: Efficacy of flavone cocktails against the parent Δ*tolC* strain and the TMOS-resistant strain ATJ029. A) Observed/Expected MIC of the 3-flavone cocktail. B) Observed/Expected MIC of the 5-flavone cocktail. Expected MIC defined as the MIC if flavones in cocktail exhibit additive synergy. **: P≤0.01. ****: P≤0.0001.

Table 1.7. Flavone cocktail efficacy.

A

3-Flavone Cocktail	MIC (μg/mL)
Apigenin	8.8
Tamarixetin	8.8
TMOS	17.6

B

5-Flavone Cocktail	MIC (μg/mL)
Apigenin	8.8
Tamarixetin	8.8
TMOS	17.6
Luteolin	17.6
3,3',4'THF	12.5

C

Cocktail	ΔtolC MIC	Expected ΔtolC MIC	$TMOS^R$ MIC	Expected $TMOS^R$ MIC
3-Flavone	0.38 ± 0.066	0.33	0.21 ± 0.037	0.5
5-Flavone	0.25 ± 0.059	0.21	0.18 ± 0.041	0.26

A). MIC's of flavones in the 3-flavone cocktail (all flavones at 1x MIC in a 1x cocktail concentration). B) MIC's of flavones in the 5-flavone cocktail (all flavones at 1xMIC in a 1x cocktail concentration, except Luteolin at 0.75x MIC due to solubility constraints). C) MIC's of flavone cocktails against the parent Δ*tolC* strain and the TMOS-resistant strain ATJ029 (designated $TMOS^R$ here). "Expected" values calculated as the next-highest dilution in the dilution series tested compared to calculated additive flavone synergy.

with high-level production of many structurally related molecules with different antibiotic MOAs that may not have extremely potent individual efficacy. This contrasts with more complex microbial antibiotic biosynthesis pathways which require large energy investments to produce a single, highly potent antibiotic[36].

After pathogen challenge, plants often produce an array of secondary metabolites that can include distinct flavone molecules. This mixture of molecules could be beneficial if the antibiotics are synergistic or additive, since this would allow pathogen control with lower concentrations of metabolites. Producing related molecules with similar structures but a diverse array of cellular targets might also be beneficial, as it would make resistance less likely to occur. To test if the different flavones acted synergistically, we made flavone cocktails comprising either 3 or 5 flavones with varied MOAs. Flavones were mixed in equal-MIC ratios in order to balance the individual activities (Table 1.7A-B), except for Luteolin which was at .75x relative MIC due to solubility constraints. We first performed MIC assays on E. coli ΔtolC strain, using the 3- and 5-flavone cocktails. We found that flavones in both cocktails exhibited additive synergy against ΔtolC: as the observed MIC matched the expected MIC of approximately 0.33X for the 3-flavone cocktail (Figure 1.9A) and 0.21X

for the 5-flavone cocktail (not 0.2X due to the slightly lower relative concentration of Luteolin) (Figure 1.9B).

We next tested if a strain selected for resistance to TMOS (ATJ029: fabZ Phe22Thr, >4x resistance to TMOS, Table 1.3) showed altered resistance to either the individual flavones or the flavone cocktails. We next tested the flavone mixtures. Since ATJ029 is more than 4-fold resistant to TMOS, one of the constituents of both cocktails, we would expect the MIC to be increased from 0.33X as expected for additive synergy in ΔtolC to 0.5X for the 3-flavone cocktail, as it should still be sensitive to two of the flavones present in the cocktail; similarly, we expected an increase from 0.21X expected in ΔtolC to 0.26X for the 5-flavone cocktail. However, we were surprised to find that ATJ029 was in fact more sensitive to both cocktails compared to ΔtolC, despite being resistant to one of the components with the 3-flavone cocktail having an MIC of 0.21X, and the 5-flavone cocktail having an MIC of 0.18X (Figure 1.9A,B, Table 1.7C).

Overall, our discovery that a mutation that grants resistance to a single flavone does not provide a selective advantage to a mixture of flavones suggests an evolutionary or ecological benefit for plants to produce diverse libraries of chemical analogues in response to pathogen challenge by safeguarding against the evolution of resistance mechanisms.

1.4 Discussion

Standard drug discovery pipelines often involve screening large libraries of compounds for killing activity, determining the mechanism of action (MOA) of bioactive molecules often through in vitro (e.g., macromolecular assays) and in silico (e.g., docking) methods[1-3]. Once candidate molecules have been identified, modifications are made to the scaffold to attempt to improve the potency of the molecule, usually indicated by a reduction in the minimum inhibitory concentration (MIC) of the modified compounds[1, 37]. Modified compounds are assumed to have the same MOA as compounds with the same backbone, as has been exemplified with known families of antibiotics such as the penicillins and fluoroquinolones[37]. Additionally, in vivo determination of MOA by generation and sequencing of resistant mutations is often time- and resource-consuming, highlighting the importance and convenience of in vitro assays to confirm suspected MOA of modified molecules[1].

In our study, we find that minor modifications – hydroxylations and methoxylations – to the flavone and flavonol backbones can entirely change the primary cellular pathway affected, as opposed to simply altering potency levels. Crucial to this study is the use of the ΔtolC strain of E. coli[38], whose deletion in the tolC drug efflux pump allows us to study the internal effects of molecules without compromising the structural

integrity of the membrane. While the strain itself is not ecologically relevant, the internal environment in plants under duress can cause permeabilization of bacterial membranes, and certain flavones have been shown to inhibit bacterial drug efflux pumps[39], leading to synergistic activity of plant defense metabolites, allowing molecules that would normally be unable to enter bacterial cells to be effective. Equally crucial to this study is the employment of Bacterial Cytological Profiling as a rapid and, importantly, unbiased technique to determine the primary cellular pathway affected by antibiotic molecules[25]. In vitro and in silico assays require researchers to already have assumed a potential target, and studies are performed against the target. BCP is able to determine the antibiotic MOA by analyzing morphological changes to cells in response to treatment without prior assumptions of the MOA of the molecule. Furthermore, while there have been many recent advances in unbiased antibiotic target determination such as thermal proteome profiling[5, 40] or analyzing changes to protein levels or RNA expression in response to differential antibiotic treatment, BCP is still valuable due to its rapidity and the lack of expensive -omics-type protocols.

Using BCP, we found at least four distinct primary antibiotic MOAs among the thirteen flavones and flavonols tested: DNA replication inhibition (3,7,4'-Trihydoxyflavone, Apigenin, Fisetin, Hispidulin, Quercetin),

cell division inhibition (Tamarixetin and Tricetin), outer membrane synthesis inhibition (TMOS and 3H573'4'TMF), and direct membrane activity (Myrcitin and Baicalein). Additionally, we identified two flavones, Luteolin and 3,3'4'-Trihydroxyflavone, that appear to have either a novel or combinatorial effect that is yet to be elucidated. These results challenge the traditional understanding of structure-activity relationship (SAR), where molecules with identical backbone structures are often assumed to have the same or similar biological activities[6].

Furthermore, our in vitro E. coli DNA gyrase and topoisomerase IV assays indicate that these flavones, with the notable exception of TMOS, do inhibit DNA replication, either by inhibiting the topoisomerase subunits directly, intercalating within the DNA, or some combination of both. The in vitro activities of flavones against both bacterial and eukaryotic topoisomerases have been well-studied, and some flavones have been investigated in potential anti-cancer studies as a result. Our studies corroborate the fact that these molecules exhibit in vitro anti-topoisomerase activity; however, our in vivo studies show that for many of these molecules, anti-topoisomerase activity is not the primary antibiotic MOA against E. coli ΔtolC. For example, Tamarixetin shows both in vivo and in vitro DNA intercalation activity; however, its BCP profile suggests that 1x MIC, treatment with Tamarixetin mimics treatment with a cell

division inhibitor (0.75x MIC), coupled with a sub-lethal (0.25x MIC) treatment of a DNA intercalator. Additionally, Baicalein showed strong in vitro activity against topoisomerases, and has been suggested previously to be a topoisomerase inhibitor[27]; however, we found that its activity at MIC was primarily that of a detergent-like compound. TMOS was the only flavone studied here to show little to no in vitro activity against DNA gyrase or topoisomerase; however, it had one of the lowest MICs amongst these compounds, and we showed that it inhibits outer membrane biosynthesis in vivo through both morphological studies and the generation of resistant mutants in the Lpx and Fab pathways.

These results highlight two weaknesses in current drug discovery pipelines, where chemically synthesized analogues of bioactive molecules are assumed to have the same or similar MOA, and determination of antibiotic MOA is often a bottleneck that is resolved by high-throughput in vitro studies. We have shown that this family of plant defense metabolites differ drastically in MOA while having the same backbone, and that their primary in vivo activity can be missed if positive results in in vitro studies or potency assays are assumed to have the same MOA.

Our studies of these plant metabolites also give us a new glimpse into the evolution of plant pathogen defense and how it differs from microbe-microbe interactions. Plant metabolites can be difficult to study,

as many are insoluble in aqueous solution, light-sensitive, unstable over long periods of time, and only transiently expressed[9, 41, 42]. These complications contribute to the fact that no successful clinical antibiotic has been isolated from plants[11], especially considering that these metabolites are often only active against bacteria at high concentrations that are physiologically relevant inside of the plant[43] but would cause cytotoxic effects if administered to humans[44]. The fact that Bacterial Cytological Profiling can identify antibiotic MOA within an hour has allowed us to avoid many of these complications pertaining to studying plant metabolites.

The multiple antibiotic mechanisms of action of flavones may represent an evolutionary advantage towards avoiding pathogen resistance [11]. We found that mutations that conferred resistance to TMOS did not confer resistance to any other flavones, indicating that a plant expressing many different flavones with varied antibiotic MOAs may be better protected against spontaneous antibiotic resistance arising in pathogens than an organism that spends many resources making large quantities of a single potent bioactive molecule. However, more in vivo and in planta experiments with ecologically relevant pathogenic and commensal strains are needed in order to further study this interaction between the plant metabolome and microbiome.

Overall, our results suggest that the flavone family of plant metabolites have different primary antibiotic mechanisms of action that are modification- and not backbone-driven, and that in vitro assays are often unable to distinguish these primary MOAs due to their reliance on already having a predetermined potential target. We also demonstrate the value of using BCP to study the in vivo antibiotic activity of plant metabolites. These results could have significant impacts in drug discovery pipelines, as well as our understanding of plant chemical defense against microbial pathogens.

1.5 Materials and Methods

Minimum Inhibitory Concentration (MIC) Assays

MICs were determined by the broth microdilution method. Compounds were added to LB media at starting concentrations of 200 and 141, 100 and 70.7, or 50 and 35.4 ug/mL depending on solubility, and serially diluted 2-fold across ten columns into a final volume of 100uL in clear sterile 96-well flat-bottom plates (Corning Product #3370). Cells were inoculated at ~$5*10^5$ CFU (starting OD_{600} = 0.005) and grown in a plate shaker at 30C, 200rpm for 24 hours. OD_{600} values were measured using a TECAN plate reader at 0, 6, and 24 hours. MICs are reported as lowest

concentration required to inhibit cells to 10% of the OD_{600} of control wells after 24hrs.

Chemical Sources

Flavones were procured from the following vendors with the following purities: Fisher (Rhamnetin 99%; Fisetin 98%; Luteolin 99%), Sigma (Baicalein 98%; Kaempferol 99%; Eupatorin 97%; 7 Hydroxyflavone 98%; 5 Hydroxyflavone 97%; 3,3',4' Trihydroxyflavone 98%; Hispidulin 98%; Quercetin (analytical standard); Eupatilin 98%; Herbacetin 98%; Rhamnazin 99%; Flavone 99%; Flavonone 98%; Sakuranetin (analytical standard)), Abcam (7,8 Dihydroxyflavone 99%; Tangeretin 97%; Nobiletin 97%; Apigenin 98%), Alpha Aesar (3 Hydroxyflavone 98%; 2',3 Dihydroxyflavone 97%; 3',4' Dihydroxyflavone 97%; Myricetin 98%), Indofine Chemicals (2' Hydroxyflavone 98%, 8 Hydroxy 7 Methoxyflavone 98%, 3,7,4' Trihydroxyflavone 99%; 5',7 Dihydroxy 8 Methoxyflavone 99%; Kaempferide 98%; Tamarexetin 99%; Tricetin 99%; Gossypetin 98%; 3,5,7,3',4'Pentamethoxyflavone 95%), and MP Biomedicals (Chrysin 99.4%). Tetramethyl-O-Scutallerin and 3-Hydroxy 6,8,3',4'-Tetramethoxyflavone were obtained as purified natural products from the NCBI's Drug Therapeutics Program (DTP), and were verified for purity by High-resolution ESI-MS. Flavonoids were stored as dry powder, and working

stocks were made at 20mg/mL or 5mg/mL in DMSO dependent upon solubility, and stored at -20C.

Bacterial Cytological Profiling

Bacterial Cytological Profiling was conducted in the same manner as in [23]. Briefly, cells were grown at 30C and treated with antibiotics at OD 0.12-0.14. At 30 minutes and 2 hours post-treatment, 1uL of dye mix (1uL 1mg/mL FM4-64, 2uL 1mg/mL SYTOX Green, 1uL 2mg/mL DAPI in 46uL T-Base) were added to 20uL of cells, and 6uL of cell-dye mixture was spotted onto agarose-LB pads (1% Agarose, 20% LB liquid medium, 80% ddH2O) and imaged by fluorescence and phase contrast microscopy with a 100x objective. As we used a strain of *E. coli* (tolC) that had not yet been fully characterized by BCP, we retested 32 control antibiotics to rebuild the control compounds database for this strain (Table 1.2). Control antibiotics were imaged at 0.5, 1, 2, and 5x MIC, while flavones were imaged at 0.5, 1, and 2x MIC due to solubility limitations. Acquisition and deconvolution of images was performed using Deltavision SoftWorx software; images were thereafter analyzed using Fiji and either quantified using CellProfiler or assembled in Adobe Photoshop.

Generation and Sequencing of Resistant Mutants by Serial Passaging

Multiple colonies of *E. coli* Δ*tolC* were combined to inoculate 1mL starter cultures in LB liquid media. Cultures were incubated with sublethal

(0.75x MIC) concentrations of antibiotics at 30C for two days. After two days, grown cultures were split 1:1000 into two new cultures, one at the previous concentration and another at a slightly higher concentration (0.75x, 1x, 1.25x, 1.5x, 2x, 2.5x, 3x, 4x). After every two days, the culture that grew at the highest concentration was again split, and generations were frozen every week. Mutant generation for each compound was conducted in biological triplicates from three separate starter colony aggregates. Final resistant mutant cultures were established when no increase in resistance was observed after more than three splits (>1 week). Increased MICs of resistant strains were reconfirmed using the microbroth dilution MIC assay described above.

Strains were sequenced on an Illumina MiSeq500-V2, through the La Jolla Institute for Immunology. We prepared samples using the Nextera DNA Flex Library Prep Kit (Cat# 20018704). Sequence analysis was performed using Geneious. Contigs were mapped to the parent strain of eRL003, MC4100 (Genbank accession no. HG_738867.1), modified to accommodate a 9kb deletion at bp ~67,500 to 76,500, as well as a few resolved SNPs between eRL003 and MC4100.

Construction of ftsZ-GFP strain

We obtained a strain of WM2026[34], which contains a C-terminally GFP-tagged FtsZ expressed under the IPTG-inducible promoter pTrc,

chromosomally integrated at the lambda attachment site alongside an ampicillin resistance marker. To generate phage lysates containing the FtsZ-GFP cassette, we added $CaCl_2$ (final concentration 5mM) to 1.5mL OD 0.5 cultures of WM2026 and incubated in a 30C roller for 15 minutes. Serial dilutions of P1 HTvir lamda phage were prepared from lysates previously from the *tolC* strain. 100uL of phage dilutions were incubated with 1.4mL of bacteria for 20 minutes at 37C, at which point we added 50uL of 1M $CaCl_2$ and 20% glucose. Cultures were then mixed with HTOP agar and plated onto LB plates. After overnight incubation, lysates were harvested by flooding plates with LB for 2 hours, centrifuging the media for 4 minutes at 13,500 rpm in a mini-centrifuge, and passed through a sterile 0.45um filter. These FtsZ-GFP phage lysates were then used to infect *tolC* by incubating 100uL of serial dilutions (10^0 to 10^{-3}) to 4mL of *tolC* that were pelleted and resuspended in 1mL of 100mM $MgSO_4$/5mM $CaCl_2$. After 20 minutes of incubation at 37C, 200uL of 1M Sodium Citrate and 1mL of fresh LB was added to each sample and rolled at 37C for 1 hour. These samples were then plated onto LB plates containing Amp100 for selection and 0.1M Sodium Citrate to inhibit further phage activity. Resulting colonies were passaged twice on Amp100/0.1M Sodium Citrate to encourage loss of phage while maintaining the FtsZ-GFP construct. The clone used in this study was notated as eRL100.

Imaging of ftsZ-GFP strain eRL100

BCP of eRL100 was conducted similarly to described above, with the following modifications: SYTOX Green was not included in the dye mix, instead adding 1 extra uL of T-Base; and cultures were induced with 30uM of IPTG at OD 0.05 for 1 hour to express GFP-tagged FtsZ before beginning antibiotic treatment (T0). Induced cultures of eRL100 normally reached OD ~0.12 after 1 hour of induction, in accordance with the normal OD at which antibiotic treatment is begun in the normal BCP workflow.

Gyrase/Topoisomerase assays

E. coli DNA Gyrase Drug Screening Kit (Catalog No. TG2001G-1KIT) and E. coli Topoisomerase IV Drug Screening Kit (TG1007-1A) were ordered from TopoGEN. Protocols were followed as provided in the kits (4 units enzyme per reaction), with compounds added to a maximum DMSO concentration of 0.5%. 1% Agarose gels were run with and without 0.5 ug/mL Ethidium Bromide.

1.6 Acknowledgements

Chapter 1, in full is currently being prepared for submission for publication of the material. Liu R., Jespersen A., Tsunemoto H., Lamsa A., Mahoney P., Pogliano J., Pogliano K. The dissertation author was the primary author of this paper.

1.7 References

1. Silver, L.L., Challenges of antibacterial discovery. Clin Microbiol Rev, 2011. 24(1): p. 71-109.

2. Theuretzbacher U., Outterson K., Engel A., Karlen A. The global preclinical antibacterial pipeline. Nat Rev Microbiol, 2020. 18(5): p. 275-285.

3. Cotsonas King, A. and L. Wu, Macromolecular synthesis and membrane perturbation assays for mechanisms of action studies of antimicrobial agents. Curr Protoc Pharmacol, 2009. Chapter 13: p. Unit 13A 7.

4. Aubrey O'Rourke, Sinem Beyhan, Yongwook Choi, Pavel Morales, Agnes P. Chan, Josh L. Espinoza, Chris L. Dupont, Kirsten J. Meyer, Amy Spoering, Kim Lewis, William C. Nierman, Karen E. Nelson. Mechanism-of-Action Classification of Antibiotics by Global Transcriptome Profiling. Antimicrob Agents Chemother, 2020. 64(3).

5. Franken, H., Mathieson, T., Childs, D. Sweetman G., Werner T., Togel I., Doce C., Gade S., Bantscheff M., Drewes G., Reinhard F., Huber W., Savitski M. Thermal proteome profiling for unbiased identification of direct and indirect drug targets using multiplexed quantitative mass spectrometry. Nat Protoc, 2015. 10(10): p. 1567-93.

6. Bryskier, A., Antimicrobial agents : antibacterials and antifungals. 2005, Washington, D.C.: ASM Press. xxx, 1426 p.

7. Webb, M.R. and S.E. Ebeler, Comparative analysis of topoisomerase IB inhibition and DNA intercalation by flavonoids and similar compounds: structural determinates of activity. Biochem J, 2004. 384(Pt 3): p. 527-41.

8. Balouiri, M., M. Sadiki, and S.K. Ibnsouda, Methods for in vitro evaluating antimicrobial activity: A review. J Pharm Anal, 2016. 6(2): p. 71-79.

9. Ahuja, I., R. Kissen, and A.M. Bones, Phytoalexins in defense against pathogens. Trends Plant Sci, 2012. 17(2): p. 73-90.

10. Schmelz, E.A., Huffaker A., Sims J., Christensen S., Lu X., Okada K., Peters R. Biosynthesis, elicitation and roles of monocot terpenoid phytoalexins. Plant J, 2014. 79(4): p. 659-78.

11. Radulovic, N.S., Blagojevic P., Stojanovic-Radic Z., Stojanovic N. Antimicrobial plant metabolites: structural diversity and mechanism of action. Curr Med Chem, 2013. 20(7): p. 932-52.

12. Andersen, E.J., Ali S., Byamukama E., Yen Y., Nepal M. Disease Resistance Mechanisms in Plants. Genes (Basel), 2018. 9(7).

13. Cowan, M.M., Plant products as antimicrobial agents. Clin Microbiol Rev, 1999. 12(4): p. 564-82.

14. Cushnie, T.P. and A.J. Lamb, Antimicrobial activity of flavonoids. Int J Antimicrob Agents, 2005. 26(5): p. 343-56.

15. Cushnie, T.P. and A.J. Lamb, Recent advances in understanding the antibacterial properties of flavonoids. Int J Antimicrob Agents, 2011. 38(2): p. 99-107.

16. Kumar, S. and A.K. Pandey, Chemistry and biological activities of flavonoids: an overview. ScientificWorldJournal, 2013. 2013: p. 162750.

17. Panche, A.N., A.D. Diwan, and S.R. Chandra, Flavonoids: an overview. J Nutr Sci, 2016. 5: p. e47.

18. Wang, T.Y., Q. Li, and K.S. Bi, Bioactive flavonoids in medicinal plants: Structure, activity and biological fate. Asian J Pharm Sci, 2018. 13(1): p. 12-23.

19. Kanakis, C.D., Tarantilis P., Polissiou M., Tamjir-Riahi H. Interaction of antioxidant flavonoids with tRNA: intercalation or external binding and

comparison with flavonoid-DNA adducts. DNA Cell Biol, 2006. 25(2): p. 116-23.

20. Morimoto, Y., Baba T., Sasaki T., Hiramitsu K. Apigenin as an anti-quinolone-resistance antibiotic. Int J Antimicrob Agents, 2015. 46(6): p. 666-73.

21. Verghese, J., Nguyen T., Oppegard L, Seivert L, Hiasi H, Ellis K. Flavone-based analogues inspired by the natural product simocyclinone D8 as DNA gyrase inhibitors. Bioorg Med Chem Lett, 2013. 23(21): p. 5874-7.

22. Górniak, I., Bartoszewski, R. & Króliczewski, J., Comprehensive review of antimicrobial activities of plant flavonoids. Phytochem Rev, 2019. 18: p. 241-272.

23. Moulishankar, A. and K. Lakshmanan, Data on molecular docking of naturally occurring flavonoids with biologically important targets. Data Brief, 2020. 29: p. 105243.

24. Lamsa, A., Lopez-Garrido J., Quach D., Riley E., Pogliano J., Pogliano K. Rapid Inhibition Profiling in Bacillus subtilis to Identify the Mechanism of Action of New Antimicrobials. ACS Chem Biol, 2016. 11(8): p. 2222-31.

25. Nonejuie, P., Burkart, M., Pogliano, K. & Pogliano, J. Bacterial cytological profiling rapidly identifies the cellular pathways targeted by antibacterial molecules. Proc Natl Acad Sci U S A, 2013. 110(40): p. 16169-74.

26. Peters, C.E., Lamsa A., Liu R., Quach D., Sugie J., Brumage L., Pogliano J., Lopez-Garrido J., Pogliano K. Rapid Inhibition Profiling Identifies a Keystone Target in the Nucleotide Biosynthesis Pathway. ACS Chem Biol, 2018. 13(12): p. 3251-3258.

27. Snyder, R.D. and P.J. Gillies, Evaluation of the clastogenic, DNA intercalative, and topoisomerase II-interactive properties of

bioflavonoids in Chinese hamster V79 cells. Environ Mol Mutagen, 2002. 40(4): p. 266-76.

28. Barb, A.W., McClerren A., Snehelatha K., Reynolds C., Zhou P., Raetz C. Inhibition of lipid A biosynthesis as the primary mechanism of CHIR-090 antibiotic activity in Escherichia coli. Biochemistry, 2007. 46(12): p. 3793-802.

29. Emiola, A., Andrews S., Heller C., George J. Crosstalk between the lipopolysaccharide and phospholipid pathways during outer membrane biogenesis in Escherichia coli. Proc Natl Acad Sci U S A, 2016. 113(11): p. 3108-13.

30. Zeng, D., Zhao J., Chung H., Guan Z., Raetz C., Zhou P. Mutants resistant to LpxC inhibitors by rebalancing cellular homeostasis. J Biol Chem, 2013. 288(8): p. 5475-86.

31. Zhang, L., Kong Y., Wu D., Zhang H., Wu J., Chen J., Ding J., Hu L., Jiang H., Shen X. Three flavonoids targeting the beta-hydroxyacyl-acyl carrier protein dehydratase from Helicobacter pylori: crystal structure characterization with enzymatic inhibition assay. Protein Sci, 2008. 17(11): p. 1971-8.

32. Geethalakshmi, R., J.C. Sundaramurthi, and D.V.L. Sarada, Antibacterial activity of flavonoid isolated from Trianthema decandra against Pseudomonas aeruginosa and molecular docking study of FabZ. Microb Pathog, 2018. 121: p. 87-92.

33. Pogliano, J., Pogliano K., Weiss D., Losick R., Beckwith J. Inactivation of FtsI inhibits constriction of the FtsZ cytokinetic ring and delays the assembly of FtsZ rings at potential division sites. Proc Natl Acad Sci U S A, 1997. 94(2): p. 559-64.

34. Si, F., Busiek K., Margolin W., Sun S. Organization of FtsZ filaments in the bacterial division ring measured from polarized fluorescence microscopy. Biophys J, 2013. 105(9): p. 1976-86.

35. Tamma, P.D., S.E. Cosgrove, and L.L. Maragakis, Combination therapy for treatment of infections with gram-negative bacteria. Clin Microbiol Rev, 2012. 25(3): p. 450-70.

36. Fischbach, M.A., C.T. Walsh, and J. Clardy, The evolution of gene collectives: How natural selection drives chemical innovation. Proc Natl Acad Sci U S A, 2008. 105(12): p. 4601-8.

37. Andersson, M.I. and A.P. MacGowan, Development of the quinolones. J Antimicrob Chemother, 2003. 51 Suppl 1: p. 1-11.

38. Husain, F., M. Humbard, and R. Misra, Interaction between the TolC and AcrA proteins of a multidrug efflux system of Escherichia coli. J Bacteriol, 2004. 186(24): p. 8533-6.

39. Solnier, J., Martin J., Bhakta S., Bucar F. Flavonoids as Novel Efflux Pump Inhibitors and Antimicrobials Against Both Environmental and Pathogenic Intracellular Mycobacterial Species. Molecules, 2020. 25(3).

40. Savitski, M.M., Reinhard F., Franken H., Werner T., Savitski M., Eberhard D. Molina D., Jafari R., Dovega R., Klaeger S. Kuster B., Nordlund P., Bantscheff M., Drewes G. Tracking cancer drugs in living cells by thermal profiling of the proteome. Science, 2014. 346(6205): p. 1255784.

41. Jorge, T.F., A.T. Mata, and C. António, Mass spectrometry as a quantitative tool in plant metabolomics. Philosophical transactions. Series A, Mathematical, physical, and engineering sciences, 2016. 374(2079): p. 20150370.

42. Sarabia, L.D., Hill, C.B., Boughton, B.A. and Roessner, U., Advances of Metabolite Profiling of Plants in Challenging Environments, in Annual Plant Reviews online. 2018. p. 629-674.

43. Curcic, M.G., Stankovic M., Radojevic I., Stefanovic O., Comic L., Tupozovic M., Djacic D., Markovic S. Biological effects, total phenolic

content and flavonoid concentrations of fragrant yellow onion (Allium flavum L.). Med Chem, 2012. 8(1): p. 46-51.

44. Sak, K. Cytotoxicity of dietary flavonoids on different human cancer types. Pharmacogn Rev, 2014. 8(16): p. 122-46.

CHAPTER 2: CHARACTERIZATION OF BIOACTIVE FUNGAL METABOLITES IN THE CHEESE MICROBIOME

Chapter 2 includes experiments and data from "Bacterial-fungal interactions revealed by genome-wide analysis of bacterial mutant fitness", Nature Microbiology 2020. The dissertation/thesis author was a secondary author on this paper, but was responsible for conducting the experiments and results described in this dissertation. The Introduction, Results, and Discussion sections have been rewritten but contain reprints of figures from this paper, while the Materials and Methods section is a reprint of a portion of the Methods section found in the publication.

2.1 Introduction

Many microbiome studies have traditionally focused on the bacterial members of microbial communities, frequently overlooking other constituents such as fungi and viruses, despite the substantial impacts they have on these ecosystems[1,2]. This bacteria-centric focus can be partially attributed to the earlier development of next-generation sequencing techniques for bacterial cells than for microeukaryotes[3]; however, recent advances in sequencing techniques have allowed for a growing interest

in studying these microeukaryotic species such as fungi, and exploring the impacts that they have on microbial ecosystems[3,4,5,6,7].

Environmental microbiomes, such as soil or water samples, are replete with fungal species and fungal-bacterial interactions; however, this very abundance of species makes it difficult to isolate mechanisms underlying species-species interactions, causing researchers to instead infer mechanisms based on -omics level surveys[8,9]. As a workaround to this problem, the cheese rind biofilm has been developed as a model microbial community with species that are genetically tractable and, importantly, multi-kingdom while on the order of ten genera[10,11]. This allows for systematic species-species interaction studies not combinatorically possible in larger, more complex environmental microbiomes.

Previous work in cheese rind biofilms has demonstrated that fungi and bacteria in these biofilms can positively and negatively impact each other's growths, through mechanisms such as cross-feeding amino acids or enabling mobility through the biofilm (positive) or through competition for vital nutrients such as iron, or secretion of bioactive antibiotic molecules (negative)[10,11,12]. The use of the high-throughput genetic screening methods RB-TnSeq[13] and RNA-Seq has further expanded our knowledge of fungal-bacterial interactions within cheese rinds. Pairing

random genetic mutations with pairwise fitness interaction studies allows for the determination of genes that are specifically beneficial or detrimental for cells only when grown in co-culture with another community member, allowing for the elucidation of the underlying mechanisms.

These genetic screens imply the importance of antimicrobial production by fungal species present in the cheese microbiome for community composition. Specifically, the deletion of MdtK[14], a drug efflux pump, from *E. coli* decreased the fitness of *E. coli* only when grown in co-culture with the fungal species. Additionally, the deletion of LaeA[15], a global regulator of fungal specialized metabolite production, from a *Penicillium* species within the cheese community led to a large decrease in the required pathways in *E. coli* for growth in co-culture conditions, indicating the presence of specialized metabolites inhibiting bacterial growth. Here, we characterize the antimicrobial effects these cheese rind biofilm fungi have against different bacterial strains using Bacterial Cytological Profiling, and show that these fungi elicit bacterial cell envelope stress via the production of antimicrobial peptides and other undetermined non-penicillin antibiotics.

2.2 Results

Adaptation of Bacterial Cytological Profiling for use on Cheese Curd Agar

Bacterial Cytological Profiling[16] has been previously developed to examine the morphological changes in cells in response to antibiotic treatment when cultured in standard laboratory media such as Luria-Bertani (LB) broth or antibiotic testing media such as cation-adjusted Mueller Hinton Broth (Ca-MHB)[17]. However, a growing body of literature suggests that cells respond to antibiotics differently depending upon the growth media used, sometimes with multiple orders of magnitude differences in MIC[18]. Furthermore, morphological responses can differ when cells are tested in media with osmo-protectants such as sucrose, which has been used to differentiate between antibiotics that target cell wall biosynthesis or are membrane active, which can result in similar phenotypes without osmoprotectants[19].

Due to the high salinity, and fat content of cheese curd agar compared to LB media, in addition to the longer timescales needed for coculture conditions, it was necessary to generate the control antibiotic training set for BCP using bacterial plated on cheese curd agar (CCA) and treated with antibiotics overnight, instead of the standard 2-hour treatment conditions in liquid LB medium used in the standard BCP protocol.

We tested fifteen different control antibiotics with varying mechanisms of action. 20µL of four different concentrations (5X, 10X, 25X,

100X MIC) of drugs were spotted onto quadrants of CCA plates and allowed to dry completely. Afterwards, 50µL of diluted cells were spread-plated onto each quadrant, allowed to dry, and grown up overnight. Zones of inhibition were visible after overnight growth, and cells at the edges of the zones of inhibition were resuspended in dye mixture and imaged (Figure 2.1).

While some cellular morphologies resulting from antibiotic treatment were consistent between CCA and LB media, clear differences are visible between the media conditions. Treatment with the DNA replication inhibitors Ciprofloxacin and Safranin-O both resulted in elongated cells with single, smooth chromosomes often removed from the poles of the cells, similar to the phenotypes in LB (Figure 2.1, 1.4). Treatment with trimethoprim also results in an elongated-cell phenotype, but with more separated and condensed chromosomes. Treatment with chloramphenicol, a protein translation inhibitor, resulted in slightly enlarged cells with rounded chromosomes, and exposure to the surfactant SDS resulted in cells with mostly normal shape, but with cell debris clearly visible; both of these phenotypes on CCA echo their counterparts in LB (Figure 2.1, 1.4).

However, distinct differences in morphological changes between CCA and LB can be seen in antibiotics targeting cell wall biosynthesis and

lipid biosynthesis. In LB, Triclosan and Cerulenin, inhibitors of Fab proteins involved in fatty acid biosynthesis, result in chains of 4 cells that have relatively normal morphology other than their chaining. However, Cerulenin treatment on CCA showed chaining but also elongation, curling, and pinching of the ends of cells. Triclosan also showed chaining, but with no clear septa between chained cells, creating the look of a single bumpy, longer cell (Figure 2.1).

With respect to cell wall biosynthesis inhibitors, several antibiotics that result in elongated cells with multiple chromosomes in LB caused spheroplasting of cells on CCA. This could be due to the high salt, protein, and lipid content of CCA acting as an osmoprotectant, as spheroplasts are often seen when cells are treated with cell wall inhibitors in LB with 0.5M sucrose as an osmoprotectant, or due to the slower growth of *E. coli* on CCA, allowing for cells slow growth enough in response to antibiotic treatment to avoid lysis. Interestingly, treatment with cloxacillin and ceftazidime resulted in a hybrid elongated-spheroplast morphology. Mecillinam treatment resulted in misshapen, semi-amorphous cells, and meropenem treatment caused shortened, ovoid cells, which appear similar to their respective phenotypes on LB (Figure 2.1, 1.4).

Figure 2.1 (Opposite page). Bacterial Cytological Profiling of Δ*tolC E. coli* treated with known antibiotics on cheese curd agar. DAPI dye stains DNA and FM4-64 dye stains bacterial membranes. SYTOX green stains nucleic acids but cannot penetrate live cells. Scale bars represent 2μm. Testing of each antibiotic at four concentrations was performed once, and cells from the edges of zones of clearing were imaged for at least 5 fields from each condition to ensure consistency in phenotype.

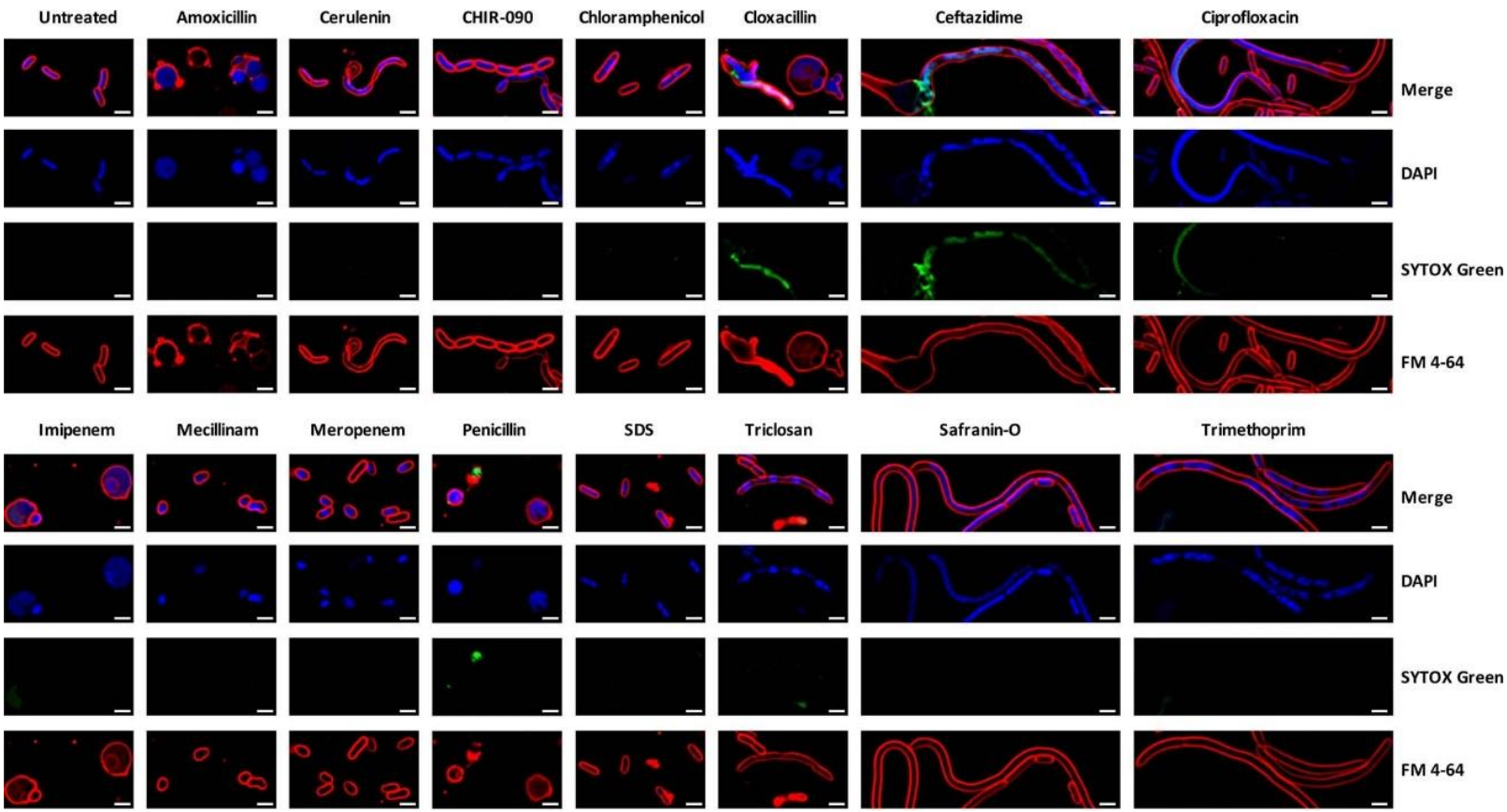
Untreated
Amoxicillin
Cerulenin
CHIR-090
Chloramphenicol
Cloxacillin
Ceftazidime
Ciprofloxacin
Merge
DAPI
SYTOX Green
FM 4-64
Imipenem
Mecillinam
Meropenem
Penicillin
SDS
Triclosan
Safranin-O
Trimethoprim
Merge
DAPI
SYTOX Green
FM 4-64

BCP of E. coli strains when grown in coculture with cheese fungus

When grown in 1:1 co-culture on CCA for a week, the fungal strains *Penicillium* sp. str. #12 (abbreviated as Pen12 here) and *Penicillium* sp. str. SAM3 were shown to significantly impact bacterial mutant fitness. Transposon mutant libraries of these bacterial species[13,20] found that strains that had mutations in genes involved in cell envelope structure, such as drug efflux pumps, envelope stress response systems, penicillin binding proteins, and lipid and peptidoglycan synthesis genes were disproportionally inhibited when grown in co-culture with these fungal strains when compared to grown alone on CCA. One mutation that specifically decreased fitness of *E. coli* when grown in coculture was in the multidrug efflux pump MdtK.

Using the BCP training set for CCA as described in the previous section, we performed BCP on WT or Δ*mdtK E. coli* cells, grown either alone on CCA or in a 1:1 mixed biofilm with SAM3 or Pen12 (Figure 2.2A.). When imaged, both WT and Δ*mdtK* cells appeared normal when grown alone on CCA. However, co-culture of WT *E. coli* with SAM3 or Pen12 resulted in slightly wider, semi-amorphous cells, mimicking the effects of treatment with Meropenem. Many cells were still phase-dark, indicating that while the cell envelopes are disrupted, a significant population of cells remain un-lysed. However, co-culture of Δ*mdtK* cells with the fungal

Figure 2.2 (Opposite page). BCP of *E. coli* grown with *Penicillium* sp. str. SAM3, *Penicillium* sp. str. 12 or Δ*laeA Penicillium* sp. str. 12 on CCA plates. The phenotype of *E. coli* grown with these fungi is similar to that seen when *E. coli* is exposed to antibiotics targeting cell wall biosynthesis. This effect is more dramatic in *E. coli* lacking the *mdtK* multidrug efflux pump. Representative fields of deconvoluted images are displayed. DAPI dye stains DNA and FM4-64 dye stains bacterial membranes. Scale bars, 2 μm. **b**, Quantification of microscopy results. The major and minor axes of individual cells were measured (all cells in the image for multiple images), and the ratio of these measurements was used as an indicator of cell roundness. Each empty circle represents an individual cell (from left to right, $n = 110$, 53, 121, 136, 181, 144, 153, 79, 70 and 73 cells examined from one independent experiment per condition). The filled circle displays the mean, and the thick bar extending from the mean displays the standard deviation. WT *E. coli* has a ratio of about 3, and the cells become rounder as the ratio approaches 1. Asterisks indicate significantly different roundness in the presence of a fungus relative to growth alone or significantly different roundness in the presence of WT *Penicillium* sp. str. 12 relative to Δ*laeA Penicillium* sp. str. 12 (unpaired two-sample Wilcoxon test $P < 0.05$). Exact P values are as follows: *E. coli–Penicillium* SAM3 versus *E. coli* alone = 3.05×10^{-13}; *E. coli–Penicillium* 12 versus *E. coli* alone = 3.55×10^{-28}; *E. coli–Penicillium* 12 versus *E. coli–*Δ*laeA Penicillium* 12 = 5.21×10^{-37}; Δ*mdtK E. coli–Penicillium* SAM3 versus Δ*mdtK E. coli* alone = 4.13×10^{-25}; Δ*mdtK E. coli–Penicillium* 12 versus Δ*mdtK E. coli* alone = 1.14×10^{-41}; Δ*mdtK E. coli–*Δ*laeA Penicillium* 12 versus Δ*mdtK E. coli* alone = 2.68×10^{-13}; Δ*mdtK E. coli–Penicillium* 12 versus Δ*mdtK E. coli–*Δ*laeA Penicillium* 12 = 1.16×10^{-7}.

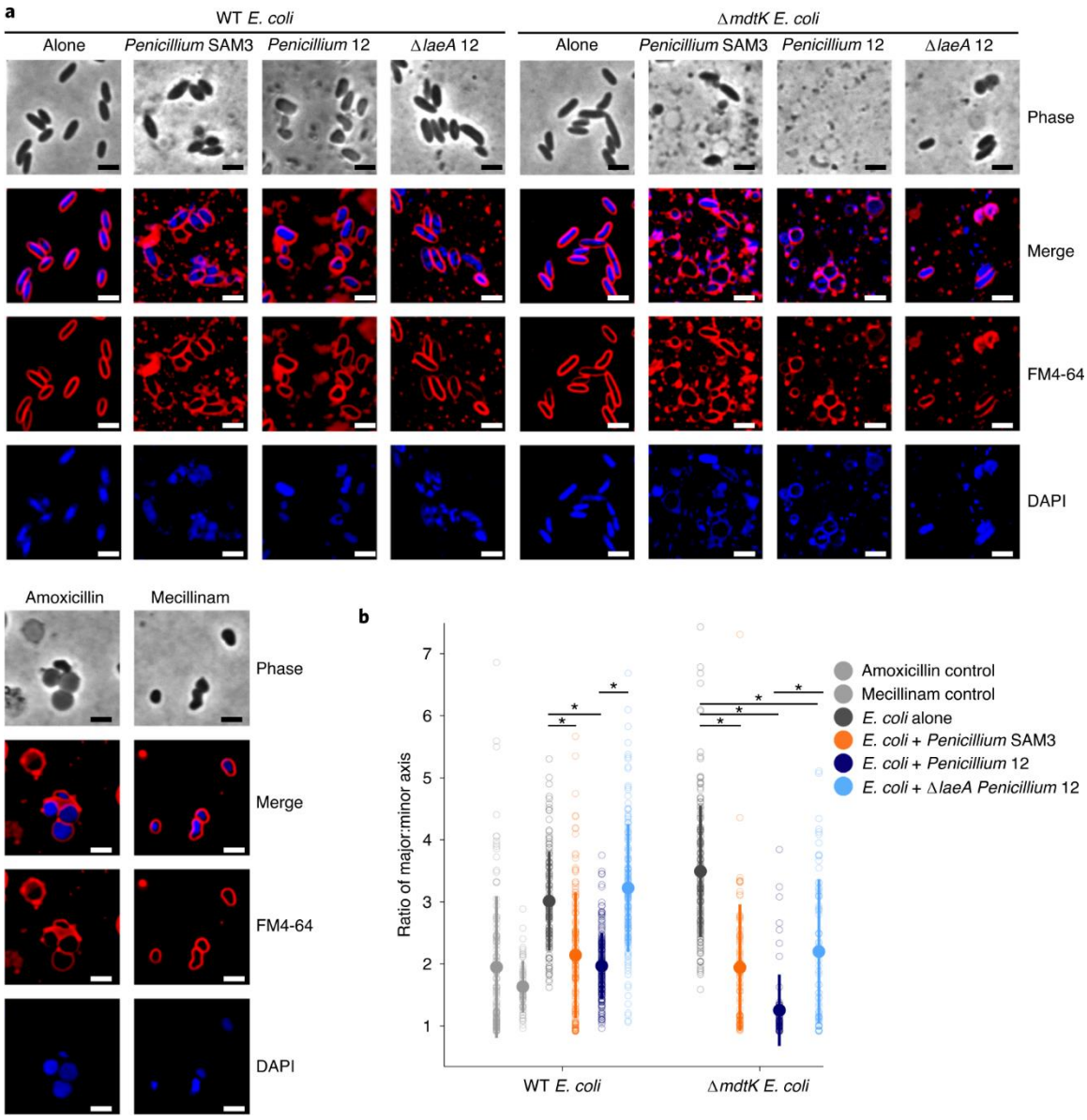
a
WT E. coli
ΔmdtK E. coli
Alone
Penicillium SAM3
Penicillium 12
ΔlaeA 12
Phase
Merge
FM4-64
DAPI
Amoxicillin
Mecillinam
b
Ratio of major:minor axis
Amoxicillin control
Mecillinam control
E. coli alone
E. coli + Penicillium SAM3
E. coli + Penicillium 12
E. coli + ΔlaeA Penicillium 12
WT E. coli
ΔmdtK E. coli

strains resulted in the formation of phase-transparent spheroplasts, indicative of the complete loss of structural integrity due to the disruption of the cell envelope as well as cell lysis. This phenotype resembles treatment of cells with Amoxicillin, which creates similar spheroplasts.

The roundness of these cells was quantified by measuring the ratio of the major and minor axes (Figure 2.2B). We found that both co-culture of WT *E. coli* with the fungal strains and Amoxicillin or Mecillinam caused significant rounding of cells. Furthermore, the Δ*mdtK E. coli* strains exhibited more severe rounding when co-cultured with Pen12 than WT *E. coli* strains, corroborating the genetic information that the Δ*mdtK* deletion reduces the fitness of the bacteria when grown in co-culture.

While the ability of *Penicillium* fungi to produce penicillins, which inhibit cell wall biosynthesis and thus induce cell envelope stress, is more than well document, penicillin biosynthesis gene clusters were not detected in these strains. Thus, the bioactive molecule or molecules are yet unknown. To try to determine which biosynthetic pathways may be responsible for producing the antimicrobial metabolites, we generated a Δ*laeA* mutant of the fungal strain Pen12. LaeA is known to be a global regulator of specialized metabolites, including antibiotic metabolites, in other closely related fungi[15]. When co-cultured with Δ*laeA* Pen12, WT *E. coli* appear to have almost no morphological defects, and are statistically

significantly more rod-shaped than when grown with Pen12 with a functional LaeA, and are quantitatively indistinguishable from cells grown on CCA alone in terms of roundness. When Δ*mdtK* cells were grown with Δ*laeA* Pen12, cells were also less round, indicating less cell envelope disruption. However, these cells did not revert to the same morphology as when grown alone on CCA. These data suggest that while LaeA is likely responsible for the production of antimicrobial metabolites that inhibit the growth of *E. coli*, there are likely other antimicrobial metabolites produced by these fungal strains not under the control of LaeA that differentially impact WT and Δ*mdtK E. coli* cells.

BCP of other bacterial strains in co-culture with Penicillium sp. str. #12.

While *E. coli* can be a causative agent of foodborne illness in cheeses, it is not a representative member in the microbial community of this cheese[21,22]. Thus, we wanted to analyze the pairwise interactions of the fungal species with other strains of bacteria. We selected *Bacillus subtilis* PY79, a Gram-positive strain for which BCP has been well studied, as well as *Pseudomonas psychrophila* str. JB418, a prominent community member of this cheese. We grew strains in a co-culture biofilm with Pen12 for a week, after which the biofilm was filtered to remove fungal matter and examined via fluorescence microscopy using the same protocol as

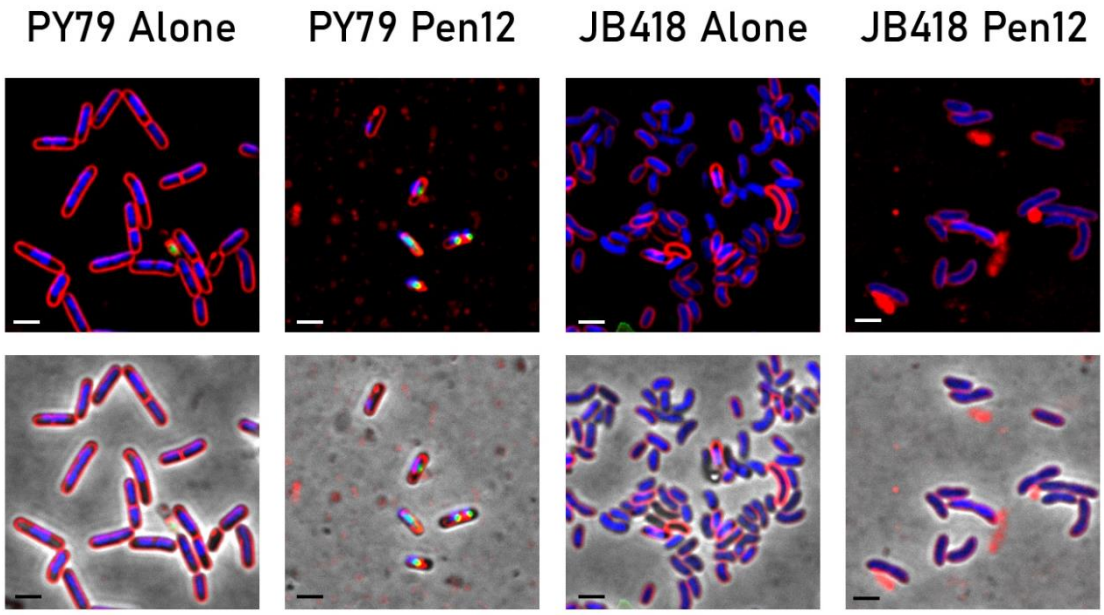

Figure 2.3 *Bacillus subtilis* PY79 and *Pseudomonas psychrophila* JB418 cultured on cheese curd agar in a biofilm for one week with and without *Penicillium* sp. str. 12 (abbreviated Pen12). Cells were scraped from the biofilm surface, resuspended in T-Base and filtered through a 5µm filter to remove fungal matter. Scale bar represents 2µm. Top row: FM4-64 (red), DAPI (blue), Sytox Green (green). Bottom row: Phase microscopy overlay.

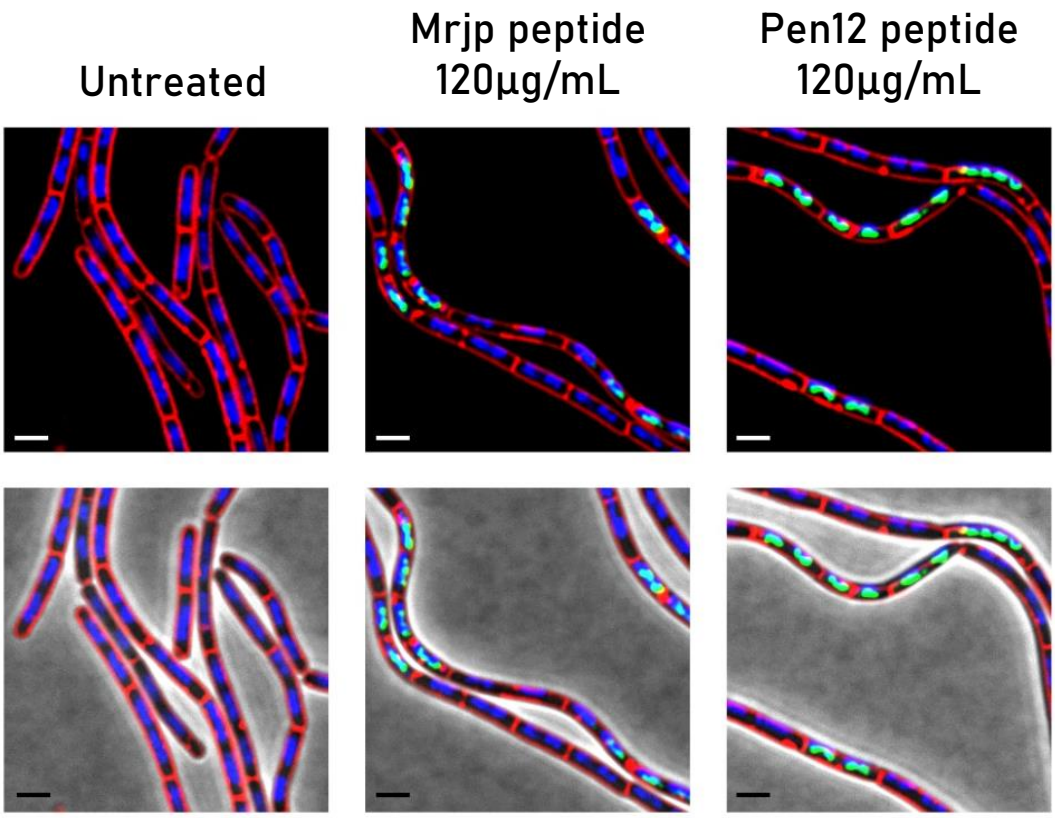

Figure 2.4. Bacterial Cytological Profiling of *Bacillus subtilis* PY79 with and without exposure to antimicrobial peptides major royal jelly protein (mrjp) and peptide produced by *Penicillium sp. str.* 12 (Pen12 peptide). Peptides were added to log-phase (OD_{600} 0.12) cultures of PY79 in LB liquid media for 30 minutes, and imaged on a 1% agarose pad slide made with 1:5 LB:T-Base. Top row: FM4-64 (red), DAPI (blue), Sytox Green (green). Bottom row: Phase microscopy overlay.

described previously (Figure 2.3). We found that co-culture with Pen12 resulted in *Bacillus* cells that were permeabilized, evidenced by the presence of SYTOX Green within the cells. Furthermore, the membrane staining with FM4-64 appears to be detracted from the cell wall, visible in the color/phase overlay. Cell debris can also be seen widely throughout the field. These phenotypes indicate cell envelope stress and permeabilization. Co-culture of *Pseudomonas psychrophila* with the fungi resulted in longer, wider cells, as well as visible cell debris. While SYTOX Green was not visible, indicating that many cells were not permeabilized or lysed, the presence of cell debris as well as the swelling morphology also corroborate the cell envelope stress phenotype seen in both *E. coli* and *Bacillus subtilis*, indicating that the antimicrobial metabolites produced by these cheese fungi likely have activity against a wide range of bacteria.

BCP of fungal antimicrobial peptides against E. coli, Bacillus subtilis and Pseudomonas psychrophila

Antimicrobial peptide (AMP) synthesis clusters were detected in *Penicillium* sp. str. #12. Interestingly, the predicted antimicrobial peptide product of these clusters were found to have homology to major royal jelly protein (mrjp) produced by bees, which is known to have

antimicrobial properties by direct membrane action[23]. To test whether these antimicrobial peptides were responsible for the cell envelope activity seen in the previous section, we conducted BCP in LB liquid media of both the fungal and bee-produced AMPS against WT *E. coli* as well as *E. coli* Δ*tolC*, a drug efflux pump knockout that sensitizes bacteria to many antibiotics. However, neither *E. coli* exhibited any visible phenotypes in response to treatment with either AMP (data not shown). To determine whether this was specific to *E. coli*, we also tested the effects of these AMPS against *Bacillus subtilis* PY79, and found that these AMPS had a direct membrane active effect against *B. subtilis,* evident by the rapid (within 30 minutes) permeabilization of cells seen without cell shape defects, as seen by the presence of Sytox green staining within cells (Figure 2.4). While the discovery of this mrjp-like AMP produced by fungi is interesting, its phenotype and activity against *E. coli* and *B. subtilis* do not completely match the phenotypes seen when these strains are co-cultured with Pen12, indicating that there are likely other antimicrobial metabolites being produced by this fungus that are yet to be isolated.

2.3 Discussion

Understanding fungal-bacterial interactions is vital to gaining a holistic understanding of microbial community dynamics[24,25]. A large part

of these interactions lie in competition, and the production of bioactive molecules plays a large role in competition, especially cross-kingdom; indeed, fungi have been long known to secrete powerful antibiotic secondary metabolites able to kill bacteria in a variety of manners[26]. Using BCP, we have provided new insight as to how fungi are able to inhibit the growth of bacteria on Cheese Curd Agar, more closely resembling the *in situ* chemical composition of the environment than standard laboratory media such as LB. The ability of BCP to be developed for virtually any environmental condition highlights its versality and potential uses to examine microbial interactions in a variety of environmental and experimental settings.

Here, we observe a mechanism by which fungi impart negative fitness on bacterial community members, and by using RB-TnSeq we are able to identify key genes involved in the antibiotic production and response in both the fungal and bacterial species. These cheese-isolated *Penicillium* species exhibit antibiotic activity that induces cell envelope stress in bacteria; however, since no penicillin-like biosynthetic clusters were identified, the causative bioactive molecule(s) are yet to be identified. Furthermore, detection of antibiotics in food products is limited, despite the prolific secondary metabolite production characteristic of *Penicillium* species[27]. Use of BCP could help to identify yet unknown

molecules by screening fermented food products for bioactivity. We also identify an AMP produced in the fungi and identify its mechanism of action as causing direct membrane damage. These results have potential impacts in both the food industry and microbial ecology, as they provide a stepping-stone for which further microbial community interactions can be observed. However, many (38%) *E. coli* genes identified in the genetic screen as important for fungal-bacterial pairwise fitness are uncharacterized or hypothetical, highlighting that many molecules and mechanisms are yet to be discovered, and that defined microbial communities such as the cheese rind biofilm can provide a useful tool for furthering examining these unknown, microbial interaction-dependent genes.

2.4 Materials and Methods

The Materials and Methods section, in full, is a reprint of material as it appears in Pierce et al., "Bacterial-fungal interactions revealed by genome-wide analysis of bacterial mutant fitness", Nature Microbiology 2020, in the Bacterial Cytological Profiling portion of the Methods section. The dissertation/thesis author was a secondary author on this paper, but was primarily responsible for conducting the experiments described in this section.

Approximately 7,000,000 WT E. coli K-12 strain BW25113 or Keio collection mdtK mutant cells[28] were inoculated alone or co-inoculated with 700,000 Penicillium sp. str. #12, Penicillium sp. str. #12 ΔlaeA, or Penicillium sp. str. SAM3 spores on 10% CCA pH 7. After 7 days of growth, 1 mL of T-Base buffer was added to the surface of the biofilms, and biofilms were scraped into the buffer. For co-culture conditions, the sample was filtered through a 0.5 µm filter to specifically remove fungal material. 2 µL of concentrated dye mix (1 µL 1 mg/mL FM4-64, 1 µL 2 mg/mL DAPI in 48 µL T-Base) were added to 20 µL of filtrate. The dye-filtrate mix was spotted onto agarose-LB pads (1% agarose, 20% LB liquid medium, 80% ddH2O) and imaged by fluorescence and phase contrast using an Applied Precision Deltavision Spectris imaging system with an Olympus UPLFLN100XO2PH objective. Control compound references on CCA medium were obtained by spotting and drying 30 µL of 5x, 10x, 25x, and 100x MIC dilutions of antibiotics onto quadrants on CCA medium pH 7 plates and then spread-plating 200 µL of log phase (OD 0.1) E. coli cultures. After two days of growth, cells near the edge of the zone of inhibition on appropriate dilution spots were resuspended in 10 µL of prediluted dye mix (1 µL 1 mg/mL FM4-64, 1 µL 2 mg/mL DAPI in 998 µL T-Base) and spotted onto agarose-LB pads and imaged as described above. Resulting images were deconvoluted using Deltavision SoftWorx

software (Applied Precision, Inc., WA, USA), analyzed using Fiji[29], and assembled in Adobe Photoshop (Adobe, CA, USA). Brightness was altered linearly in Fiji to aid visualization. For quantification of cell roundness, we defined the cell major axis as the longest possible line along the cell, and the cell minor axis was measured as the longest possible line orthogonal to the cell major axis. Cell measurements were obtained via the measure tool in Fiji[29], and single-cell major and minor axes measurements were collated. Pixel to micron ratio was set as 15.6 as per the microscope specifications. Major/minor axis ratio was calculated for all cells in the field. 26 Number of fields was chosen to ensure measurement of at least 50 cells for each experimental condition. Individual ratio values for each cell were plotted via R package ggplot2 (v.3.2.1)[30], and differences in major:minor ratios in the presence of a fungus relative to growth alone or with WT Penicillium sp. str. #12 relative to ΔlaeA Penicillium sp. str. #12 were determined based on an unpaired two-sample Wilcoxon test p-value < 0.05.

2.5 Acknowledgements

Chapter 2, in part, is a reprint of the material as it appears in Nature Microbiology 2020. Pierce, E.C., Morin, M., Little, J.C., Liu R.B., Tannous J., Keller N.P., Pogliano K., Wolfe B.E., Sanchez L.M., Dutton R.J. Bacterial–

fungal interactions revealed by genome-wide analysis of bacterial mutant fitness. Nat Microbiol (2020). The dissertation author was a co-author on this paper.

2.6 References

1. Laforest-Lapointe, I. & Arrieta, M.-C. Microbial eukaryotes: a missing link in gut microbiome studies. *mSystems* 3, e00201-17 (2018).

2. Huseyin, C. E., O'Toole, P. W., Cotter, P. D. & Scanlan, P. D. Forgotten fungi—the gut mycobiome in human health and disease. *FEMS Microbiol. Rev*. 41, 479–511 (2017).

3. Huffnagle, G. B. & Noverr, M. C. The emerging world of the fungal microbiome. *Trends Microbiol.* 21, 334–341 (2013).

4. de Phillips, F., Laiola, M., Blaiotta, G. & Ercolini, D. Different amplicon targets for sequencing-based studies of fungal diversity. *Appl. Environ. Microbiol.* 83, e00905-17 (2017).

5. Lindsay, A. K. & Hogan, D. A. *Candida albicans*: molecular interactions with *Pseudomonas aeruginosa* and *Staphylococcus aureus*. *Fungal Biol. Rev*. 28, 85–96 (2014).

6. Spraker, J. E. Wiemann P., Baccile J., Venkatesh N., Schumacher J., Schroeder F., Sanchez L., Keller N. Conserved responses in a war of small molecules between a plant-pathogenic bacterium and fungi. *mBio* 9, e00820-18 (2018).

7. Khalid, S. Baccile J., Spraker J., Tannous J., Imran M., Schroeder F., Keller N. NRPS-derived isoquinolines and lipopetides mediate antagonism between plant pathogenic fungi and bacteria. *ACS Chem. Biol.* 13, 171–179 (2018).

8. Wagg, C., Schlaeppi, K., Banerjee, S., Kuramae, E. E. & van der Heijden, M. G. A. Fungal–bacterial diversity and microbiome complexity predict ecosystem functioning. *Nat. Commun.* 10, 4841 (2019).

9. Tourneroche, A. Lami R., Hubas C., Blanchet E., Vallet M., Escoubeyrou K., Paris A., Prado S. Bacterial–fungal interactions in the kelp

endomicrobiota drive autoinducer-2 quorum sensing. *Front. Microbiol.* 10, 1693 (2019).

10. Wolfe, B. E., Button, J. E., Santarelli, M. & Dutton, R. J. Cheese rind communities provide tractable systems for in situ and in vitro studies of microbial diversity. *Cell* 158, 422–433 (2014).

11. Zhang, Y., Kastman, E. K., Guasto, J. S. & Wolfe, B. E. Fungal networks shape dynamics of bacterial dispersal and community assembly in cheese rind microbiomes. *Nat. Commun.* 9, 336 (2018).

12. Morin, M., Pierce, E. C. & Dutton, R. J. Changes in the genetic requirements for microbial interactions with increasing community complexity. *eLife* 7, e37072 (2018).

13. Wetmore, K. M., Price M, Waters R, Lamson J, He J, Hoover C, Blow M, Bristow J, Butland G, Arkin A, Deustchbauer A. Rapid quantification of mutant fitness in diverse bacteria by sequencing randomly bar-coded transposons. *mBio* 6, e00306-15 (2015).

14. Bay DC, Stremick CA, Slipski CJ, Turner RJ. Secondary multidrug efflux pump mutants alter Escherichia coli biofilm growth in the presence of cationic antimicrobial compounds. Res Microbiol. 2017 Apr;168(3):208-221

15. Bok JW, Keller NP. LaeA, a regulator of secondary metabolism in Aspergillus spp. Eukaryot Cell. 2004 Apr;3(2):527-35. doi: 10.1128/ec.3.2.527-535.2004. PMID: 15075281; PMCID: PMC387652.

16. Nonejuie, P., Burkart, M., Pogliano, K. & Pogliano, J. Bacterial cytological profiling rapidly identifies the cellular pathways targeted by antibacterial molecules. *Proc. Natl Acad. Sci. USA* 110, 16169–16174 (2013).

17. Quach D.T., Sakoulas G., Nizet V., Pogliano J., Pogliano K. "Bacterial Cytological Profiling (BCP) as a Rapid and Accurate Antimicrobial

Susceptibility Testing Method for *Staphylococcus aureus*. EBioMedicine 4: 95-103 (2016).

18. Kumaraswamy M, Lin L, Olson J, Sun CF, Nonejuie P, Corriden R, Döhrmann S, Ali SR, Amaro D, Rohde M, Pogliano J, Sakoulas G, Nizet V. Standard susceptibility testing overlooks potent azithromycin activity and cationic peptide synergy against MDR Stenotrophomonas maltophilia. J Antimicrob Chemother. 2016 May;71(5):1264-9. doi: 10.1093/jac/dkv487. Epub 2016 Jan 31. PMID: 26832758; PMCID: PMC4830416.

19. Gupta, N, Liu R, Shin S, Sinha R, Pogliano J, Pogliano K, Griffin J, Nizet V, Corriden R. "SCH79797 improves outcomes in experimental bacterial pneumonia by boosting neutrophil killing and direct antibiotic activity." *The Journal of antimicrobial chemotherapy* vol. 73,6 (2018): 1586-1594.

20. Pierce, E.C., Morin, M., Little, J.C. Liu R, Tannous J, Keller N, Pogliano K, Wolfe B, Sanchez L, Dutton R. Bacterial–fungal interactions revealed by genome-wide analysis of bacterial mutant fitness. *Nat Microbiol* (2020).

21. Choi, K.-H., Lee, H., Lee, S., Kim, S. & Yoon, Y. Cheese microbial risk assessments—a review. *Asian-Australas. J. Anim. Sci.* 29, 307–314 (2016).

22. Perrin, F, Tenehaus-Aziza, Michel V, Miszczycha S, Bel M, Sanaa M. Quantitative risk assessment of haemolytic and uremic syndrome linked to O157:H7 and non-O157:H7 shiga-toxin producing Escherichia coli strains in raw milk soft cheeses: quantitative risk assessment of HUS linked to pathogenic STEC in cheese. Risk Anal. 35, 109–128 (2015).

23. Brudzynski K, Sjaarda C Honey Glycoproteins Containing Antimicrobial Peptides, Jelleins of the Major Royal Jelly Protein 1, Are Responsible for the Cell Wall Lytic and Bactericidal Activities of Honey. PLOS ONE 10(4): e0120238. (2015)

24. Scherlach, K., Graupner, K. & Hertweck, C. Molecular bacteria–fungi interactions: effects on environment, food, and medicine. *Annu. Rev. Microbiol.* 67, 375–397 (2013).

25. de Boer, W., Folman, L. B., Summerbell, R. C. & Boddy, L. Living in a fungal world: impact of fungi on soil bacterial niche development. *FEMS Microbiol. Rev.* 29, 795–811 (2005).

26. Tarkka, M. T., Sarniguet, A. & Frey-Klett, P. Inter-kingdom encounters: recent advances in molecular bacterium–fungus interactions. *Curr. Genet.* 55, 233–243 (2009).

27. Laich, F., Fierro, F. & Martín, J. F. Production of penicillin by fungi growing on food products: identification of a complete penicillin gene cluster in *Penicillium griseofulvum* and a truncated cluster in *Penicillium verrucosum*. *Appl. Environ. Microbiol.* 68, 1211–1219 (2002).

28. Baba, T. Ara T, Hasegawa M, Takai Y, Okumura Y, Baba M, Datsenko K, Tomita M, Wanner B, Mori H. Construction of *Escherichia coli* K-12 in-frame, single-gene knockout mutants: the Keio collection. *Mol. Syst. Biol.* 2, 2006.0008 (2006).

29. Schindelin, J. Arganda-Carreras I, Frise E, Kaynig V, Longair M, Pietzch T, Preibisch S, Rueden C, Saalfeld S, Schmid B, Tinivez J, White D, Hartenstein V, Eliceiri K, Tomancak P, Cardona A. Fiji: an open-source platform for biological-image analysis. *Nat. Methods* 9, 676–682 (2012).

30. Wickham, H. *ggplot2: Elegant Graphics for Data Analysis* (Springer Science+Business Media, 2009).

CHAPTER 3: SCH79797 IMPROVES OUTCOMES IN EXPERIMENTAL BACTERIAL PNEUMONIA BY BOOSTING NEUTROPHIL KILLING AND DIRECT ANTIBIOTIC ACTIVITY

Chapter 3, in full, is a reprint of material as it appears in Gupta N, Liu R, Shin S, et al. "SCH79797 improves outcomes in experimental bacterial pneumonia by boosting neutrophil killing and direct antibiotic activity" in the Journal of Antimicrobial Chemotherapy, 2018. The dissertation/thesis author was second author on this paper, and was responsible for conducting the experiments related to determination of antibiotic mechanism of action described in this paper.

3.1 Introduction

Severe pneumonia is the most common cause of respiratory failure and sepsis among critically ill patients with a mortality rate approaching 40%–50% in the most severe cases.[1–3] Other than timely antibiotic therapy and supportive care, there have been no proven pharmacological therapies for this condition. Given the rapid emergence of antibacterial resistance among pathogenic bacteria, the ability to effectively treat severe bacterial pneumonia and sepsis has been significantly impaired. This has been particularly observed among enteric Gram-negative organisms (Escherichia coli, Pseudomonas aeruginosa and Klebsiella

pneumoniae), which are frequent causes of severe pneumonia in the ICU. Therefore, novel therapies are needed to aid in the management of this complex syndrome.[4]

Protease-activated receptors (PARs) are G protein-coupled, seven-transmembrane receptors that have a unique mechanism of activation that involves cleavage of the N-terminal region by coagulation-based serine proteases.[5] PAR1 was the initial PAR discovered and is activated by a variety of enzymes, though thrombin is the principal agonist under physiological conditions. PAR1 is expressed by a variety of cell types including endothelial cells, epithelial cells and bone marrow-derived haematopoietic cells. Classically, PAR1 activation on endothelial cells by thrombin triggers a vascular disruptive phenotype, so that at areas of inflammation and coagulation there is fluid extravasation into organs and into third spaces (e.g. peritoneal cavity).[6–9] In this study, we sought to determine the role of intrapulmonary PAR1 antagonism in a murine model of Gram-negative pneumonia using a well described and widely employed antagonist, SCH79797. We focused on the potential effects of SCH79797 on neutrophils, since these are the predominant inflammatory cells present in acute bacterial pneumonia.

The literature in this area is somewhat limited with conflicting results but suggests that there may be time-dependent roles of PAR1 antagonism

in experimental models of sepsis with early blockade leading to beneficial outcomes. Kaneider et al.[10] published a report demonstrating that early activation of PAR1 in a sepsis model was harmful, whereas late activation is beneficial via a PAR2-dependent mechanism. The authors utilized unique cell-penetrating peptides, pepducins, that specifically targeted the third intracellular loop of PAR1 to dissect the time-dependent effects of PAR1 activation in sepsis.[10] In 2012, Schouten et al.[11] used a pneumococcal pneumonia model in mice to show that PAR1 impairs host defence against infection. They presented data demonstrating that PAR1 #/# mice had improved survival early after infection, lower bacterial burden and less inflammatory cell influx than WT mice.[11] And, in 2013, Khoufache et al.[12] examined the effect of PAR1 antagonism and deficiency in a murine model of influenza A pneumonia. They reported that treatment with a PAR1 antagonist improved outcomes in mice with influenza infection.[12] However, Camerer et al.[13] published an article in 2006 reporting that PAR1 #/# mice did not have improved survival or inflammatory indices in an experimental model of sepsis using intraperitoneal endotoxin.

In terms of neutrophils and PAR1 specifically, there are reports indicating that neutrophils express PAR1 and other PARs,[14] and that PAR1 antagonism has been shown to influence neutrophil recruitment in an

experimental pneumonia model.[15,16] However, the literature is sparse in terms of describing the effects of PAR1 antagonism on neutrophil function directly.

Our hypothesis was that PAR1 antagonism with SCH79797 would be protective in murine E. coli pneumonia and sepsis and modulate neutrophil activity in the lung. The results demonstrated that SCH79797 did improve survival, lung injury and bacterial clearance in our model of bacterial pneumonia through neutrophil boosting of bacterial killing as well as a direct antibiotic effect. However, these results were not seen with the newer-generation PAR1 antagonist vorapaxar (SCH530348), suggesting that SCH79797 may be acting through both PAR1-dependent and PAR1-independent effects, which has been previously reported.[17]

3.2 Methods

Murine E. coli pneumonia model and treatment with SCH79797

All mice used in this study were male C57BL/6J mice (Jackson Labs) between 12 and 15 weeks of age. Mice were housed under standard conditions in a clean facility at the University of California, San Diego (UCSD) approved by the Association for Assessment and Accreditation of Laboratory Animal Care (AAALAC) and all experiments were approved by the UCSD Institutional Animal Care and Use Committee (IACUC).

E. coli strain K1 was used in all in vivo and in vitro models in this study (originally isolated from the blood of a patient with biliary sepsis; provided by Xiao Su, MD, PhD, Institut Pasteur of Shanghai). Intratracheal (IT) instillation of E. coli (1 million cfu) into mice was accomplished using a previously described protocol of direct visual instillation.[18] SCH79797 (Tocris Bioscience) was administered IT as a treatment for E. coli pneumonia at 6 h post-infection. See Supplementary Methods (available as Supplementary data at JACOnline) for more details.

Bronchoalveolar lavage and lung injury analyses

Bronchoalveolar lavage (BAL) was done using a previously published protocol.19 Lungs were harvested and processed in a standard fashion and lung injury was scored using an established method.[19,20] See Supplementary Methods for details.

Mouse neutrophil isolation

Mouse neutrophils were isolated from the bone marrow of tibias and femurs of adult, male C57BL/6J mice using a previously published protocol.[21] The purity of the neutrophils was assessed by doing a cytospin of an aliquot of cells, fixing the cells on a slide and then doing a hematoxylin and eosin (H&E) stain (90% purity confirmed by this method). See Supplementary Methods for details.

Mouse neutrophil quantitative real-time PCR and western blotting for PAR1 expression

RNA and protein were isolated from mouse neutrophils using standard techniques. Quantitative real-time PCR (qPCR) was done to analyse gene expression of PAR1 in neutrophils and western blotting was performed to determine whole-cell PAR1 protein expression. Bone marrow-derived mesenchymal stem cells (MSCs) were used as a positive control, as they have been recently shown to express PAR1 by our group.[22] See Supplementary Methods for full details of the methods used for these analyses.

Neutrophil bacterial killing and reactive oxygen species assays

Neutrophil bacterial killing assays were done, using a previously published protocol, with SCH79797 to determine the effects of this compound on killing efficiency.[23] Reactive oxygen species (ROS) production was measured as has been previously published by our group.[23] See Supplementary Methods for details.

Mouse neutrophil extracellular trap visualization and quantification

In order to ascertain whether the increase in neutrophil killing of bacteria by SCH79797 correlates with neutrophil extracellular trap (NET) formation, studies were done to visualize and quantify NETs using a protocol that our group has previously published.[23] See Supplementary

Methods for complete details. Vorapaxar was also tested to determine whether the effects seen were generalizable to the class of PAR1 antagonists. A protein kinase C (PKC) inhibitor was used in some conditions to determine whether this pathway is involved in NET formation, since PKCs have been previously reported to be required for phorbol myristate acetate (PMA)-induced NETs.[24]

Mouse neutrophil cathelicidin-related antimicrobial peptide expression analysis

Neutrophils were isolated as above and resuspended in Hank's balanced salt solution (HBSS) with calcium and magnesium. Cells were plated at a concentration of 1 million cells per 250 lL in a 24-well tissue culture plate in the presence of SCH79797 (10 lM), PMA (25 nM) or E. coli (3 million cfu). Stimulation was added in a 50lL volume so the final total volume was 300 lL per well. Each condition was done in triplicate. The plate was then centrifuged at 1600 rpm for 5min and then incubated at 37C for 3 h, after which 3 lL of the conditioned medium from each sample was applied directly onto a nitrocellulose membrane and allowed to completely dry. The membrane was blocked with appropriate buffer (LiCor) and cathelicidin-related antimicrobial peptide (CRAMP) protein was then detected and visualized using standard techniques (rabbit anti-

mouse CRAMP antibody, 1:500, Novus Biologicals; secondary goat anti-rabbit antibody, 1:10 000, LiCor).

Image J software (NIH) was then used to quantify the CRAMP immunoblot in terms of densitometry of the respective conditions tested.

Human neutrophil isolation and analyses with SCH79797

Human neutrophils were isolated as previously described using a Polymorphprep kit (Axis-Shield, Dundee, Scotland).[23] Analyses for NET formation and NET-based killing assays were carried out in a manner similar to that used for mouse neutrophils and as previously published.[23]

Assessment of direct antibacterial effect of SCH79797

To determine whether there was a direct antibacterial effect of SCH79797 that may, in part, account for the protective in vivo effects observed, we carried out two different assays to measure how SCH79797 influences E. coli growth in vitro: (i) a continuous assessment of E. coli growth kinetics over 24 h; and (ii) a killing assay to quantify growth or killing of E. coli after 6 h. Separate conditions using vorapaxar were included to ascertain whether the effects seen with SCH79797 were applicable to other PAR1 antagonists. In addition, we tested the killing activity of SCH79797 against Gram-positive bacteria using an isolate of MRSA (TCH1516). See Supplementary Methods for details.

Determination of mechanism of SCH79797 antibacterial action

Bacterial cytological profiling was utilized to determine the antibiotic mechanism of action of SCH79797 as has been previously published by our group.[25,26] Bacillus subtilis was used as a Gram-positive bacterium against which to test the activity of SCH79797 given our group's experience with this strain for morphological studies. See Supplementary Methods for details. Of note, experiments in high-sucrose medium were done to discriminate between cell membrane and cell wall effects of SCH79797. Published images were taken using fluorescent microscopy.

Statistical analyses

Survival data was analysed using a log-rank test, while the majority of the other data is presented as mean +SD for each group analysed. An unpaired, two-sided Student's t test was used for most comparisons between two sets of data. If multiple groups of data were compared simultaneously, an ANOVA was used. A P value ,0.05 was used for statistical significance.

3.3 Results

PAR1 antagonism with SCH79797 improves survival in murine E. coli pneumonia

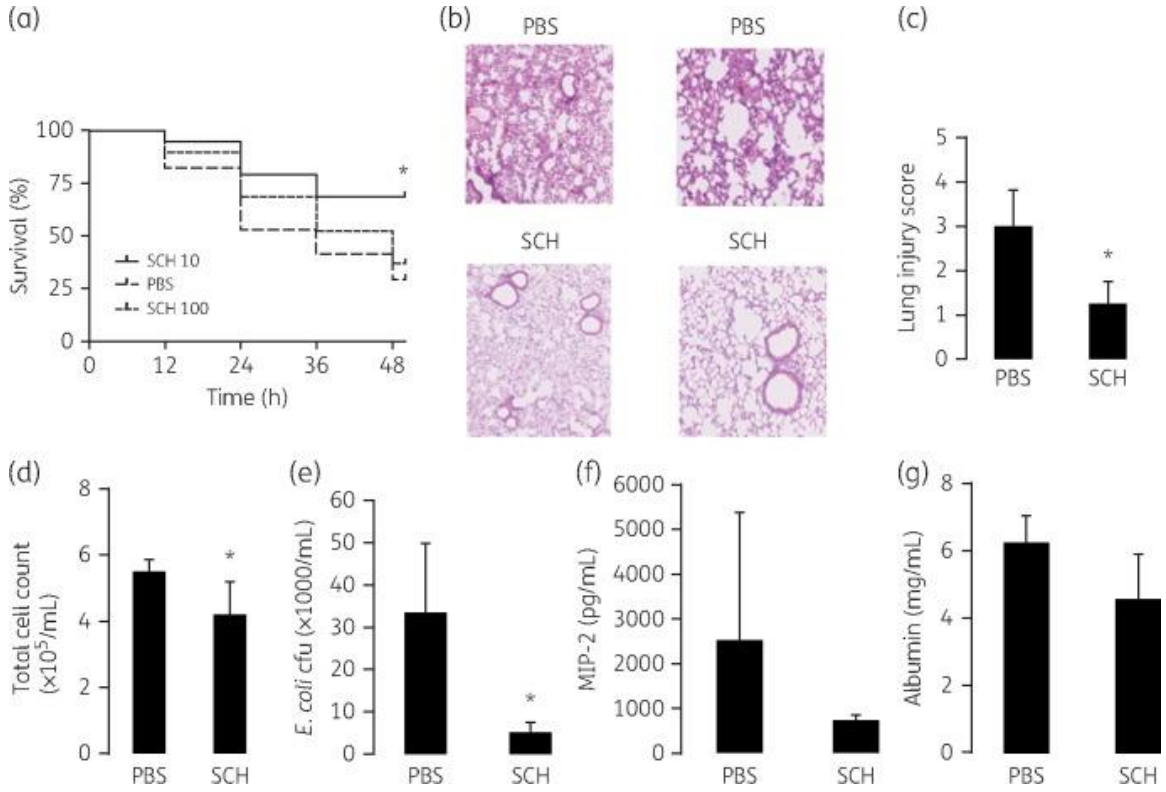

Figure 3.1. SCH79797 significantly improves survival, lung injury and inflammation in murine *E. coli* pneumonia. SCH79797 at 10 μM was determined to be the most effective dose when given as a treatment 6 h after infection (a; $n = 17–19$ per group, $^*P < 0.05$ for 10 μM SCH79797, SCH 10, versus PBS; 100μM SCH79797 (SCH 100) provided no survival advantage versus PBS). H&E staining of lungs demonstrated less lung injury in mice treated with SCH79797 10 μM (SCH) at 24 h post-infection (b and c; $n = 3$ lungs per group for lung injury score analysis, $^*P < 0.05$ for SCH- versus PBS-treated groups, data as mean ± SD). BAL at 24 h showed reduced inflammatory cell influx (d), reduced bacterial burden (e) and a trend towards a reduction in both inflammatory cytokine levels (f) and vascular permeability (g) with SCH treatment ($n = 6$ per group for all analyses, $^*P < 0.05$ and $P = 0.16$ for macrophage inflammatory protein-2 (MIP-2) concentrations and $P = 0.055$ for albumin concentrations, data as mean ± SD). This figure appears in colour in the online version of *JAC* and in black and white in the print version of *JAC*.

When SCH79797 was administered via the IT route 6 h after establishment of E. coli pneumonia there was a significant improvement in survival at 48 h post-infection in the group of mice treated with 10 lM SCH79797 (SCH79797-treated mice" 68% versus PBS-treated mice" 29%, P , 0.05). Mice given a higher dose of SCH79797 (100lM) had no improvement in survival compared with control mice treated with PBS (Figure 3.1a).

SCH79797 reduces lung injury, bacterial burden and markers of inflammation

Treatment with 10 lM SCH79797 6 h after E. coli infection resulted in a significant reduction in alveolar oedema 24 h after infection as determined by scoring of lung histological sections (Figure 3.1b and c). In addition, BAL studies done 24 h after infection showed a significant reduction in bacterial burden and inflammatory cell influx and a trend towards lower neutrophil chemokine levels (Figure 3.1d–f). Also, there was a near-significant reduction in the quantity of alveolar total protein level with treatment with SCH79797 at 10 lM (Figure 3.1g), but not when higher doses of SCH79797 were used (data not shown).

Mouse neutrophils express PAR1 and SCH79797 boosts neutrophil killing activity

Bone marrow-derived neutrophils demonstrated evidence of PAR1 gene and protein, albeit at low levels when compared with bone marrow-

derived MSCs (Figure 3.2a and b). Incubation of neutrophils with SCH79797 (10 lM) significantly increased bacterial killing of E. coli when assessed after 3 h of stimulation to allow for formation of NETs. The addition of DNase, to disrupt the NETs, eliminated the effect of SCH79797 on neutrophil killing (Figure 3.2c). Of note, SCH79797 also increased neutrophil killing of bacteria after only 30min of stimulation, but this effect was not as pronounced and did not reach a statistical level of significance (data not shown).

SCH79797 stimulated several pathways by which neutrophils classically kill bacteria including increasing ROS activity (Figure 3.2d), NET formation as seen visually and quantitatively (Figure 3.2e and f) and CRAMP release (Figure 3.2g). SCH79797-induced NET formation was significantly reduced by pre-incubation with the conventional PKC inhibitor Go6976. PMA was used as a positive control for these mechanistic studies and SCH79797 boosted neutrophil killing activities in a manner similar to or greater than that measured with PMA. Importantly, vorapaxar did not result in any measurable increase in NET formation suggesting that the effect seen with SCH79797 is not generalizable among the class of PAR1 antagonists.

Figure 3.2 (Opposite page). SCH79797 augments neutrophil killing of *E. coli* by several mechanisms. Neutrophils (PMNs) express low levels of the PAR1 gene and protein as evidenced by qPCR (a; $n = 3$ per group, $^{**}P < 0.01$ for PMN versus MSCs and $\#P < 0.01$ for negative control (neg ctrl) versus PMN and neg ctrl versus MSCs, data as mean ± SD) and western blotting (b). SCH79797 at 10 μM (SCH) increased mouse neutrophil killing efficiency (c) and ROS production (d) significantly, while the addition of DNase eliminated the enhanced bacterial killing seen with SCH79797 ($n = 6$ per group for killing and $n = 3$ per group for ROS assay, $^{**}P < 0.01$ for PMN + SCH versus unstimulated (unstim) PMN, $\#P < 0.01$ for PMN + SCH + DNase versus PMN + SCH and $\surd P < 0.01$ for PMN + PMA versus unstim PMN, data as mean ± SD). Fluorescent imaging demonstrated qualitatively more NET formation with incubation of SCH79797 at 10 μM and this effect was reduced with the PKC inhibitor Go6976 at 10 μM (e). Quantitative analysis of NET formation showed a significant increase with 25 nM PMA and 10 μM SCH79797 and this effect was significantly reduced with pre-incubation with the PKC inhibitor Go6976. Vorapaxar 10 μM (Vorapax), however, did not result in any appreciable increase in NET formation compared with unstimulated neutrophils (f; $n = 4$–8 per group, $^{**}P < 0.01$ for PMA and SCH versus unstim, $\#P < 0.01$ for Go6976 + PMA versus PMA and $\surd P < 0.01$ for Go6976 + SCH versus SCH, data as mean ± SD). SCH79797 at 10 μM significantly increased the release of the antimicrobial peptide CRAMP from neutrophils at a level that approximates that seen with PMA (g; $n = 6$ per group, $^{**}P < 0.01$ compared with unstim PMN, data as mean ± SD). This figure appears in colour in the online version of *JAC* and in black and white in the print version of *JAC*.

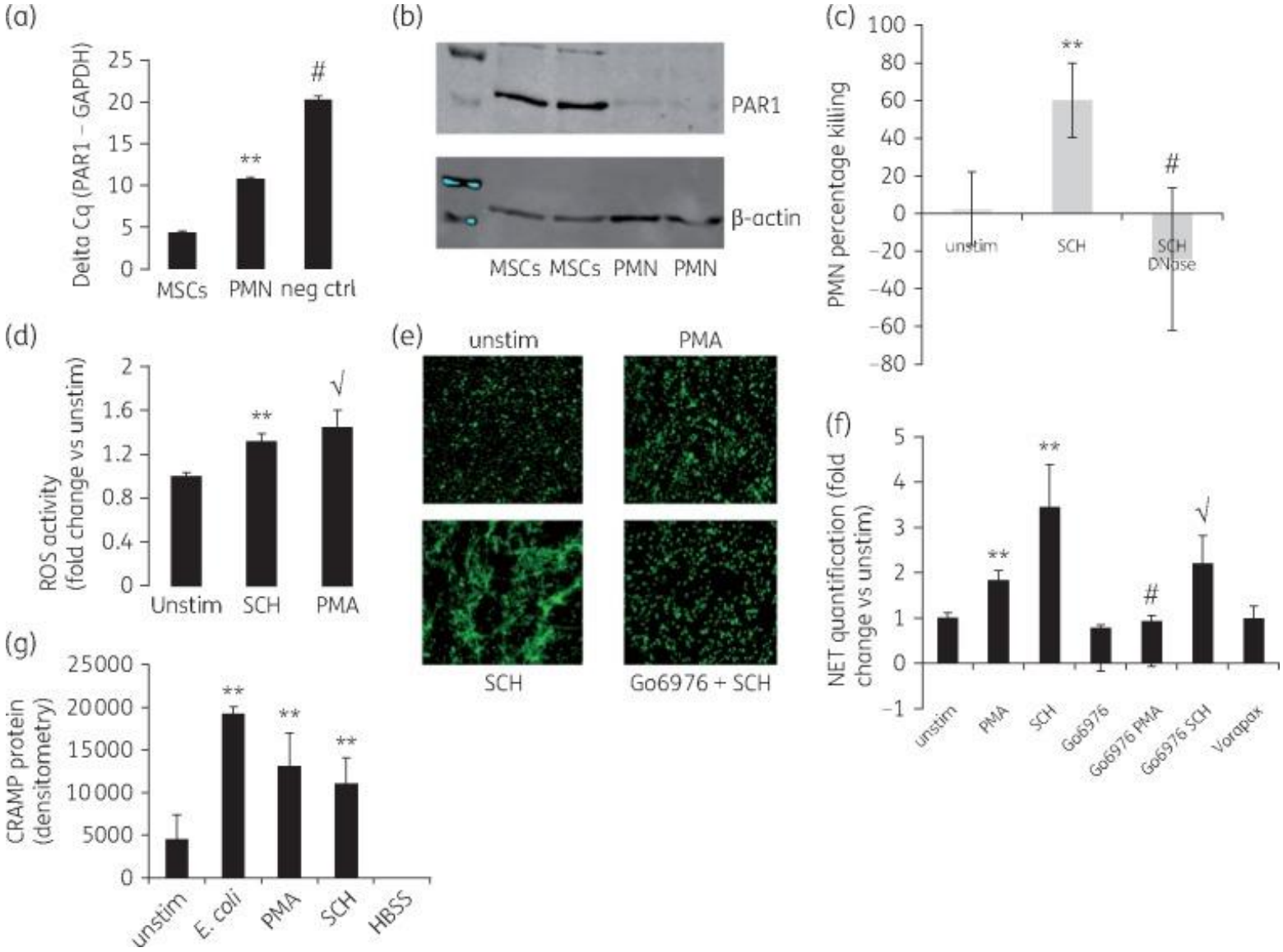
(a)
Delta Cq (PAR1 – GAPDH)
25
20
15
10
5
0
**
#
MSCs
PMN
neg ctrl
(b)
PAR1
β-actin
MSCs MSCs PMN PMN
(c)
PMN percentage killing
100
80
60
40
20
0
−20
−40
−60
−80
**
#
unstim
SCH
SCH DNase
(d)
ROS activity (fold change vs unstim)
2
1.6
1.2
0.8
0.4
0
**
√
Unstim
SCH
PMA
(e)
unstim
PMA
SCH
Go6976 + SCH
(f)
NET quantification (fold change vs unstim)
5
4
3
2
1
0
−1
**
**
#
√
unstim
PMA
SCH
Go6976
Go6976 PMA
Go6976 SCH
Vorapax
(g)
CRAMP protein (densitometry)
25000
20000
15000
10000
5000
0
**
**
**
unstim
E. coli
PMA
SCH
HBSS

Figure 3.3. (Opposite Page) SCH79797 increases NET formation in human neutrophils and enhances their bacterial killing capacity. Fluorescent imaging showed that SCH79797 (SCH) at a dose of 10 μM increased NET formation compared with unstimulated (unstim) neutrophils and this was partially reduced with the PKC inhibitor Go6976 at 10 μM (a). Quantification of NET formation demonstrated significantly higher levels of NETs with 10 μM SCH79797, similar to that seen with the positive control, PMA. Vorapaxar 10 μM (Vorapax) stimulation did not result in an increase in NET formation compared with unstimulated neutrophils (b; $n = 4$ per group, $^{*}P < 0.05$ for PMA versus unstim and $^{**}P < 0.01$ for SCH versus unstim, data as mean ± SD). SCH79797 at 10 μM significantly increased human neutrophil killing of *E. coli* and this was reversed by the addition of DNase (c; $n = 4$ per group, $^{*}P < 0.05$ for SCH versus unstim and $\surd P < 0.05$ for SCH + DNase versus SCH, data as mean ± SD). This figure appears in colour in the online version of *JAC* and in black and white in the print version of *JAC*.

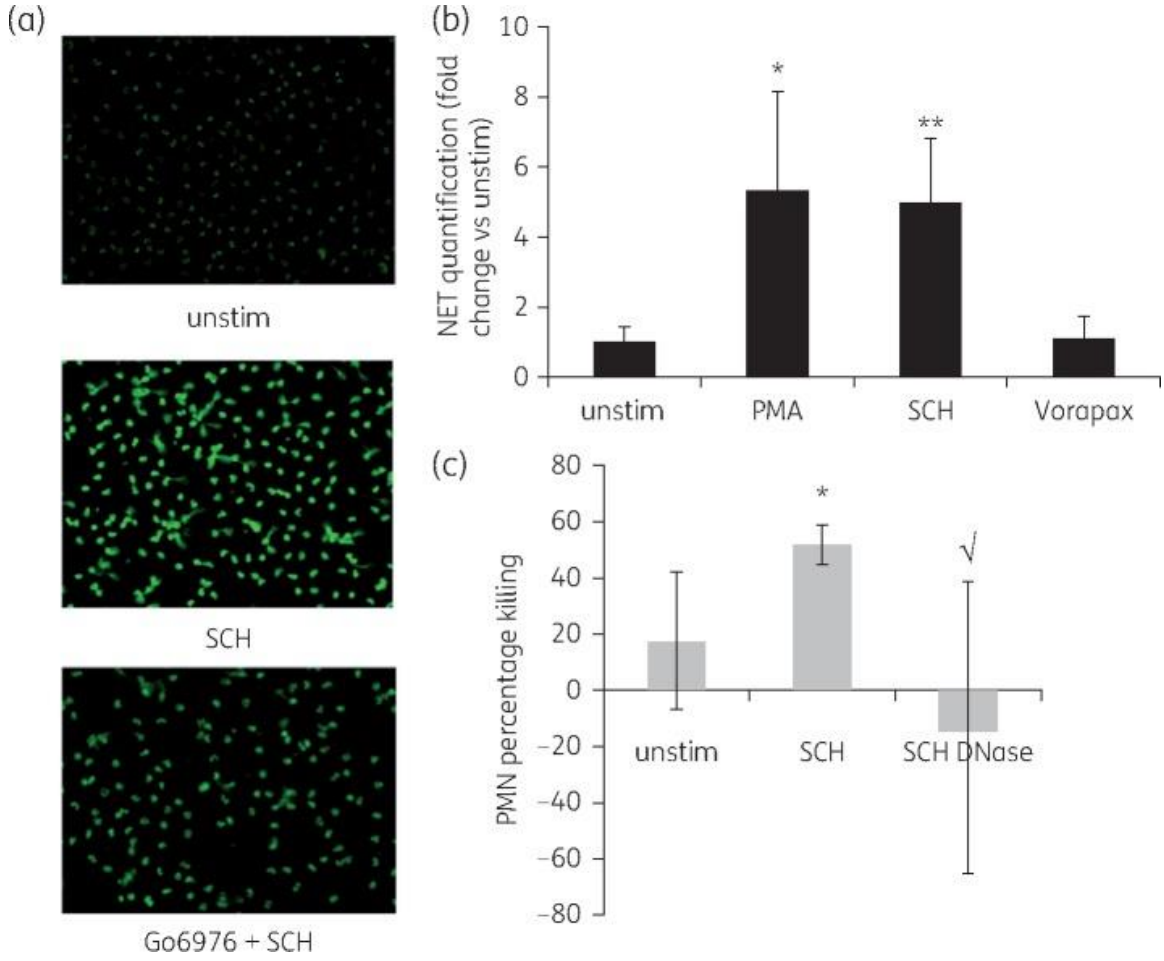
(a)
unstim
SCH
Go6976 + SCH
(b)
NET quantification (fold change vs unstim)
10
8
6
4
2
0
*
**
unstim
PMA
SCH
Vorapax
(c)
PMN percentage killing
80
60
40
20
0
−20
−40
−60
−80
*
√
unstim
SCH
SCH DNase

SCH79797 induces NETs in human neutrophils and enhances their bacterial killing

To determine whether the findings in mouse neutrophils extend to human neutrophils, studies assessing the effects of SCH79797 on human neutrophil function were carried out, similar to those done with mouse neutrophils. Initially, it was determined that human neutrophils do express the transcript for PAR1 by qPCR (data not shown). Then, fluorescent microscopy demonstrated that SCH79797, at a dose of 10 IM, led to significant NET formation in human neutrophils (Figure 3.3a and b). As with the mouse neutrophil studies, the use of the PKC inhibitor Go6976 partially reduced the formation of NETs (Figure 3.3a). Quantification of NET formation also demonstrated a significant increase with SCH79797 at 10 IM that closely approximated the positive control, PMA (Figure 3.3b). However, vorapaxar did not result in any measurable increase in NET formation as was seen in the mouse neutrophil studies (Figure 3.3b). In addition, human neutrophil killing activity was significantly improved with SCH79797 (10 IM) and this effect was completely eliminated with the addition of DNase as seen in Figure 3.3(c). These findings are also consistent with what was observed with mouse neutrophils and demonstrate the importance of SCH79797-induced NETs in mediating bacterial killing.

Figure 3.4 (Opposite page). SCH79797 has a direct antibiotic effect through disruption of the bacterial membrane. SCH79797 (SCH) significantly impaired the growth of *E. coli* over the course of 24 h starting at a concentration of 1 μM (a; $n = 3$ per condition, $^{*}P < 0.05$ versus *E. coli* alone) and resulted in no bacterial growth when used between 10 and 100 μM (a; $n = 3$ per condition, $^{**}P < 0.01$ versus *E. coli*). After 6 h, SCH79797 significantly reduced *E. coli* growth at a concentration of 10 μM, and, at 100 μM, SCH79797 resulted in approximately 95% killing of *E. coli*. Vorapaxar (Vorapax) at 10 and 100 μM did not significantly suppress *E. coli* growth (b; $n = 3$ per group, $^{**}P < 0.01$ versus positive control (pos ctrl) DMSO condition, data as mean ± SD). The mechanism of SCH79797's antibiotic effect was determined through cytological profiling of SCH79797 (c–h). Δ*tolC E. coli* cells were treated with 2% DMSO (c, e and g) or 25 μM (5 × MIC) SCH79797 (d, f and h). (c and d): 30 min post-treatment, LB medium. (e and f): 2 h post-treatment, LB medium. (g and h): 2 h post-treatment, LB medium with 0.5 M sucrose. Cell membranes are stained with FM4–64 (red). DNA is stained with the membrane-permeable dye DAPI (blue) and the membrane-impermeable dye SYTOX Green (green). The presence of SYTOX Green indicates cells with compromised membranes; thus, SYTOX Green is normally absent from untreated cells. Scale bars = 2 μm. This figure appears in colour in the online version of *JAC* and in black and white in the print version of *JAC*.

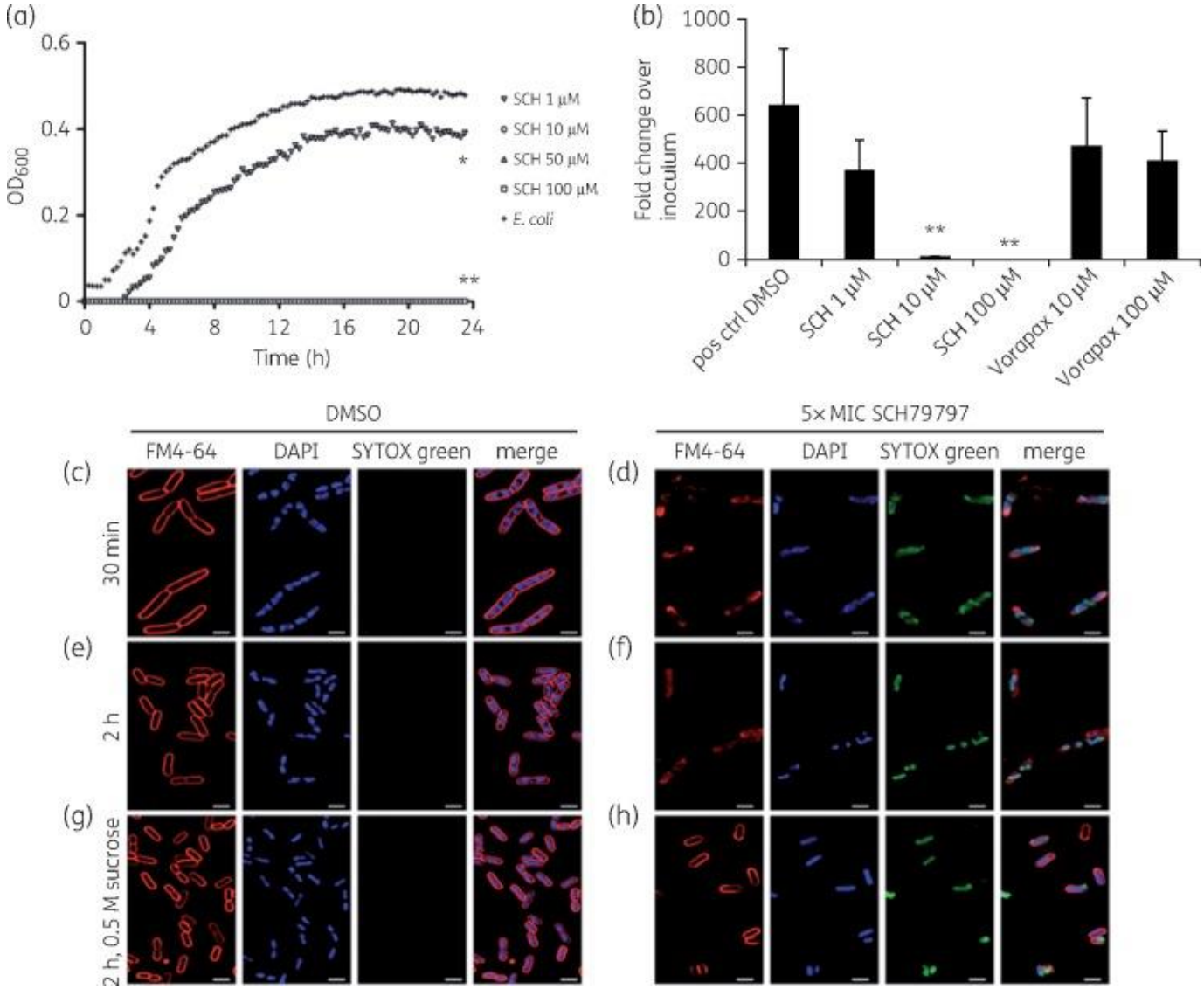
(a)
0.6
0.4
0.2
0
OD600
0
4
8
12
16
20
24
Time (h)
SCH 1 μM
SCH 10 μM
SCH 50 μM
SCH 100 μM
E. coli
*
**
(b)
1000
800
600
400
200
0
Fold change over inoculum
**
**
pos ctrl DMSO
SCH 1 μM
SCH 10 μM
SCH 100 μM
Verapax 10 μM
Verapax 100 μM
DMSO
5× MIC SCH79797
FM4-64
DAPI
SYTOX green
merge
(c)
(d)
30 min
(e)
(f)
2 h
(g)
(h)
2 h, 0.5 M sucrose

SCH79797 exhibits direct antibacterial activity targeting the membrane

The Bioscreen assay demonstrated that SCH79797, starting at 1lM, inhibited E. coli growth compared with the positive control of E. coli alone in growth medium (Figure 3.4a). Concentrations of SCH79797 that were 10lM and greater led to no apparent growth of E. coli as detected by the Bioscreen assay. When separate analyses were carried out to quantify the bacterial counts after 6 h of incubation of SCH79797 with E. coli, 10lM SCH79797 led to significant suppression of growth, while 100lM led to pronounced bacterial killing (Figure 3.4b). However, vorapaxar did not significantly reduce bacterial growth when tested at 10 and 100lM. These comparisons were made in reference to the initial inoculum of E. coli plated per well.

Using bacterial cytological profiling, it was determined that SCH79797 used at 25 lM (5% the calculated MIC) resulted in substantial E. coli lysis and exposure of DNA to the membrane-impermeable dye SYTOX Green (Figure 3.4c–f). This was seen at both the 30min and 2 h timepoints. The rapid permeabilization of E. coli at 30min suggests a membrane-active effect, but this finding could also be due to a potent inhibition of cell wall biosynthesis (Figure S1A and B, available as Supplementary data at JAC Online). To distinguish between a membrane-active or cell wall-inhibitory effect of SCH79797, E. coli was treated with SCH79797, D-

cycloserine or polymyxin B under osmotic stabilization conditions with 0.5 M sucrose (Figure 3.4g and h and Figure S1E and F). In the absence of sucrose, SCH79797, the cell wall biosynthesis inhibitor D-cycloserine and the membrane-active polymyxin B cause cell permeability at 30min and cellular debris can be seen alongside cells with minimal shape defects at 2 h (Figure 3.4d and f and Figure S1A–D). However, at 2 h of treatment in the presence of sucrose, cells treated with D-cycloserine formed rounded shapes with minimal membrane permeabilization (Figure S1E), whereas cells treated with SCH79797 and polymyxin B maintained a shape typical of cells grown in sucrose but were still permeabilized (Figure 3.4h and Figure S1F). The morphological similarity between cells treated with SCH79797 and polymyxin B, especially under osmotically stabilizing conditions, indicates that SCH79797 acts as a membrane-active compound and not a cell wall biosynthesis inhibitor.

In testing the activity of SCH79797 against Gram-positive bacteria, it was observed that SCH79797 led to significant bacterial membrane disruption of B. subtilis as early as 30min after incubation (Figure S2A–D). Furthermore, SCH79797 showed significant growth suppression of MRSA at a dose of 1 lM and substantial bactericidal activity at 10lM (Figure S3).

3.4 Discussion

PARs are G protein-coupled receptors that have a unique mechanism of activation and are predominantly cleaved and activated by coagulation-based serine proteases. PAR1 is the principal target of thrombin and sits at the fulcrum of inflammation and coagulation in response to infection. The role of PAR1 in experimental models of infection has been investigated to some extent, but there is still uncertainty as to whether activation is beneficial or harmful in this setting. We undertook the current study to determine whether intrapulmonary PAR1 antagonism with SCH79797 would have protective effects in an experimental model of E. coli pneumonia in mice. Our data yielded the following main results: (i) SCH79797 significantly improved survival, reduced lung injury and inflammation, and enhanced bacterial clearance when given as a treatment; (ii) neutrophils express low levels of PAR1 and SCH79797 boosts killing of E. coli by enhancing ROS production, NET formation and CRAMP release; and (iii) SCH79797 has direct, potent antibacterial effects against E. coli. When we tested a newer-generation PAR1 antagonist that has been used in clinical trials, vorapaxar, we observed that there was no effect on NET formation or direct bacterial killing. These results suggest that the in vivo effects obtained with SCH79797 are probably a combination of PAR1- dependent and -independent effects.

In relation to the existing literature on PAR1 in experimental models of sepsis, our findings are most consistent with the findings reported by Khoufache et al.[12] regarding the beneficial effects of SCH79797 administration in a model of influenza pneumonia. The publication by Schouten et al.[11] is also congruent with our results as they report that PAR1 #/# mice have improved outcomes in a model of pneumococcal pneumonia. Our study does provide some additional insights into the effects of SCH79797 on neutrophil function by demonstrating that SCH79797 enhances neutrophil killing of bacteria through several possible mechanisms, including ROS production, NET formation and CRAMP release. The induction of NET formation by SCH79797 was particularly robust and exceeded the quantity seen with the positive control PMA when using mouse neutrophils. NETs have been recognized in the literature as potent antimicrobial networks of chromatin and granule proteins since their initial description.[27] NETs have been postulated to increase the concentration of antimicrobial factors, which aid in bacterial killing, and our finding of an increase in CRAMP release during the same approximate time period may synergize with the formation of NETs to result in enhanced killing. The parallel increase in ROS and NET formation is consistent with reports in the literature that suggest these two pathways are interlinked.[24] Furthermore, the observed inhibition of NET formation by

the conventional PKC inhibitor Go6976 is also consistent with previous studies demonstrating that PKC isoforms are implicated in the generation of NETs.[23,24] Importantly, we were able to demonstrate that our findings using SCH79797 with mouse neutrophils did extend to human neutrophils, which also showed robust NET formation and enhanced killing with SCH79797. However, there is experimental literature demonstrating that NETs are pathogenic in models of lung injury and that targeting NETs may have therapeutic potential.[28–30] In this study, the stimulation of NET formation by SCH79797 may have conflicting effects by having a beneficial effect in promoting bacterial clearance but potentially exacerbating the development of lung injury. The net effect of NET formation in vivo is probably dependent on how extensive the NETs are within the lung and the resultant balance of these competing effects.

In addition to the boosting the effect on neutrophil killing, we observed that SCH79797 had direct, potent antibacterial effects against E. coli. Using both the Bioscreen analysis system and direct killing assays, we were able to demonstrate that SCH79797 had bacteriostatic effects at a concentration of 10 IM and significant bactericidal activity at 100 IM. Using bacterial cytological profiling, we then were able to ascertain that SCH79797 exhibits rapid permeabilization of bacteria to the DNA dye, SYTOX green, indicating membrane disruption. This is the first description of

a PAR1 antagonist exhibiting antibiotic properties, to our knowledge. Furthermore, SCH79797 exerted significant antibacterial effects against Gram-positive bacteria as assessed by morphological (B. subtilis) and killing (MRSA) assays. Of note, the newer generation PAR1 antagonist vorapaxar had no effect on bacterial growth and did not induce NET formation as mentioned above. These findings support the possibility that SCH79797 is exerting PAR1-independent effects on neutrophils and on bacteria directly and are consistent with prior reports of SCH79797 exhibiting PAR1- independent functions.[17]

Although we did identify two possible mechanisms to explain the therapeutic effect of the PAR1 antagonist, SCH79797, our study did not explore the effects of this compound on other cells known to express PAR1. This includes endothelial cells, epithelial cells and fibroblasts in the lung parenchyma and possibly other immune cells such as macrophages and dendritic cells. It is likely that SCH79797 also affects some of these cell types, which may explain the dose-dependent effects we observed in vivo. In this context, it is important to note that lower doses of SCH79797 led to a greater survival benefit and a greater reduction in vascular permeability, consistent with the fact that higher doses of SCH79797 can have deleterious effects on endothelial cells and other cell types.[17,31] We focused on neutrophils primarily because they are the predominant

innate immune cells present in the alveolar space during the acute phase of pneumonia, comprising up to 90% of the total inflammatory cell component (assessed by cytospin and H&E staining of BAL fluid). Therefore, we anticipated that effects of SCH79797 on neutrophils would have a significant impact on lung injury and mortality in a pneumonia model. Understanding the relative contributions of the various effects of SCH79797 (neutrophil boosting, direct bacterial killing and reduction in vascular permeability) in the current model is difficult to ascertain specifically and the mortality benefit seen with SCH79797 treatment probably represents a summation of these actions.

In addition to the limitations outlined above, another important factor to consider that was not addressed in the current project is the role of other PARs in mediating neutrophil killing of bacteria and the pathogenesis of bacterial pneumonia. Our data (not shown) show that mouse neutrophils do appear to express mRNA for all PARs and have detectable protein expression for PAR1 and PAR2 under basal conditions. Therefore, it is highly likely that other PARs are playing a role in regulating neutrophil activity in response to bacterial infection and that different bacterial strains activate distinct PARs on neutrophils through the production of proteases. These areas will be the focus of future studies.

In conclusion, we have demonstrated that treatment with intrapulmonary PAR1 antagonism using SCH79797 exhibits significant protective effects in a mouse model of E. coli pneumonia. These effects can probably be explained, in part, through the observations that SCH79797 boosts neutrophil killing of bacteria and has direct antibiotic properties. Some of the effects observed with SCH79797 are probably PAR1 independent, because a newergeneration PAR1 antagonist vorapaxar did not produce similar results on neutrophil function or bacterial killing. SCH79797 and PAR1 antagonism more generally, may have therapeutic implications for patients with severe, antibiotic-resistant pneumonia, but understanding which effects are PAR1 dependent and elucidating the optimal, therapeutic concentration will be very important in any translational effort.

3.5 Supplementary data

Supplementary Methods and Figures S1 to S3 are available as Supplementary data at JAC Online.

3.6 Acknowledgments

Chapter 3, in full, is a reprint of the material as it appears in the Journal of Antimicrobial Chemotherapy 2018. Gupta, N., Liu R., Shin. S.,

Sinha R., Pogliano J., Pogliano K., Griffin J., Nizet V., Corriden R. "SCH79797 improves outcomes in experimental bacterial pneumonia by boosting neutrophil killing and direct antibiotic activity." The Journal of Antimicrobial Chemotherapy vol. 73,6 (2018). The dissertation author was a co-author on this paper.

3.7 References

1. Bellani G, Laffey JG, Pham T. Fam E, Brochard L, Esteban A, Gattinoni L, van Haren F, Larsson A, McAuley D, Ranieri M, Rubenfield G, Thompson B, Wrigge H, Slutsky A, Pesenti A. Epidemiology, patterns of care, and mortality for patients with acute respiratory distress syndrome in intensive care units in 50 countries. JAMA 2016; 315: 788–800.

2. Rubenfeld GD, Caldwell E, Peabody E., Weaver J, Martin D, Neff M, Stern E, Hudson L. Incidence and outcomes of acute lung injury. N Engl J Med 2005; 353: 1685–93.

3. The ARDS Definition Task Force. Acute respiratory distress syndrome: the Berlin Definition. JAMA 2012; 307: 2526–33.

4. Ventola CL. The antibiotic resistance crisis: part 1: causes and threats. P T 2015; 40: 277–83.

5. Coughlin SR. How the protease thrombin talks to cells. Proc Natl Acad Sci USA 1999; 96: 11023–7.

6. Hollenberg MD, Mihara K, Polley D. Suen J, Han A, Fairlie D, Ramachandran R. Biased signaling and proteinase-activated receptors (PARs): targeting inflammatory disease. Br J Pharmacol 2014; 171: 1180–94.

7. Gieseler F, Ungefroren H, Settmacher U. Hollenberg M, Kaufmann R. Proteinase-activated receptors (PARs)—focus on receptor-receptor-interactions and their physiological and pathophysiological impact. Cell Commun Signal 2013; 11: 86.

8. Lin H, Liu AP, Smith TH. Trejo J., Cofactoring and dimerization of proteinase-activated receptors. Pharmacol Rev 2013; 65: 1198–213.

9. Mosnier LO, Sinha RK, Burnier L. Bouwens E, Griffin J. Biased agonism of protease-activated receptor 1 by activated protein C caused by noncanonical cleavage at Arg46. Blood 2012; 120: 5237–46.

10. Kaneider NC, Leger AJ, Agarwal A. Nguyen N, Perides G, Derian C, Covic L, Kuliopulos A. 'Role reversal' for the receptor PAR1 in sepsis-induced vascular damage. Nat Immunol 2007; 8: 1303–12.

11. Schouten M, van't Veer C, Roelofs JJ. Levi M, van der Poll T. Protease-activated receptor-1 impairs host defense in murine pneumococcal pneumonia: a controlled laboratory study. Crit Care 2012; 16: R238.

12. Khoufache K, Berri F, Nacken W. Vogel A, Delenne M, Camerer E, Coughlin S, Cermeliet P, Lina B, Rimmelzwaan G Planz O, Ludwig S, Riteau B. PAR1 contributes to influenza A virus pathogenicity in mice. J Clin Invest 2013; 123: 206–14.

13. Camerer E, Cornelissen I, Kataoka H. Duong D, Zheng Y, Coughlin S. Roles of protease-activated receptors in a mouse model of endotoxemia. Blood 2006; 107: 3912–21.

14. Wang Y, Gu Y, Lucas MJ.. Expression of thrombin receptors in endothelial cells and neutrophils from normal and preeclamptic pregnancies. J Clin Endocrinol Metab 2002; 87: 3728–34.

15. Mercer PF, Williams AE, Scotton CJ. Jose R, Sulikowski M, Moffatt J, Murray L, Chambers R. Proteinase-activated receptor-1, CCL2 and CCL7 regulate acute neutrophilic lung inflammation. Am J Respir Cell Mol Biol 2014; 50: 144–57.

16. Jose RJ, Williams AE, Mercer PF, Sulikowski M, Brown J, Chambers R. Regulation of neutrophilic inflammation by proteinase-activated receptor 1 during bacterial pulmonary infection. J Immunol 2015; 194: 6024–34.

17. Di Serio C, Pellerito S, Duarte M, Massi D, Naldini A, Cirino G, Prudovsky I, Santucci M, Geppetti P, Marchionni N, Masotti G, Tarantini F. Protease-activated receptor 1-selective antagonist SCH79797 inhibits cell proliferation and induces apoptosis by a protease-activated receptor 1-independent mechanism. Basic Clin Pharmacol Toxicol 2007; 101: 63–9.

18. Su X, Looney MR, Robriquet L, Fang X, Matthay M. Direct visual instillation as a method for efficient delivery of fluid into the distal airspaces of anesthetized mice. Exp Lung Res 2004; 30: 479–93.

19. Gupta N, Su X, Popov B. Lee J, Serikov V, Matthay M. Intrapulmonary delivery of bone marrow-derived mesenchymal stem cells improves survival and attenuates endotoxin-induced acute lung injury in mice. J Immunol 2007; 179: 1855–63.

20. Mrozek JD, Smith KM, Bing DR. Meyers P, Simonton S, Connett J, Mammel M. Exogenous surfactant and partial liquid ventilation: physiologic and pathologic effects. Am J Respir Crit Care Med 1997; 156: 1058–65.

21. Looney MR, Su X, Van Ziffle JA, Lowell C, Mattay M. Neutrophils and their Fcγ receptors are essential in a mouse model of transfusion-related acute lung injury. J Clin Invest 2006; 116: 1615–23.

22. Gupta N, Sinha RK, Xu X. Nizet V, Matthay M, Griffin J. R41Q-PAR1 mutation eliminates the therapeutic capacity of bone marrow derived mesenchymal stem cells in murine *E. coli* pneumonia. Am J Respir Crit Care Med 2015; 191: A6152. (Abstract).

23. Corriden R, Hollands A, Olson J, Derieux J, Lopez J, Chang J, Gonzalez D, Nizet V. Tamoxifen augments the innate immune function of neutrophils through modulation of intracellular ceramide. Nat Commun 2015; 6: 8369.

24. Gray RD, Lucas CD, MacKellar A, Li F, Hiersemenzel K, Haslett C, Davidson D, Rossi A. Activation of conventional protein kinase C (PKC) is critical in the generation of human neutrophil extracellular traps. J Inflamm (Lond) 2013; 10: 12.

25. Nonejuie, P., Burkart, M., Pogliano, K. & Pogliano, J. Bacterial cytological profiling rapidly identifies the cellular pathways targeted by antibacterial molecules. Proc Natl Acad Sci USA 2013; 110: 16169–74.

26. Lamsa A, Lopez-Garrido J, Quach D, Riley E, Pogliano J, Pogliano K. Rapid inhibition profiling in *Bacillus subtilis* to identify the mechanism of action of new antimicrobials. ACS Chem Biol 2016; 11: 2222–31.

27. Brinkmann V, Reichard U, Goosmann C. Fauler B, Uhlemann Y, Weiss D, Weinrauch Y, Zychlinsky A. Neutrophil extracellular traps kill bacteria. Science 2004; 303: 1532–5.

28. Caudrillier A, Kessenbrock K, Gilliss BM, Nguyen J, Marques M, Monestier M, Toy P, Werb Z, Looney M. Platelets induce neutrophil extracellular traps in transfusion-related acute lung injury. J Clin Invest 2012; 122: 2661–71.

29. Bosmann M, Ward PA.. Protein-based therapies for acute lung injury: targeting neutrophil extracellular traps. Expert Opin Ther Targets 2014; 18: 703–14.

30. Liu S, Su X, Pan P, Zhang L, Hu Y, Tan H, Wu D, Liu B, Li H, Li H, Li Y, Dai M, Li Y, Hu C, Tsung A. Neutrophil extracellular traps are indirectly triggered by lipopolysaccharide and contribute to acute lung injury. Sci Rep 2016; 6: 37252.

31. Zania P, Kritikou S, Flordellis CS, Maragoudakis M, Tsopanoglou N. Blockade of angiogenesis by small molecule antagonists to protease-activated receptor-1: association with endothelial cell growth suspension and induction of apoptosis. J Pharmacol Exp Ther 2006; 318: 246–54.

Chapter 4: Conclusion and Future Directions

Understanding the interactions between species is vital to our understanding of biology. These interactions, or symbioses, can come in many forms, and can be neutral, beneficial, or detrimental to any organism involved. One extremely common type of symbiosis is competition: where two (or more) organisms are in conflict with each other, usually for access to nutrients, space, or other necessities. In many such cases, a simple solution is for one organism to attempt to kill the other.

In the prokaryotic-eukaryotic interface, warfare is often chemical. Specifically, various eukaryotic species including plants, fungi, and animals have been well documented throughout scientific history to produce antibiotic metabolites able to kill bacteria, either to capitalize on nearby resources or to prevent infection. This dissertation has focused on the use of Bacterial Cytological Profiling (BCP) to explore how bacteria are affected by bioactive, antibiotic molecules present in the prokaryotic/eukaryotic interface.

In chapter 1, I discuss a family of plant defense metabolites called the flavones. Antibiotics are often grouped into families by their backbone structure, and antibiotics within the same family normally differ by various chemical modifications to the backbone, such as hydroxylation,

methoxylation, acetylation, and more. Antibiotics within the same family are widely considered to have the same antibiotic mechanism of action (MOA); namely, what bacterial cellular process they inhibit. This MOA is most often attributed to the activity of the backbone structure of these antibiotic molecules; for example, the beta-lactam ring belonging to the penicillin family, which conjugates to proteins in bacteria essential for the synthesis of the cell wall. The minor modifications, on the other hand, are thought to alter different properties of the drugs, such as solubility, stability, and avoidance of bacteria resistance.

When studying flavones, I discovered that their primary antibiotic MOA can differ based off of the modifications to the same exact backbone structure. Moreover, *in vitro* DNA replication inhibition experiments failed to realize that anti-DNA replication was not the primary MOA of many of the antibiotic flavones. I found that in addition to inhibiting DNA replication and membrane integrity, which are well characterized in previous literature, certain flavones also exhibit activity against outer membrane biosynthesis and cell septation machinery. These results are exciting, as the current paradigm throughout drug discovery pipelines are that antibiotic backbones are responsible for conferring an antibiotic's potency. Once a candidate molecule is found, modifications are made to try to improve its potency, but are assumed to have the

same MOA; as such, resulting libraries of molecules are screened *in vitro* or *in silico* for activity against an assumed target. Our results show that, in contrast to the current understanding of antibiotic structure-activity relationship (SAR), plant flavones' antibiotic MOAs are also driven by their modifications, and that *in vitro* and *in silico* studies fail to differentiate the new MOAs.

In Chapter 2, I explore how BCP can be used to observe metabolic warfare in a microbial community. By examining the defined microbial community of cheeses, we identified genes that were responsible for bacterial fitness specifically when grown in a co-biofilm with various fungal species. By using RB-TnSeq combined with BCP, we identified MdtK as important for bacterial survival under co-culture conditions, LaeA as important for fungal killing of bacteria, as well as the general MOA by which the fungi impede the growth of the bacteria – by secreting metabolites, including AMPs, that disrupt the bacterial cell envelope.

These results are important for several reasons. Firstly, I am pairing a wide genetic screen with phenotypic validation. Many genetic screens are good for "fishing" expeditions, where huge numbers of genes get filtered into a smaller number of candidates. However, even the smaller number of candidates that come out of these screens can take painstakingly long to validate through traditional means of knockouts,

identification, extraction, and fractionation of metabolic products, and retesting and reconfirming. As the BCP pipeline is rapid and facile, it provides another possible filtering step that can narrow down candidates from genetic screens even further, facilitating research on the production of antibiotic molecules by different species.

Additionally, these results are a proof-of-concept that BCP can be applied to more diverse, ecologically and/or clinically relevant situations. There is an ever-growing body of evidence showing that laboratory conditions often do not represent ecological conditions – which can be seen in examples such as the great plate count anomaly, where an estimated 1% or fewer of species can even be cultured in the lab, and in clinics, where antibiotics such as ciprofloxacin can have MICs many orders of magnitude lower (more potent) against bacteria grown on LB when compared to the same strain in patients or in media representative of conditions eukaryotic cells normally experience. The successful application of BCP to cheese curd agar paves the way for essentially creating bespoke analysis parameters for any experimental condition, which may allow for the better understanding of antibiotic efficacy in clinical settings, or metabolic warfare in various ecosystems.

In Chapter 3, I use BCP to examine the chemical SCH79797 that achieves antibacterial activity both through immune signaling pathways

and through its antimicrobial effect. This type of dual-purpose function is uncommon, and further adds to our understanding of how drugs have multiple activities, especially in complex environments such as the human immune system and infection sites. These results further highlight the complexity of clinically relevant settings in compared to standard antibiotic laboratory testing conditions, as drugs originally isolated for different primary activities such a neutrophil recruitment can exhibit antimicrobial effects, or vice versa. These can lead to interesting synergies or antagonisms that might only be experienced *in vivo*, and missed with traditional antibiotic susceptibility tests. While the BCP used in this study involved standard laboratory conditions to test the effects of SCH79797 in isolation from milieu of other biotic and abiotic antimicrobial agents inside the body, our adaptation of BCP to other experimental conditions in Chapter 2 may allow for an avenue for adapting it to be used directly on clinical samples or settings. This could have significant impacts in the pathology and infectious diseases fields, as normal laboratory tests require overnight culturing of pathogens and subsequent susceptibility testing; however, microscopy-based techniques similar to BCP could be developed for more rapid, possibly point-of-care determination of antibiotic susceptibility of infections. This, in turn, could lead to improved

diagnosis and prognosis of antibiotic-resistant bacterial infections, which are seen in millions of people in the United States yearly.

While this dissertation explores my work on the antibiotic metabolite interface between eukaryotic and prokaryotic species, much more research remains to be done to fully understand the mechanisms underlying these interactions. Specifically, while BCP can quickly identify the essential cellular pathway affected by a molecule, it cannot always identify the exact molecular target of the antibiotic. In Chapter 1, I showed that flavones with varying modifications primarily impacted different cellular pathways. These pathways affected were verified using genetic mutant screens and *in vitro* enzymatic activity assays; however, the genetic mutations found to grant resistance to the flavones are likely suppressor mutations and not in the actual molecular target. Therefore, it is worthwhile to further identify the molecular target of TMOS, NSC102049, Tamarixetin, and Tricetin, the former two of which inhibit outer membrane biosynthesis, and the latter two which inhibit cell septation. Furthermore, treatment with Luteolin resulted in a cellular morphology previously not seen before with treatment with any single antibiotic. It is possible that Luteolin has a pleotropic effect, simultaneously inhibiting multiple pathways and leading to its unique curled-cell phenotype. Therefore, studies with antibiotic combinations could be conducted in order to

phenocopy treatment with Luteolin, which may lend insight into the pathways that Luteolin inhibits. Alternatively, genetic mutants resistant to other subgroups of flavones could be tested against Luteolin, in the chance that these mutants would be resistant to one of the molecule's effects but not the other(s), leading to the possible elucidation of Luteolin's MIC.

Given the wealth of plant defense metabolite families that include many structurally related compounds that differ by minor modifications such as hydroxylations and methoxylations, it is possible that some of the other defense metabolite families exhibit the same modification-based activity seen in the flavones. This would lend further credence to our finding that minor modifications can completely change the primary cellular pathway affected by antibiotics. Furthermore, it would lend further insight into how plants defend against microbial pathogens – employing a 'scorched earth' policy of broadly effective antibiotics as opposed to producing an antibiotic that is extremely potent but only has one target. While the latter would certainly be more useful for clinical antibiotic development, further understanding the former will better our understanding of the plant microbiome and plant-microbial interactions.

With respect to Chapter 2, possible future research includes identifying the causative agents for the antibiotic activity seen, and the

determination and classification of hypothetical or uncharacterized genes shown to impart differential fitness between when the bacteria are grown alone or in a co-biofilm. We have identified a biosynthetic cluster in Penicillium *sp.* 12 that is hypothesized to produce an AMP similar to a bee royal jelly protein. Future research can be done to further characterize the AMPs produced by these fungal species, and their potential role competition with bacterial species. Furthermore, fractionation of the fungal-bacterial cobiofilms may allow us to determine other antibiotic molecules produced by cheese fungi, which has potential implications in food safety and stability, as well as impacting the human microbiome when large quantities of these fermented foods are consumed. Finally, I can further investigate bacterial strains that have knockouts in hypothetical proteins shown to have reduced fitness when grown in co-culture. As I saw with the Δ*mdtK* strain, it is likely that some of the strains will deletions in these hypothetical proteins will have sicker phenotypes when grown in a co-biofilm than the wild-type strains; performing BCP on these strains may help identify some of these genes as important for antibiotic resistance.

I would like to see long-term future research utilizing Bacterial Cytological Profiling focusing on adapting the technique to many more ecosystems or environmental conditions, in order to better understand

how bacteria are impacted by bioactive metabolites *in situ*. There are countless biological niches with seemingly infinite combinations of organisms, and perhaps the easiest way to understand how these community members interact is by direct observation. This mantra is shared in the growing field of metagenomics, which seeks to analyze genetic information in environmental samples without introducing culturability biases. Combination of BCP with other microscopy-based techniques such as Fluorescence in situ Hybridization (FISH) could allow for the identification of target species within diverse environmental samples, where individual members of the target species identified via FISH could be then filtered through and analyzed using BCP, allowing us to study 'rare' or unculturable species and how they are affected by antibiotic metabolites.

Furthermore, the development of BCP for usage in more environmental conditions could include mimicking human tissue to better diagnose infections diseases such as necrotizing fasciitis, or it could include environments that are nutrient-poor, such as seawater, which harbor diverse species that are often difficult to culture in laboratory settings. Furthermore, because many antibiotics are more effective against actively growing cells, using standard laboratory conditions to study bacteria that naturally occur in nutrient-poor ecosystems will very

likely engender incorrect or at the very least ecologically irrelevant conclusions. The ability to conduct BCP directly on environmental samples would be extremely powerful, and lead to a better understanding of microbial ecology and symbioses between eukaryotes and prokaryotes.